UNIVERSITA' DEGLI STUDI DI MILANO-BICOCCA

Facoltà di Scienze Matematiche, Fisiche e Naturali

Dipartimento di Biotecnologie e Bioscienze

Dottorato in Biotecnologie Industriali, XXVII ciclo

Spatial control of mitotic exit and spindle positioning

in budding yeast

Ilaria Giusy Scarfone

Anno Accademico 2013/2014

Spatial control of mitotic exit and spindle positioning in budding yeast

Ilaria Giusy Scarfone

Matricola 760866

Tutor: Dr. Simonetta Piatti

Università degli Studi di Milano-Bicocca
Piazza dell'Ateneo Nuovo 1, 2126 Milano

Dipartimento di Biotecnologie e Bioscienze
Piazza della Scienza 2, 20126 Milano

To all the people in my life who touch my heart

Contents

Abstract

The asymmetrically dividing yeast *S. cerevisiae* assembles a bipolar spindle well after establishing the future site of cell division (i.e. the bud neck) and the division axis (i.e. the mother-bud axis). A surveillance mechanism called spindle position checkpoint (SPOC) delays mitotic exit and cytokinesis until the spindle is properly positioned relative to the mother-bud axis, thereby ensuring the correct ploidy of the progeny. SPOC relies on the heterodimeric GTPase-activating protein (GAP) Bub2/Bfa1 that inhibits the small GTPase Tem1, in turn essential for activating the mitotic exit network (MEN) kinase cascade and cytokinesis. The Bub2/Bfa1 GAP and the Tem1 GTPase form a complex at spindle poles that undergoes a remarkable asymmetry during mitosis when the spindle is properly positioned, with the complex accumulating on the bud-directed spindle pole. In contrast, the complex remains symmetrically localized on both poles of misaligned spindles. The mechanism driving asymmetry of Bub2/Bfa1/Tem1 in mitosis is unclear. Furthermore, whether asymmetry is involved in timely mitotic exit is controversial.

By constitutively tethering Bub2 or Bfa1 to a spindle pole body component, which leads to symmetric recruitment of the Bub2/Bfa1/Tem1 complex at spindle poles throughout the cell cycle, we find that, surprisingly, symmetry does not impair mitotic exit, while,

3

conversely, it abolishes SPOC response. Furthermore, it facilitates mitotic exit of MEN mutants, likely by increasing the residence time of Tem1 at spindle poles where it gets active.

We also investigated the mechanism by which the GAP Bub2/Bfa1 controls GTP hydrolysis on Tem1 and generated a series of mutants leading to constitutive Tem1 activation. These mutants are SPOC-defective and invariably lead to symmetrical localization of Bub2/Bfa1/Tem1 at spindle poles, indicating that GTP hydrolysis is essential for asymmetry.

Strikingly, all mutant or chimeric proteins leading to symmetric localization of Bub2/Bfa1/Tem1 lead to increased symmetry at spindle poles of the Kar9 protein that mediates spindle positioning. Kar9 symmetry in turn causes spindle misalignment in metaphase. Thus, asymmetry of the Bub2/Bfa1/Tem1 complex is crucial to control Kar9 distribution and spindle positioning during mitosis.

Riassunto

Nelle cellule che si dividono asimmetricamente, il corretto posizionamento del fuso mitotico lungo l'asse di polarità cellulare è un elemento fondamentale affinché le due cellule figlie ereditino i fattori di polarità in maniera corretta. La regolazione della divisione asimmetrica è capitale per le cellule staminali, che distribuiscono i fattori di pluripotenza in modo disomogeneo tra le due cellule figlie. Alterazioni nei meccanismi di controllo del posizionamento del fuso mitotico hanno effetti deleteri nelle divisioni di cellule staminali e promuovono la tumorigenesi.

Il lievito *Saccharomyces cerevisiae* rappresenta un ottimo sistema modello per studiare la regolazione del posizionamento del fuso mitotico in relazione alla progressione del ciclo cellulare e al controllo della polarità cellulare. Essendo la divisione di *S. cerevisiae* anch'essa asimmetrica, i meccanismi responsabili del corretto posizionamento del fuso rivestono un'importanza fondamentale in quest'organismo. Per questo motivo, più pathways ridondanti si sono evoluti per posizionare correttamente il fuso mitotico in *S.cerevisiae.* E' inoltre presente un meccanismo di sorveglianza del ciclo cellulare chiamato Spindle Position Checkpoint (SPOC), che blocca la progressione del ciclo cellulare e l'uscita dalla mitosi qualora il fuso mitotico non sia correttamente allineato lungo l'asse di divisione cellulare. Il bersaglio molecolare dello

SPOC è la GTPasi Tem1 che controlla sia il posizionamento del fuso che l'uscita dalla mitosi. La GTPase-activating protein dimerica Bub2/Bfa1 inibisce l'attivazione di Tem1 fin tanto che il fuso mitotico non è correttamente orientato. Tem1, Bfa1 e Bub2 formano un complesso eterotrimerico ai poli del fuso mitotico, dove risiedono i centri organizzatori dei microtubuli (Spindle Pole Bodies o SPBs). Il complesso Bub2/Bfa1/Tem1 si distribuisce in maniera asimmetrica, accumulandosi solo sullo SPB diretto nella gemma, se il fuso mitotico si allinea correttamente in anafase. Nel caso, invece, in cui il fuso non sia correttamente orientato, il complesso si localizza in modo simmetrico ed equamente distribuito sui due SPBs. Lo scopo di questa tesi è stato di investigare l'importanza fisiologica della peculiare distribuzione del complesso Bub2/Bfa1/Tem1 in relazione al posizionamento del fuso.

Attraverso la caratterizzazione di mutanti nei siti catalitici di Tem1 e Bub2, abbiamo dimostrato una relazione diretta tra l'attività GTPasica del complesso eterotrimerico e la distribuzione asimmetrica dello stesso in anafase. Inoltre, attraverso lo studio di proteine chimeriche, che reclutano costitutivamente il complesso eterotrimerico su entrambi gli SPBs in maniera simmetrica, abbiamo dimostrato che l'asimmetria del complesso Bub2/Bfa1/Tem1 non regola la progressione del ciclo

cellulare e l'uscita dalla mitosi, ma il posizionamento del fuso mitotico lungo l'asse di divisione cellulare e la corretta distribuzione asimmetrica della proteina Kar9, che partecipa a sua volta ad uno dei pathways di posizionamento del fuso.

Introduction

Asymmetric cell division

Although cell division is commonly thought to involve the equal distribution of cellular components between the two daughter cells, in nature there are many examples of cells that divide asymmetrically. Asymmetric cell division generates two daughter cells genetically equivalent but that differ in fate and/or in size and cytoplasmic material (Fig.1).

Figure 1 Symmetric versus asymmetric cell division. Simple schemes of symmetric and asymmetric cell division. The former generates two identical daughter cells, whereas the latter generates two daughter cells which differ in fate/size/cytoplasmic material (Adapted from Li R., 2013).

In all organisms, ranging from bacteria to mammals, asymmetric cell divisions generate cell diversity (reviewed in Hawkins and Garriga, 1998) and play a major role in the development of multicellular organisms (reviewed in Horvitz and Herskowitz, 1992). Asymmetric cell division is

an intrinsic feature of some unicellular organisms, such as the budding yeast *Saccharomyces cerevisiae* or the prokaryote *Caulobacter crescentus*, and has been extensively studied in invertebrate model systems, such as the embryos of the worm *Caernorhabditis elegans* and the neuroblasts of the fruit fly *Drosophila melanogaster* (Fig. 2).
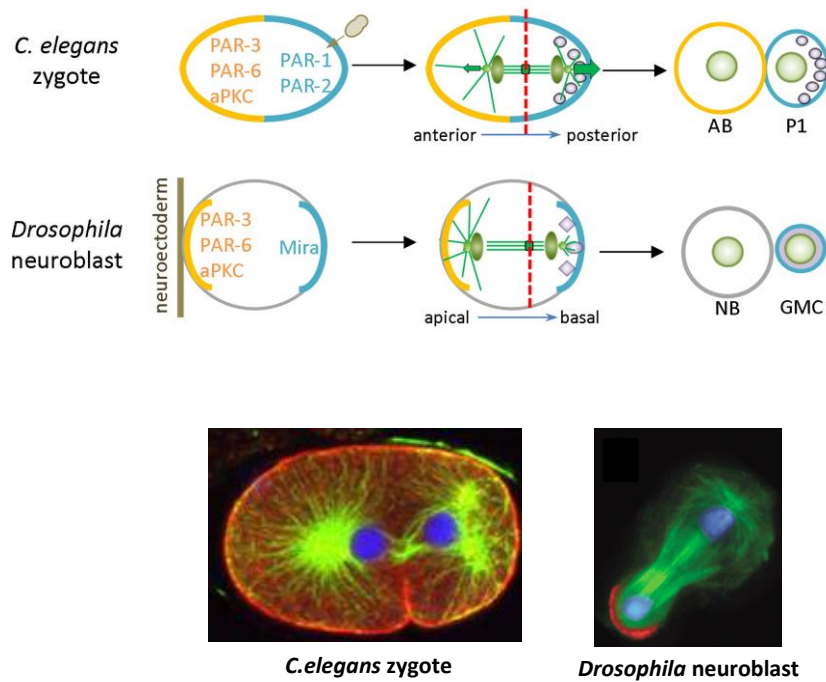

Figure 2 Asymmetric cell division in mitotic animal cells. *C.elegans* zygotes and *Drosophila* embryonic neuroblasts divide asymmetrically after establishment of cell polarity and proper position and orientation of the spindle (Adapted from Li R., 2013).

In mammals, the asymmetry of meiotic divisions is essential for the formation of a functional female gamete (Brunet and Verlhac, 2011). A rising interest towards asymmetric cell division derives from its relevance in stem cell biology, whereby a single stem cell produces two daughter cells and simultaneously directs their differential fate: one retains its stem cell identity while the other becomes specialized and loses stem cell properties (Mukherjee et al., 2014). Remarkably, impairment of asymmetric cell division in *Drosophila* neuronal stem cells induces a cancer-like state (Gateff, 1978; Humbert et al., 2003). This leads to interesting connections between defects in asymmetric cell division and the generation of a stem cell pool that loses control over growth and proliferation to form eternally proliferating deadly tumours (Barker et al. 2009).

Asymmetric outcomes of a cell division can be specified by two general mechanisms: asymmetric segregation of intrinsic fate determinants or asymmetric placement of daughter cells into microenvironments that provide extrinsic signals directing cells to different states (reviewed in Yamashita and Fuller, 2008).

During intrinsic asymmetric cell division, polarity factors are first concentrated to specific locations to define the poles of cell division, in

addition, the centrosomes become morphologically and functionally different to correctly respond to polarity cues (Yamashita et al., 2010). In eukaryotic cells ranging from bacteria to yeast to animal cells, GTPases of the Rho family are widely employed in regulating cell polarity (Schonegg et al., 2007; Jaffe et al., 2008). Several lines of evidence indicate that the localization of the GTP-bound active form of many GTPases in specific cortical domains of the cell activates downstream effectors that regulate intracellular structural reorganization (Craddock et al., 2012; Betschinger et al., 2003; Jaffe et al., 2008). Afterwards the spindle orients according to the polarity cues in order to segregate one set of chromosomes towards a given set of polarity determinants and the other away from it, thereby generating two unequal daughter cells (Tsou et al., 2003). Correct spindle positioning is therefore critical to preserve the right lineage of asymmetrically dividing cells. Accordingly, spindle mispositioning in asymmetrically dividing stem cells, which normally generate one daughter stem cell with self-renewal potential and one cell destined to differentiation, steers tumorigenesis by increasing the pool of undifferentiated stem cells (reviewed in Gonzales, 2007; reviewed in Siller and Doe, 2009). Surveillance mechanisms, or checkpoints, must therefore respond to spindle positioning errors and delay cell cycle

progression until the mitotic spindle is properly oriented with respect to the cell polarity axis (Caydasi et al., 2010; Yamashita et al., 2010).

The budding yeast *Saccharomyces cerevisiae* is a widely recognized model system to study asymmetric cell division. It divides asymmetrically by budding and generates a daughter cell smaller than the mother, which might be considered as a primitive stem cell because it undergoes many more rounds of cell division than the mother cell (reviewed in Yamashita and Fuller, 2008) (Fig.3).
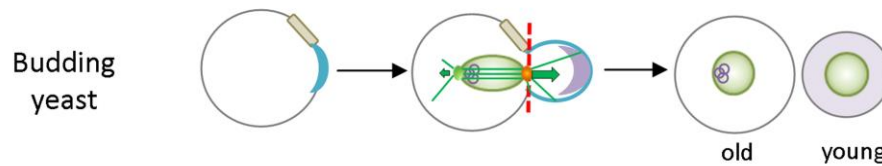
Figure 3 Asymmetric cell division in budding yeast *Saccharomyces cerevisiae.* In yeast, cell polarity and the predetermined division site control the positioning of the mitotic spindle (Adapted from Li R., 2013)

In budding yeast, the future site of cytokinesis is established in early G1 by the accumulation of determinants that define the site of bud emergence (bud neck) and stimulate the reorganization of the actin network to fuel polarized growth and transport into the bud (reviewed in

Moore and Cooper 2010). Continued polarized growth towards this site, coupled with the assembly of a non-expanding bud neck, leads to the enlargement of the bud (reviewed in Li, 2013). Afterwards, the mitotic spindle must elongate along the polarity axis of the cell in order to ensure accurate chromosome segregation between the mother and the daughter cell. Only after the spindle is properly positioned the two cells are separated by the process of cytokinesis at the bud neck (Fig.4).

Figure 4 Budding yeast cell cycle. Mitotic division of a single yeast cell: after DNA replication and SPB duplication (blue), a bipolar spindle (green) assembles between the two SPBs, embedded in the nuclear envelope (yellow). At the anaphase onset mitotic spindle elongates along the mother-bud axis, hence mitotic exit and cytokinesis can occur.
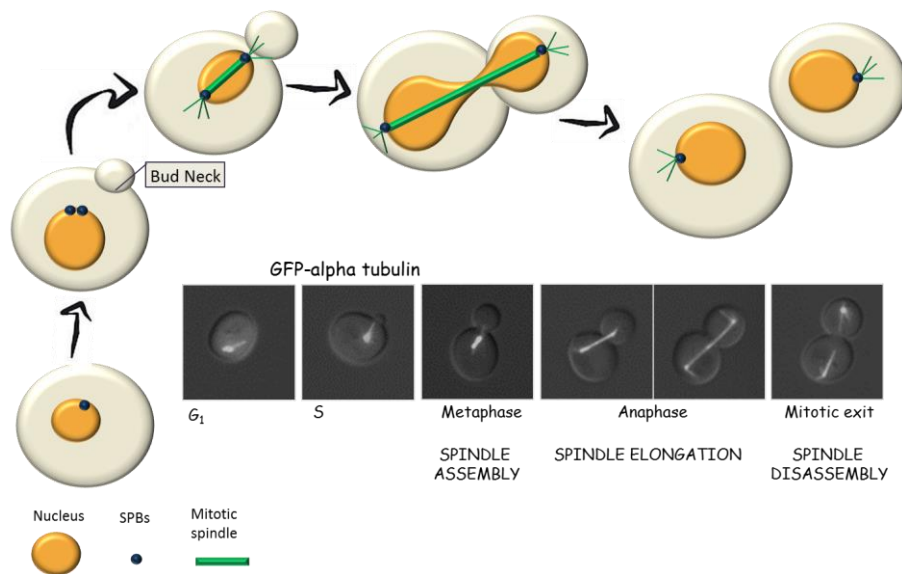
Unlike higher eukaryotic cells, yeast undergoes a close mitosis, without nuclear envelop breakdown. Therefore the position of the mitotic spindle corresponds to the nuclear position. The microtubule-organizing centers, named spindle pole bodies or SPBs (the equivalent of mammalian centrosomes) are multi-layered structures embedded in the nuclear envelope and thus structurally distinct from centrosomes (Araki et al., 2006). However, centrosomes and SPBs are functionally equivalent organelles in that both use a similar γ-tubulin-based mechanism for microtubules nucleation (Knop and Schiebel, 1997; Soltys and Borisy, 1985). SPBs orchestrate proper spindle positioning by regulating both intranuclear spindle assembly and elongation, as well as astral (or cytoplasmic) microtubules (cMTs) interactions with the cell cortex. Upon binding to the cortex, force applied by molecular motors to cytoplasmic microtubules is transmitted to the spindle, producing displacement of the latter along with the nucleus (Adames and Cooper, 2000).

Spindle positioning

The mitotic spindle is an elongated dynamic structure that ensures the separation of the two genomes during mitosis. It consists of three classes of microtubules (MTs) nucleated from the two spindle poles: (1) kinetochore MTs attach to the chromosomes to separate the two genomes at anaphase; (2) interpolar MTs form an antiparallel array between the spindle poles and are implicated in positioning the furrow at cytokinesis; (3) astral MTs dynamically anchor the mitotic spindle to the cortex and also participate in furrow positioning (reviewed in Glotzer, 2009; Tanaka, 2010).

In animal cells, spindle position determines the location of contractile ring assembly (Cao and Wand, 1996). Thus, placing a spindle in the centre of the cell will result in daughter cells of equal size. In symmetrically dividing human cells two mechanisms act co-ordinately to centre the spindle during anaphase: one directed by the microtubule-based motor dynein, the other by asymmetric plasma membrane elongation in response to spindle mispositioning. (Kiyomitsu and Cheeseman, 2013). Moreover, in human dividing cells, micro-environmental forces applied on the cell body induce a polarization of dynamic subcortical actin structures that

correlate with spindle movements and direct spindle orientation during mitosis (Fink et al., 2011).

Accurate positioning of spindles is essential for asymmetric cell divisions. The predominant model for spindle positioning in asymmetrically dividing systems involves attachment of the microtubule based motor dynein to the cortex, where it exerts a pulling force on astral microtubules that extend from the spindle poles to the cell cortex, thereby displacing the spindle. This model, termed "cortical pulling", has been extensively investigated in *C. elegans* and *Drosophila* models, whereas in cells of Chordata, Nematoda and Arthropoda phyla, where spindles have no astral microtubules, other mechanisms for spindle positioning must be at work (reviewed in McNally, 2013). In mouse oocytes, a vesicle-based mechanism of actin network modulation is also essential for asymmetric positioning of the meiotic spindle (Holubcová et al., 2013).

Spindle positioning in budding yeast requires either one of two redundant pathways, one that depends on the APC (Adenomatous Polyposis Coli)-related protein Kar9, and the other on dynein (Moore et al., 2008) (Fig.5). Either pathway is dispensable for cell viability, whereas inactivation of both is lethal (Miller and Rose 1998).
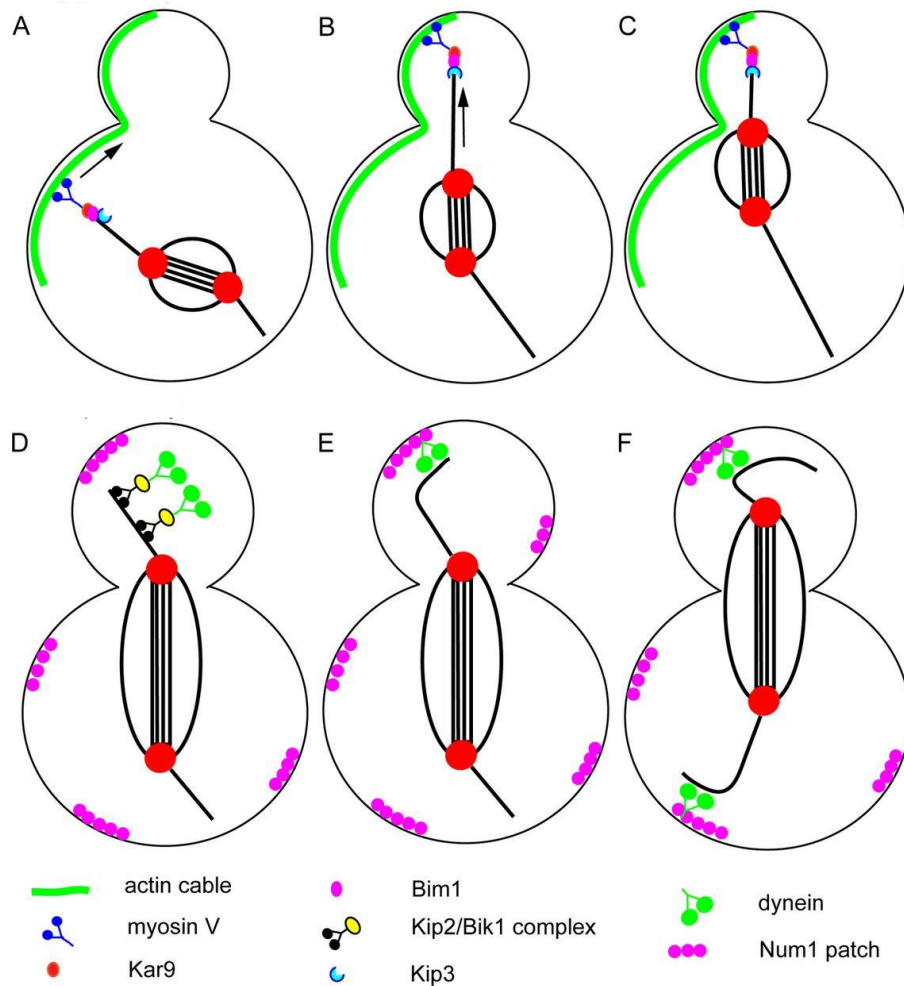
Figure 5 Spindle positioning in budding yeast. Schematic diagram of the two sequential spindle positioning pathways of budding yeast. In the Kar9 pathway **(A-C)** Myo2 transports the plus end of an astral microtubule towards the bud tip on a polarized actin cable. Once the plus end has reached the bud cortex, the plus‑end depolymerase Kip3 is activated to allow pulling of the spindle pole toward the bud neck. In the dynein pathway **(D-F)** the contact of dynein with the cortical protein Num1 allows dynein to pull the spindle toward the bud. (Adapted from McNally, 2013).

The Kar9 pathway acts mainly in metaphase and mediates the transport of microtubule ends along actin cables. Microtubule ends interact with Myo2, the myosin-V motor that walks along actin filaments via Kar9 and Bim1 (Lee et al., 2000). The translocation of Kar9 from the SPB to the cMT plus ends requires its interaction with the plus end-directed motor protein Kip2 and is important for proper function (Maekawa et al., 2003) One critical feature of Kar9 activity is its asymmetric localization to astral microtubules emanating from one of the two SPBs, the bud-oriented SPB. The selective recruitment of Kar9 to a specific set of microtubules ensures that only one end of the mitotic spindle is oriented towards the bud (Liakopoulos et al., 2003). The second pathway of spindle positioning acts predominantly in anaphase and is controlled by the minus end- directed motor dynein (Yeh et al., 1995). Bik1 and Kip2 target dynein to the plus end of cMTs where it probes its cortical receptor Num1 and gets activated. Dynein activation promotes its translocation towards the MT minus ends that slide along the cortex (reviewed in Moore and Cooper, 2010). These sliding events generate pulling and pushing forces for spindle movements that place the nucleus at the bud neck and orient the mitotic spindle with respect to the division axis.

The accuracy of spindle positioning requires the two poles of the mitotic spindle to become morphologically and functionally distinct from each other and to respond differently to polarity cues (Hotz et al., 2012). Observations in mammalian cultured cells suggest that structural differences between older and younger centrioles can be used to confer differential behaviour on mother and daughter centrosomes. In vertebrate cells, the mother centriole remains near the cell centre while the daughter migrates extensively throughout the cytoplasm (Piel et al., 2000). Differential behaviour of the two centrosomes during interphase appears to underlie the stereotyped orientation of the spindle in *Drosophila*, where the mother centrosome is normally segregated into the cell that maintains stem cell identity (Yamashita et al., 2007). Centrosome asymmetry has been indeed implicated in stem cell fate maintenance in both flies and vertebrates (Singh et al., 2014). Similarly, SPBs segregate non-randomly in budding yeast, such that the bud inherits normally the old SPB (Pereira et al., 2001) and asymmetric organization of astral microtubules stems from an outstanding structural asymmetry of the spindle pole bodies (Juanes et al., 2003). Differences between the mother and daughter spindle pole bodies appear to be used

in establishing the stereotyped orientation of the mitotic spindle and, therefore, successful cell division.

Mitotic exit and cytokinesis

Mitosis is the process by which a eukaryotic cell splits in two. The division of the cell involves a transient but profound reorganization to ensure the coordinated distribution of cellular material between the daughter cells (Hotz et al., 2014). Because the tiniest error in this process can have detrimental consequences for the cell, mitotic progression is tightly regulated.

The cell cycle control machinery is conserved from yeast to human and centered on cyclin-dependent kinases (CDKs). The activity of CDKs depends on the phosphorylation on a conserved threonine by CDK-activating kinase (CAK) (Tassan et al., 1994). The most prominent mitotic kinase is Cdk1 (Cdc28 in budding yeast) that mediates entry into mitosis through the interaction with its partners, cyclins. Cdk1 is a protein ubiquitously expressed throughout the cell cycle and its activity is controlled directly by phosphorylation and indirectly through proteolysis of its cyclin binding partners (Noton and Diffley, 2000; Lowe et al., 1998). Activatory phosphorylations of Cdk1/cyclin complexes by Polo-like kinases, Aurora-kinases and NIMA-related kinases lead to centrosome maturation and separation, bipolar spindle formation, nuclear envelope breakdown and chromatin condensation (Eckerdt and Strebhardt, 2006;

Osmani et al., 1991; Hannak et al., 2001; Crosio et al., 2002), whereas inhibitory phosphorylations by the Wee1-like kinases and checkpoint kinases restrain mitotic entry during the normal cell cycle (Wee1), in response to DNA damage (Wee1, Chk1 and Chk2) or spindle assembly errors (Bub-related kinases) (Yeh et al., 2009; Abrieu et al., 2001; Lampson and Kapoor, 2005)

While mitotic entry is triggered by Cdk-dependent phosphorylation of mitotic substrates, mitotic exit starts with the inactivation of Cdk1 and the dephosphorylation of its targets. The protein phosphatase 2A (PP2A) together with its B55 regulatory subunit is a major activity dephosphorylating Cdk1 targets in most eukaryotic cells (Baro et al., 2012; Wang et al., 2014). As a consequence, the mitotic spindle breaks down, chromosomes decondense, and cytokinesis can occur. Although little is known about how mitotic exit is triggered in most systems, studies in yeast achieved an unprecedented understanding of the regulatory circuits that control this phase of the cell cycle and drive the ordered events of cell division and separation (reviewed in Weiss, 2012). In the budding yeast *Saccharomyces cerevisiae* mitotic exit is controlled by the protein phosphatase Cdc14, which dephosphorylates CDK substrates, turns on cyclin proteolysis and activates the cyclin B-CDK inhibitor Sic1

(Visintin et al, 1998). Cdc14 is highly conserved, although in many organisms its orthologues are not essential for mitotic exit (reviewed in Mocciaro and Schiebel, 2010). Yeast cells lacking Cdc14 function arrest division in telophase, with chromosome masses segregated between mother and daughter cells by a fully elongated mitotic spindle (Grandin et al., 1998; Luca et al., 2001). Because of its key function in mitotic exit, Cdc14 activity is tightly regulated. Premature Cdc14 activation is prevented by its reclusion in the nucleolus through tight binding to the Net1/Cfi1 inhibitor throughout most of the cell cycle (Visintin et al., 1999; Shou et al., 2002). Cdc14 is partially released into the nucleoplasm at the metaphase to anaphase transition by the FEAR (Cdc fourteen early anaphase release) pathway, whereas the MEN (mitotic exit network) drives its full release also into the cytoplasm later in anaphase, thus allowing it to dephosphorylate its targets (Fig. 6). While the FEAR is dispensable for mitotic exit, the MEN is absolutely required for this process (Stegmeier et al., 2002).
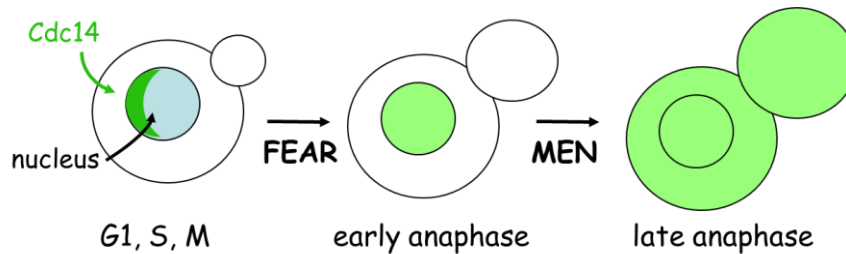
Figure 6 FEAR and MEN. Cdc14 is sequestered in the nucleolus during a large window of the cell cycle, it is partially released into the nucleoplasm at the metaphase to anaphase transition by the FEAR pathway, whereas the MEN drives its full release also into the cytoplasm later in anaphase

The Polo-like kinase Cdc5 controls both FEAR and MEN pathways and increases the activity of Cdc14, playing a role that is not yet fully understood (reviewed in Weiss 2012). The phosphatase PP2A associated with its regulatory subunit Cdc55 is critical to retain Cdc14 inside the nucleolus (Queralt et al., 2006), by counteracting CDK-mediated phosphorylation of Net1 (Kerr et al., 2011). The proteins Zds1 and 2 associate with PP2A^{Cdc55} (Queralt et al., 2008; Wicky et al., 2011) and regulate the nuclear pool of this phosphatase (Calabria et al., 2012). Upon inhibition of PP2A^{Cdc55} the FEAR pathway gets activated and Esp1 triggers the release of Cdc14 by promoting CDK phosphorylation of Net1 (Queralt et al., 2006; Sullivan and Uhlmann 2003; Azzam et al., 2004). The Esp1-associated protein Slk19 and the redundant Spo12 and Bns1

proteins are necessary for optimal Cdc14 early release (Visintin et al., 2003). The FEAR-mediated activation of Cdc14 in anaphase is thought to regulate spindle dynamics and to contribute to timely activation of the MEN (Stegmeier et al., 2002; Havens et al., 2010). However, consistent with its non-essential nature, FEAR-driven Cdc14 release cannot drive full exit from mitosis.

Complete mitotic exit requires the MEN, which promotes robust relocalization of Cdc14 in the cytoplasm, leading to full dephosphorylation of CDK substrates (Visintin et al., 1998; Jaspersen et al., 1998). MEN is a protein kinase cascade triggered by the small G protein Tem1 and includes Cdc15 (direct target of Tem1) and the Mob1/Dbf2 kinase complex (Fig. 7).
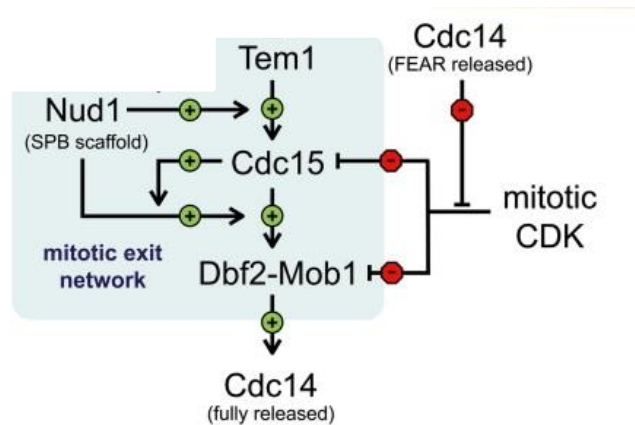
Figure 7 The logic of the MEN (Adapted from Weiss, 2012) Tem1 triggers the MEN cascade by promoting SPB recruitment of Cdc15 kinase, which activates Dbf2-Mob1 at the SPBs. Dbf2-Mob1 promotes the full release of Cdc14 from the nucleolus into the cytoplasm. Fully released Cdc14 inactivates the mitotic cyclin/Cdk and reverses the Cdk-dependent phosphorylation of several Cdk substrates, including Cdc15 and Mob1, thereby fueling MEN activation and triggering mitotic exit (Visintin et al, 1998; Stegmeier and Amon, 2004).

During mitosis most MEN components are localized to the SPBs. Localization at the spindle poles is critical for the system's activation in response to proper spindle position and is mainly accomplished at the cytoplasmic face of the SPBs through association to the SPB scaffold Nud1 (Gruneberg et al., 2000; Luca et al., 2001; Rock and Amon 2011). Nud1 connects the γ-tubulin binding protein Spc72 to the SPB outer plaque and is thus an important anchor for cytoplasmic microtubules (Pereira et al., 1999; Gruneberg et al., 2000).

31

The G protein Tem1 appears to be the first MEN component loaded onto Nud1 at the SPB (Visintin and Amon, 2001; Valerio-Santiago and Monje-Casas, 2011) and its recruitment promotes Cdc15 loading to SPBs and activation. Once activated, Cdc15 first phosphorylates the scaffold Nud1. This creates a phospho-docking site on Nud1, to which the effector kinase complex Dbf2-Mob1 binds in order to be activated by Cdc15, translocate to the nucleus and trigger Cdc14 release (Rock et al., 2013). Both Tem1 localization at SPBs and its nucleotide state are important for MEN control. A dimeric complex made of Bub2 and Bfa1 has GTPase-activating protein (GAP) activity and promotes the GDP-bound inactive form of Tem1, thereby preventing premature exit from mitosis or aberrant mitosis in case of spindle misposition (Geymonat et al., 2002; Fraschini et al., 2006). Bub2 and Bfa1 form a heterotrimeric complex with Tem1, where Bub2 carries the GAP activity and Bfa1 mediates the interaction between Bub2 and Tem1 (Ro et al., 2002; Geymonat et al., 2002). Furthermore Bfa1 behaves as a guanine nucleotide dissociation inhibitor (GDI), stabilizing Tem1 binding to GTP/GDP (Geymonat et al., 2002; Fraschini et al., 2006: Geymonat et al., 2009).

The polo kinase Cdc5 inactivates Bub2/Bfa1 by directly phosphorylating Bfa1 and thereby positively regulates the MEN (Hu et al., 2001, Kim et

al., 2012). Additionally, several polarity proteins, such as the PAK kinases Ste20 and Cla4, also participate to MEN regulation (Höfken and Schiebel, 2002; Seshan et al., 2002; Chiroli et al., 2003).

A similarly organized pathway, the Septation Initiation Network (SIN), promotes cytokinesis in fission yeast (Furge et al., 1998; Fankhauser and Simanis, 1994), but is not required for mitotic exit in this organism.

Several observations indicate that Tem1 activation is necessary but not sufficient to promote mitotic exit. Indeed, covalent tethering of Tem1 to SPBs promotes its activation and increases Cdc15 levels at spindle poles, but does not promote premature mitotic exit (Valerio-Santiago and Monje-Casas, 2011). Similarly, fusion of Cdc15 to the SPBs leads to premature activation of the Dbf2 kinase, but not premature mitotic exit (Rock and Amon, 2011).

Although the prevailing MEN function is closely coupled with the final stages of mitosis, recent observations MEN components also have important functions earlier on during the cell cycle. These include a role in orienting the mitotic spindle in metaphase (Hotz et al., 2012) and in stabilizing early mitotic transcripts, such as *CLB2* and *SWI5* (Trcek et al., 2011). Moreover Tem1 plays a critical role in the latest stage of cell division by regulating the timing of cytokinesis (Lippincott et al., 2001).

This suggests that MEN components have different functions in different cell cycle stages. Because several MEN (and SIN) components can also be found in higher eukaryotic systems, from plants to human, similar pathways might also exist in multicellular eukaryotes to survey the correct pattern of asymmetric cell division during development (reviewed in Bedhomme et al., 2008).

Once mitotic exit has been completed, cytokinesis can occur. Cytokinesis is the complex process that mediates the physical separation of dividing cells after chromosome segregation. In animal cells, a contractile ring, composed of actin and myosin filaments, forms a cleavage furrow midway between the spindle poles (Maupin and Pollard, 1986; Dechant and Glotzer, 2003; reviewed in Mierzwa and Gerlich, 2014) (Fig. 9).
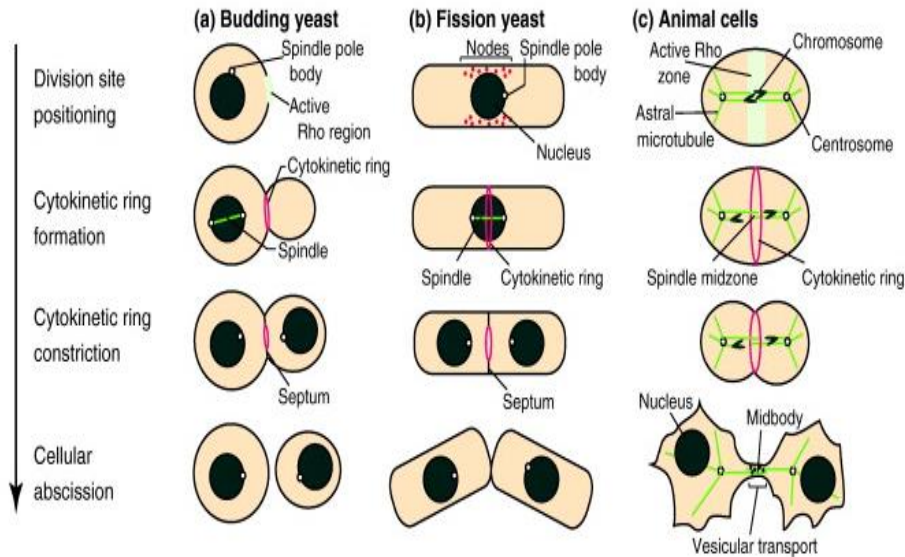
Figure 9 Schematic representations of the process of cytokinesis in (a) the budding yeast *S. cerevisiae*, (b) the fission yeast *S. pombe* and (c) animal cells. Examples of cells at individual stages of cytokinesis are presented, with progression through the cell cycle oriented downward. In budding yeast and animal cells, the cytokinetic apparatus is positioned and assembled from an active Rho region (Bohnert and Gould, 2011)

The positioning of the cleavage furrow involves continuous communication between the anaphase spindle and the cell cortex. The small GTPase RhoA accumulates at the equatorial cell cortex and promotes assembly and contraction of the actomyosin ring (Bement et al., 2005). Similarly, in budding yeast the contraction of an actomyosin ring at the bud neck, although not essential, facilitates the physical

scission of mother and daughter cells (Bi et al., 1998). The GTPase Rho1, i.e. the counterpart of mammalian RhoA, becomes concentrated at the bud neck during late mitosis and, similar to RhoA, promotes ring assembly and contraction (Yoshida et al., 2006). Septins, which belong to a family of conserved GTP-binding proteins, play a critical role in cytokinesis. Whereas little is known about the mechanism in higher eukaryotes, in budding yeast they act as a scaffold that tethers cytokinetic components (Lee et al., 2002). In *S. cerevisiae* and *Candida* septins polymerize into filaments that assemble as a ring at the bud neck.

Regulation of spindle position by MEN components

As mentioned above, although MEN function in the final stage of mitosis is certainly the most prominent, recent studies suggest that MEN is active also early in mitosis, being involved in spindle positioning during metaphase and in establishing Kar9 asymmetry (Hotz et al., 2012) (Fig.8). In wild type cells, the spindle positioning protein Kar9 accumulates asymmetrically, localizing specifically to astral microtubules emanating from the old spindle pole body (SPB) and driving its segregation to the bud (Leisner et al., 2008). Upon MEN impairment, by inactivation of Nud1, Tem1, Cdc15, Dbf2, or its paralog Dbf20 function, Kar9 fails to localize to only one SPB's aster microtubules in early mitosis (Hotz et al., 2012).
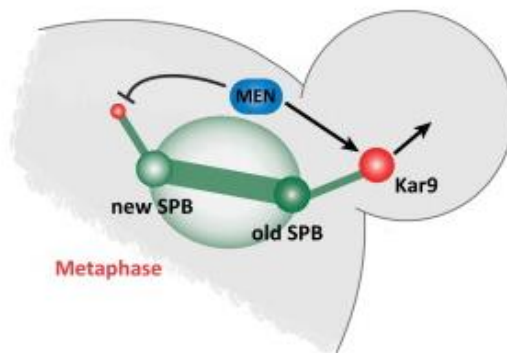

Figure 8 The MEN promotes specification of spindle pole body (SPB) fate and the asymmetric accumulation of Kar9 with respect to old and new SPBs in metaphase (Adapted from Hotz and Barral, 2014)

Recent studies have shed light on the regulation of Kar9 asymmetry (Liakopoulos et al., 2003; Moore et al., 2006; Moore and Miller, 2007; Leisner et al., 2008; Meednu et al., 2008; Kammerer et al., 2010; Cepeda-Garcıa et al., 2010). Interestingly direct phosphorylation by Dbf2 and Dbf20 is required for Kar9 asymmetry in metaphase (Hotz et al., 2012), and other posttranslational modifications of Kar9 protein might also contribute to its asymmetric distribution. Nevertheless, it remains unclear how SPB identity is specified and how Kar9 asymmetry is directed toward the old SPB (reviewed in Hotz and Barral, 2014).

Cells lacking Kar9 align their spindles with the mother-bud axis in early anaphase in a dynein-dependent manner (Adames and Cooper, 2000; Carminati and Stearns, 1997; Grava et al., 2006), because the Kar9- and dynein-dependent pathways can compensate for the absence of the other (Miller and Rose, 1998). However, only the Kar9 pathway specifies SPB inheritance (Pereira et al., 2001; Moore et al., 2006). Therefore, upon MEN inactivation, inheritance of old and new SPB between mother and daughter cell is randomized as a consequence of Kar9 symmetric distribution at spindle poles (Hotz et al., 2012). Nud1 specifies the identity of SPBs, leading to the stabilization of Kar9 asymmetry toward the old one. MEN-dependent phosphorylation of Kar9 mediates this

stabilization (Hotz et al., 2012). Surprisingly, the downstream MEN phosphatase Cdc14 does not participate to this newly discovered function of the MEN, as *cdc14-1* mutant cells aligned properly their metaphase spindles and show a canonical asymmetric distribution of Kar9. Deletion of *LTE1* and *KIN4*, which both act upstream of MEN (see below), also has no effect on spindle positioning and Kar9 localization. Taken together, these data indicate that the SPB component Nud1 and the MEN proteins Tem1, Cdc15, and Dbf2/20 contribute to the control of Kar9 distribution and metaphase spindle position under a regulatory network different than the one regulating MEN components for mitotic exit (Hotz et al., 2012).

Mitotic Checkpoints

To ensure that cell cycle events occur in the correct order, eukaryotes have developed surveillance mechanisms, named checkpoints, which control the order and timing of cell cycle transitions (reviewed in Hartwell and Weinert 1989). Cell cycle checkpoints ensure that critical events such as DNA replication and chromosome segregation are completed with high fidelity. They respond to various errors in critical cell cycle processes by transiently arresting cell cycle progression and providing time for error correction. Checkpoint loss results in genomic instability and has been implicated in the evolution of normal cells into cancer cells (reviewed in Elledge 1996). Due to the conservation of the cell cycle regulatory machinery among all eukaryotes, many components of the checkpoints have homologues within the taxon. Therefore, insights of the molecular mechanism governing the checkpoints came to a great extent from studies on yeast. The Spindle Assembly Checkpoint (SAC) monitors the sister chromatid tension/attachment to the mitotic spindle via a specialized chromatid structure called kinetochore. It is sufficient that a single kinetochore is not properly attached to the spindle to trigger SAC-mediated cell cycle arrest (Chen et al., 1996;; Pangilinan and Spencer, 1996; Farr and Hoyt, 1998). As a consequence, SAC prevents

40

chromosome missegregation (Dobles et al., 2000; reviewed in Musacchio and Salmon, 2007) (Fig10A). Multiple proteins, such as the Mps1 and Bub1 kinases or Mad1 and Mad2 proteins, are required for the correct function of the SAC. Upon treatment with nocodazole, a drug that depolymerises microtubules, wild type yeast cells arrest in mitosis as large budded cells, whereas SAC mutants fail to block the cell cycle progression and undergo aberrant mitosis (Li and Murray, 1991; Wang and Burke, 1995).

During asymmetric cell division, the mitotic spindle must be correctly aligned with respect to the polarity axis in order to ensure accurate chromosome segregation. Spindle positioning errors in budding yeast are monitored by a surveillance mechanism, referred to as spindle position checkpoint (SPOC), that delays mitotic exit and cytokinesis to provide the time for proper spindle realignment (reviewed in Caydasi and Pereira, 2012) (Fig.10B). Experimental evidence suggests that pathways similar to the SPOC might control cell cycle progression in response to spindle mispositioning in other asymmetrically dividing eukaryotic cells (Cheng et al., 2008).
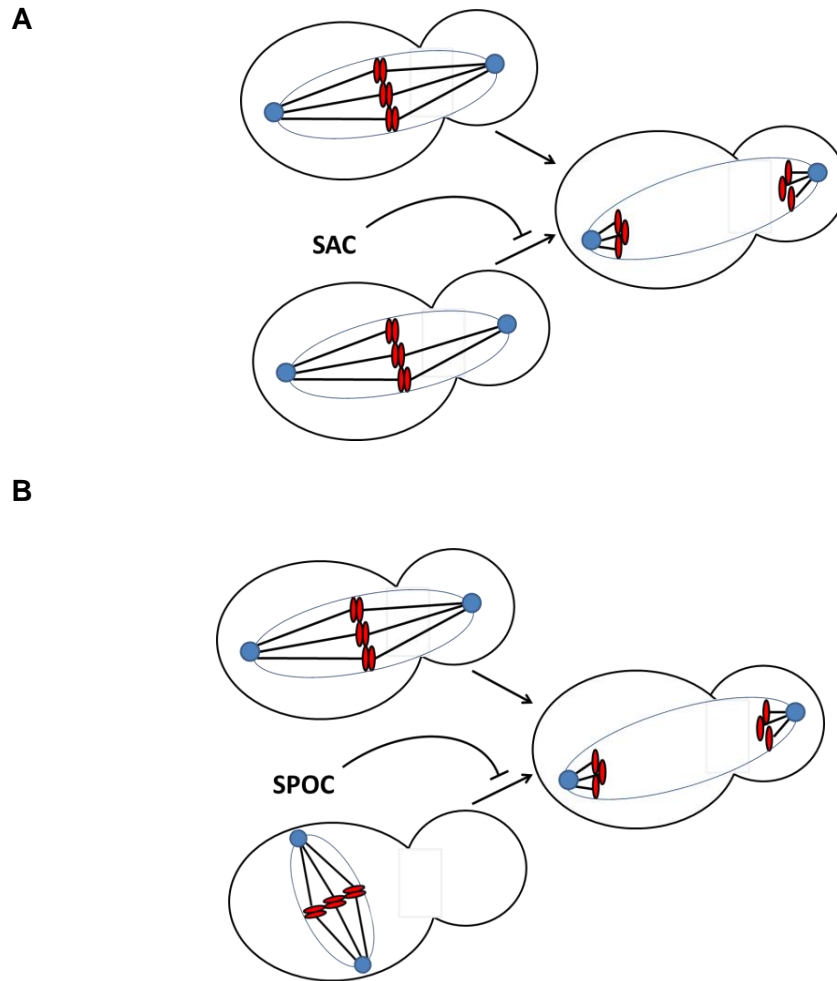
Figure 10 (A) Spindle Assembly Checkpoint (SAC) The mitotic spindle segregates chromosomes to opposite poles. Correct bipolar attachment of chromosomes to the spindle is monitored by the SAC. **(B) Spindle Position Checkpoint.** In a normal situation, spindle elongation delivers one spindle pole to the bud and the other to the mother, leading to mitotic exit and cytokinesis. In cells that fail to position properly the spindle, anaphase spindle elongation occurs within the mother cells and mitotic exit is delayed by the SPOC.

The first evidence for a pathway that may act as an inhibitor of mitotic exit in budding yeast came from studies on mutants lacking dynein heavy chain (*dyn1*, Yeh et al., 1995). In these cells anaphase takes place within the mother with quite high frequency, suggesting that spindle mispositioning does not prevent the onset of anaphase. Nonetheless, these mutants inhibit cell division until spindle movements eventually deliver one spindle pole with the associated chromosomes into the bud. Since then, several studies elucidated the molecular mechanisms of SPOC operation in *Saccharomyces cerevisiae*. They are described in detail in the next chapter.

Controlling mitotic exit and cytokinesis in yeast: the Spindle Position Checkpoint

The Mitotic Exit Network is the target of a signaling mechanism named spindle position checkpoint (or SPOC), that blocks mitotic exit when the spindle is not properly oriented, in order to ensure the inheritance of a complete set of chromosomes to both mother and daughter cells. SPOC-mediated inhibition of the MEN prevents the formation of aneuploid or polyploid cells after cytokinesis (reviewed in Bardin and Amon, 2001; Piatti et al., 2006). The target of the SPOC is a small GTPase called Tem1, which acts as molecular switch for the activation of the MEN kinase cascade. As mentioned above, the MEN effector of Tem1 is the kinase Cdc15, which in turn promotes the activation of the downstream Mob1/Dbf2 kinase complex that ultimately leads to activation of the Cdc14 phosphatase (reviewed in Stegmeier et al., 2004). Upon spindle misalignment the two-component GTPase-activating protein (GAP) Bub2/Bfa1 inactivates Tem1 by stimulating GTP hydrolysis (Fraschini et al., 2006; Geymonat et al., 2002). The Kin4 protein kinase is a key component of the SPOC (Pereira and Schiebel, 2005). During spindle misalignment Kin4 phosphorylates Bfa1, thereby preventing the inhibitory phosphorylation of the GAP Bub2/Bfa1 by the

polo kinase Cdc5 (D'Aquino et al., 2005; Pereira and Schiebel, 2005) (Fig.11)
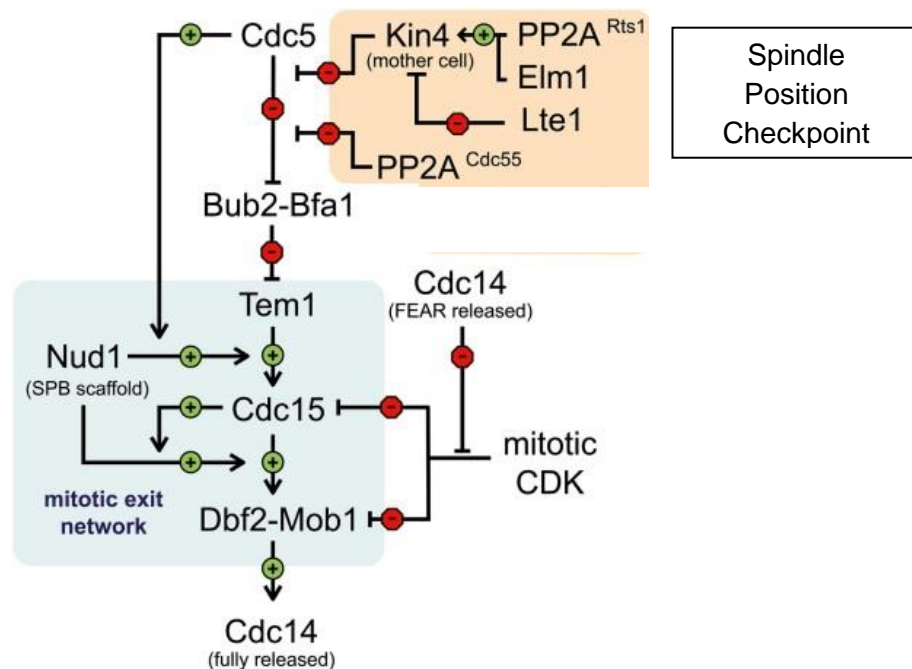
Figure 11 Spindle position checkpoint (SPOC) (Adapted from Weiss, 2012) Misalignment of the mitotic spindle activates Bfa1-Bub2 via Kin4, hence Tem1 is inhibited. Phosphorylation by the protein kinase Elm1 is essential for Kin4 catalytic activity (Caydasi et al, 2010; Moore et al, 2010). Rts1 regulatory subunit of the protein phosphatase 2A (PP2A), provides proper Kin4 localization at the SPBs and at the mother cell cortex by promoting Kin4 dephosphorylation (Chan and Amon, 2009; Caydasi et al, 2010). Daughter-specific protein Lte1 inactivates Kin4 and excludes it from the dSPB during an unperturbed anaphase (Falk et al, 2011).

During the unperturbed cell cycle Kin4 is strategically restricted to the mother cell compartment, where it is thought to sense the anomalous persistence of both SPBs in anaphase. In addition, it is present on both SPBs of misaligned spindles (D'Aquino et al., 2005; Pereira and Schiebel, 2005). Bud-residing protein Lte1 promotes mitotic exit by controlling the localization of the kinase Kin4. Lte1 physically interacts with Kin4 and excludes it from the bud (Bertazzi et al 2011; Falk et al., 2011). At low temperature deletion of *LTE1* is lethal (Shirayama et al., 1994; Pereira and Schiebel, 2005), in this condition mitotic exit is blocked and cells arrest in anaphase with an abnormal presence of Kin4 in the dSPB of a high percentage of cells (Bertazzi et al., 2011; Falk et al., 2011). The Elm1 kinase and the Rts1 regulatory subunit of the protein phosphatase 2A (PP2A) contribute to the SPOC by controlling Kin4 activity (Caydasi et al., 2010; Moore et al., 2010; Chan and Amon, 2009). The function of PP2A^{Rts1} consists in the regulation of the phosphorylation status of Kin4 and promoting its localization to the mother cortex and the SPBs (Chan and Amon, 2009), whereas Elm1 phosphorylates Kin4 on T209 and is required for Kin4 catalytic activity (Caydasi et al., 2010; Moore et al., 2010). Localization of MEN and SPOC proteins to the SPBs

changes during the cell cycle, in that some proteins (like Cdc15, Mob1 and Dbf2) are loaded on both SPBs at the anaphase onset, whereas other proteins (like Tem1, Bfa1 and Bub2) are present on both SPBs already in metaphase and their localization becomes much more asymmetric in anaphase, when they preferentially accumulate on the bud-directed SPB (Monje-Casas et al., 2009; Caydasi et al., 2009). Interestingly, the position of the spindle seems to play a role in controlling the asymmetric localization of Tem1, Bub2 and Bfa1 in anaphase. Indeed, these proteins localize less strongly but more symmetrically on the two SPBs when a misoriented spindle elongates within the mother cell and the SPOC turns on (Caydasi et al., 2009; Molk et al., 2004; Pereira et al., 2000). Whether the asymmetric localization of Tem1 or its GAP is important for triggering MEN signalling remains to be elucidated. Remarkably, the SIN counterparts of several MEN components also localize asymmetrically on SPBs during anaphase, with the homologs of the GAP components Bub2 (Cdc16) and Bfa1 (Byr4) occupying one SPB, while the GTP-bound form of the GTPase Spg1 and its effector kinase Cdc7 occupy the other (Cerutti et al., 1999; Li et al., 2000). SIN asymmetry has been proposed to be crucial for timely cytokinesis, as *cdc16* and *byr4* mutants where Spg1 and Cdc7 are symmetric in

47

anaphase undergo multiple rounds of septation (Li et al., 2000; Sohrmann et al., 1998).

Kin4 was found to increase the turnover of the Bub2/Bfa1 complex at SPBs (Caydasi and Pereira, 2009). However, Kin4 alone is unable to break Bfa1 symmetry at yeast centrosomes. Instead, phosphorylation of Bfa1 by Kin4 creates a docking site on Bfa1 for the 14-3-3 family protein Bmh1, which in turn weakens Bfa1-centrosome association and promotes symmetric Bfa1 localization when the SPOC is turned on (Caydasi et al., 2014).

Regulation of Tem1

Considering the importance of the Tem1 GTPase in activation of the MEN pathway, spindle positioning and cytokinesis, it is crucial for yeast cells to finely regulate Tem1 activity. Like all GTPases, Tem1 is active when bound to GTP and inactive in its GDP-bound form (Fig. 12).

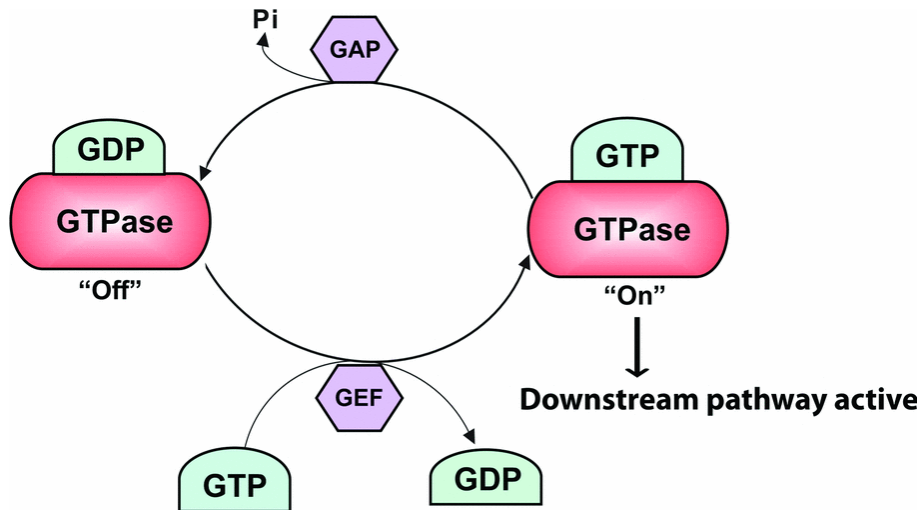**Figure 12 GTPase cycle.** GTPases cycle between the inactive 'off' GDP-bound state and the active 'on' GTP-bound state. The inactive state occurs by stimulation of intrinsic GTPase hydrolysis activity by GAPs. Activation is facilitated by GEFs to load GTP and dissociate GDP, allowing interaction with downstream effectors and in turn activation of downstream signalling pathways (Xiong et al., 2012).

The common element of the GTPase superfamily is the 160-180 residue G domain involved in nucleotide binding (reviewed in Bourne et al., 1990). Within the G domain two flexible "switch regions", referred to as Switch I and II undergo the most dramatic structural rearrangement upon GTP hydrolysis and therefore define the major conformational changes conferred by GTP versus GDP binding (reviewed in Vetter et al., 2001). On the basis of sequence alignment with human Ras, Switch I and II in Tem1 correspond to residues 50-55 and 77-84, respectively.

Upon spindle misalignment the two-component GTPase-activating protein (GAP) Bub2/Bfa1 inactivates Tem1 by stimulating GTP hydrolysis (Fraschini et al., 2006; Geymonat et al., 2002). GTPase-activating proteins accelerate GTP hydrolysis, promoting the GDP-bound inactive form of GTPases (reviewed in Bourne et al., 1991; and Schweins et al., 1994). The GAP activity of the Bub2/Bfa1 complex resides on Bub2, which carries a TBC domain (Tre-2, Bub2 and Cdc16; (reviewed in Neuwald et al., 1997), whereas Bfa1 mediates Bub2 interaction with Tem1 and prevents Tem1 dissociation from guanine nucleotides, thereby acting as GDI (guanine-nucleotide dissociation inhibitor) (Fraschini et al., 2006; Geymonat et al., 2009; Geymonat et al., 2002; Ro et al., 2002).

Often, the release of GDP from GTPases is a slow and thermodynamically unfavourable reaction. This is why GTPase activation requires in most cases the intervention of nucleotide exchange factors (GEFs) that catalyse the release of GDP, promoting its replacement by GTP (reviewed in Bourne et al., 1991). The identity of the GEF(s) for Tem1, if any, remains elusive. The early proposal based on genetic data that the Lte1 protein might be the GEF for Tem1, has not been confirmed by biochemical assays (Geymonat et al., 2009). Therefore, if inactivation of a GEF for Tem1 could play any role in the SPOC, besides Tem1 inhibition by the GAP Bub2/Bfa1, remains to be established.

Beside its nucleotide state, Tem1 activity also depends on its localization. Tem1 loading onto the SPBs is an essential step to trigger the mitotic exit cascade (Valerio-Santiago and Monje-Casas, 2011). Furthermore, the daughter cell-specific protein Amn1 that physically interacts with Tem1 (Wang et al., 2003) competes with Cdc15 for binding Tem1 both *in vitro* and *in vivo,* hence inhibiting the MEN pathway.

The function of Tem1 could also be regulated by post-translational modifications. This kind of regulation, such as phosphorylation and ubiquitylation is wide spread in nature. Indeed, SDS-electrophoresis

shows that Tem1 migrates as a doublet (Ro et al., 2002; Wang and Ng,

2006), but this modification is not cell cycle-dependent.

Spatial distribution of MEN and SPOC components

As already mentioned, several components of MEN and SPOC are localized to SPBs via Nud1 (reviewed in Fraschini et al., 2008; Caydasi et al., 2010). With the exception of the Tem1 GTPase, the downstream MEN effectors are diffused in the cytoplasm throughout most of the cell cycle and become recruited to the SPBs mostly after anaphase onset (Menssen et al., 2001; Visintin et al., 2001). The SPOC regulators Bub2 and Bfa1 are loaded to SPBs already in metaphase, like Tem1.

Interestingly, the distribution of Tem1 and its inhibitors Bub2/Bfa1 changes during the cell cycle. In metaphase, these proteins localize only partially asymmetrically to the SPBs (Fig. 13) (Molk et al., 2004; Pereira et al., 2000; Monje-Casas and Amon, 2009; Valerio-Santiago and Monje-Casas, 2011). Both Bub2 and Bfa1 are necessary for Tem1 recruitment to the SPBs throughout most of the cell cycle, whereas in late mitosis Tem1 can bind to SPBs independently of the Bub2/Bfa1 complex (Pereira et al., 2000). The Kin4 protein kinase keeps the GAP complex in the active state by preventing the inhibitory phosphorylation of Bfa1 by Cdc5, thus behaving as a MEN inhibitor (Hu et al., 2001; D'Aquino et al., 2005; Pereira and Shiebel, 2005; Maekawa et al., 2007).

Figure 13 Schematic representation of localization patterns of MEN and SPOC components. Localization of MEN and SPOC components changes throughout the cell cycle

Kin4 localizes to the mother cell cortex and during anaphase also to the SPB remaining in the mother cell, whereas the MEN activator Lte1 localizes to the bud (Chan and Amon, 2010). As the mitotic spindle elongates during anaphase, the distribution of Tem1 and Bub2/Bfa1 changes. Now the proteins are strongly asymmetrically bound to the SPB that enters the bud, thus escaping from the Kin4 inhibitory zone and entering the compartment where Lte1 resides (reviewed in Caydasi et al., 2010). The migration of the SPB carrying Tem1 into the bud, is probably what triggers MEN activation and leads to mitotic exit and cytokinesis

(Caydasi et al., 2009). Upon activation, Tem1 starts recruiting Cdc15 and Dbf2/Mob1 to the SPBs.

It should be emphasized that whereas the Bub2/Bfa1 complex seems to completely disappear from the mother-bound SPB in anaphase, Tem1 remains in low amounts on this SPB (Pereira et al., 2000; Bardin et al., 2000; Molk et al., 2004). In addition, while the majority of Tem1 binds to SPBs through its interaction with Bub2/Bfa1, a relatively small pool of Tem1 binds symmetrically to both SPBs in a GAP-independent manner (Pereira et al., 2002; Valerio-Santiago and Monje-Casas, 2011). Time-lapse analysis of Tem1-GFP in cells with the double deletion of *BUB2* and *BFA1* showed that this GAP-independent pool of Tem1 does not change in levels from metaphase until mid-anaphase. In contrast, a prominent increase in the levels of Bub2/Bfa1-independent loading of Tem1-GFP on SPBs is observed after spindle disassembly, suggesting that it is not required for mitotic exit (Caydasi et al., 2009). Up to date, the exact role of the GAP-independent Tem1 fraction is not ascertained.

SPOC activation leads to changes in the localization pattern of its players (Fig.14). Tem1 and its regulators Bub2/Bfa1 that normally localize to the bud-directed SPB (referred to as dSPB, as opposed to the mSPB that stays in the mother cell) during anaphase, are symmetrically distributed

on both spindle poles upon spindle misalignment, albeit at reduced levels in comparison to the dSPB during normal mitosis (Pereira et al., 2000).

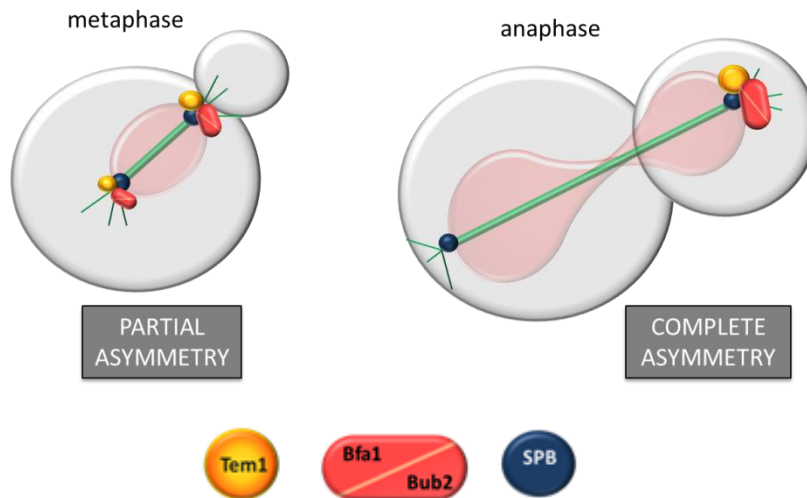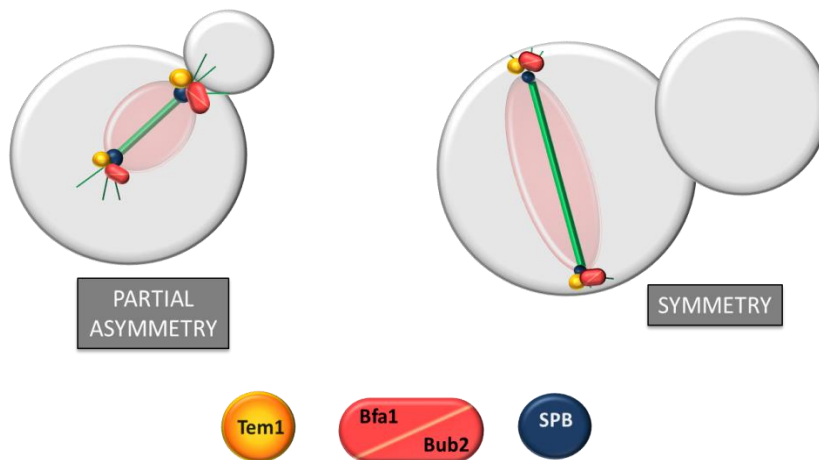**Figure 14 Schematic representation of localization patterns of MEN and SPOC components.** Localization of MEN and SPOC components changes upon spindle mispositioning and SPOC activation.

This change in the protein localization is crucial for the SPOC function and is mediated by Kin4 (Caydasi and Pereira, 2009). As already mentioned, Kin4 localizes to the mother cortex throughout the cell cycle (shortly also to the mSPB in mid-anaphase) but in cells with mispositioned spindles the kinase associates with both SPBs, where it

phosphorylates and activates the GAP Bub2/Bfa1, thereby inhibiting the MEN (Maekawa et al., 2007). In contrast, localization of Cdc5 (GAP inhibitor) to the spindle poles does not change upon spindle mispositioning (Maekawa et al., 2007).

When the SPOC is turned on, Kin4 activates the GAP by phosphorylating Bfa1 on serines S150 and S180 (Maekawa et al., 2007). FRAP measurements showed that this event promotes the rapid turnover of the GAP at both SPBs (Caydasi and Pereira, 2009). Since Tem1 association with SPBs is highly dynamic in the presence of Bub2/Bfa1, the levels of Tem1 on SPBs during spindle misalignment also decrease (Caydasi and Pereira, 2009). As a consequence, when the SPOC is active, Tem1 and its regulators Bub2/Bfa1 are mostly dispersed in the cytoplasm.

Chimeric proteins obtained by fusing Bub2 or Bfa1 to the structural SPB component Cnm67 cause unscheduled mitotic exit in the presence of mispositioned spindles, which led to the proposal that high turnover of Bub2/Bfa1 might be important to inhibit Tem1 in the cytoplasm during SPOC activation (Caydasi and Pereira, 2009). Conversely, a modified version of Bub2 carrying 9 myc epitopes at the C terminus localizes the GAP and Tem1 rather symmetrically at SPBs and prevents mitotic exit in some sensitized MEN mutant backgrounds (Fraschini et al., 2006).

In order to shed light onto the relationship between Bub2/Bfa1 symmetry and SPOC response, during this thesis we carried out the characterization of a series of mutants altering either the Bub2/Bfa1 subunits or Tem1 and causing symmetric localization of Tem1 and its GAP during properly oriented anaphase. Remarkably, these mutant proteins as a whole tend to activate, rather than inhibit, the MEN. In addition, they lead to more symmetric distribution of Kar9 on spindle poles and to spindle positioning defects, indicating that a delicate balance between MEN activation and inactivation is required for proper spindle alignment.

Results

Bub2 GAP activity involves a 'dual finger' mechanism and promotes Bub2/Bfa1 disappearance from the mother SPB

The catalytic mechanism of GTPase-activating proteins (GAPs) requires an 'arginine-finger', where the lateral chain of a conserved arginine (R85 for Bub2, Fraschini et al., 2006; Neuwald et al., 1997), interacts with the nucleotide-binding site of a G protein, thus stimulating hydrolysis of the γ-phosphate. A new catalytic mechanism, called "dual finger", was proposed for the family of GAPs with TBC (Tre-2, Bub2 and Cdc16) domain. According to the dual finger mechanism a conserved glutamine residue contributes to stimulate GTP hydrolysis together with the canonical catalytic arginine (Pan et al., 2006).

To investigate if Bub2 acts indeed via a dual finger mechanism, we generated a mutant Bub2 variant, Bub2-Q132L, where we replaced by leucine the conserved glutamine at position 132 that identifies the glutamine finger on the basis of sequence alignment (Pan et al., 2006). Bacterially purified His-tagged Tem1, Maltose Binding Protein (MBP)-tagged Bfa1 and glutathione-S transferase (GST)-tagged Bub2 or Bub2-Q132L proteins were used in *in vitro* GTPase assays, as previously described (Fraschini et al., 2006; Geymonat et al., 2002). The rate of GTP hydrolysis and dissociation was measured using Tem1 bound to

γ[^{32}P]-GTP, whereas the rate of GTP dissociation alone was measured using Tem1 bound to the non-hydrolysable GTP analogue γ[^{35}S]-GTP (Fig.1A). As shown in figure 1A, the kinetics of radioactivity loss from wild type Tem1 loaded with either γ[^{32}P]-GTP or γ[^{35}S]-GTP were very similar, suggesting that Tem1 on its own mostly dissociates GTP without hydrolysing it. The presence of Bfa1 stabilized Tem1 in the GTP-bound form, whereas Bub2 stimulated Tem1 GTPase activity in the presence of Bfa1, but not GTP dissociation. Interestingly, Bub2-Q132L did not display any GAP activity towards GTP-bound Tem1 (M. Venturetti, PhD thesis), behaving as the GAP–dead mutant Bub2-R85A previously characterized (Fraschini et al., 2006). Furthermore, it did not stimulate GTP dissociation, exactly like wild type Bub2 (M. Venturetti, PhD thesis).

In vivo, the Q132L substitution completely abolished the checkpoint function of Bub2. Indeed, similar to *bub2Δ* cells, *bub2-Q132L* cells escaped the mitotic arrest upon nocodazole treatment, as indicated by their ability to re-replicate their chromosomes (Fig. 1A)*.*

Checkpoint response to spindle misalignment was also impaired in *bub2-Q132L* cells. Indeed, when spindle mispositioning was induced by *DYN1* or *KAR9* deletion (Miller et al. 1998; Yeh et al., 1995) *bub2-Q132L* cells did not arrest in mitosis as large budded cells but re-budded, similar

to *bub2Δ* cells (Fig. 1B). Thus, consistent with the proposed model (Pan et al., 2006), Bub2 GAP activity, and thereby its role in the SPOC, relies on a dual finger mechanism involving two catalytic residues, R85 and Q132.

A
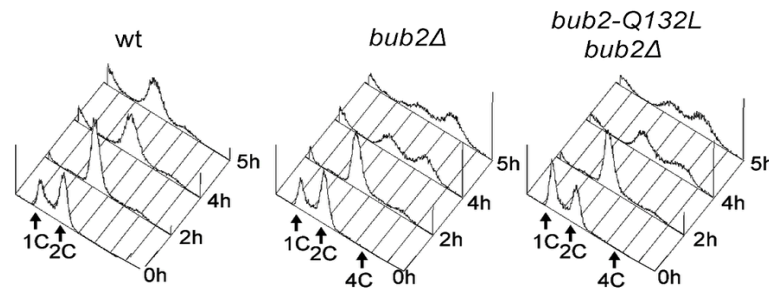
B
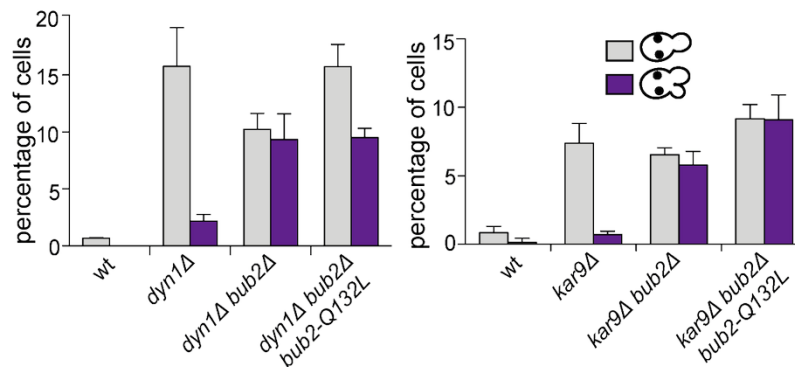
Figure 1 A: Exponentially growing cultures of the indicated strains were shifted to nocodazole-containing medium at t=0. Cell samples were withdrawn at the indicated time for FACS analysis of DNA contents. **B**: The percentage of cells with binucleate cell bodies accompanied or not by a checkpoint defect (indicated by re-budding in the absence of proper chromosome segregation) was scored in cycling cultures of the indicated strains shifted either 14°C for 16h (left graph) or to 37°C for 3h (right graph)

The *bub2-Q132L* allele did not accelerate mitotic exit during the unperturbed cell cycle. Indeed, synchronized *bub2-Q132L* cells could divide and disassemble bipolar spindles with wild type kinetics (Fig. 2A-B).

A
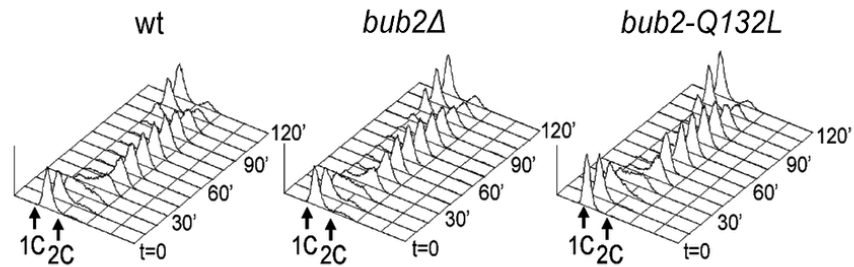
B
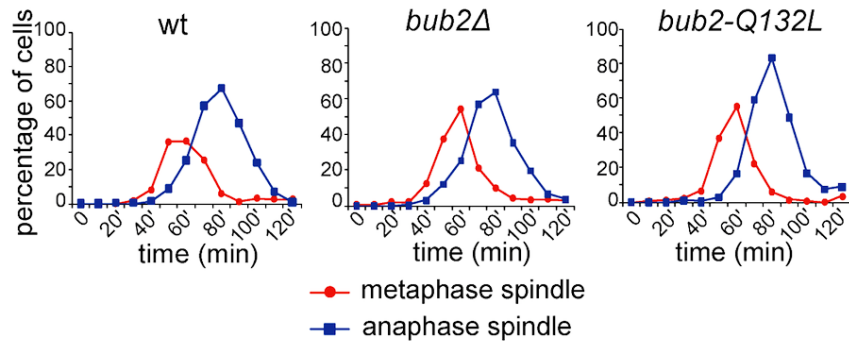
Figure 2 Exponentially growing cells with the indicated genotypes were arrested in G1 by α-factor and released into fresh medium at time 0. At 70' after the release α-factor was re-added to prevent cells from entering a second cell cycle. Cell samples were collected for FACS analysis of DNA content **(A)** and for tubulin staining by indirect immunofluorescence **(B)**.

Furthermore, kinetics of degradation of the main mitotic cyclin Clb2 were very similar in wild type and *bub2-Q132L* cells (Fig. 3). Interestingly, we found that cell cycle-dependent phosphorylation of Bfa1, which promotes mitotic exit (Hu et al., 2001), was abolished in *bub2-Q132L* cells, in agreement with the recent proposal that it requires Bub2 activity (Valerio-Santiago et al., 2013).
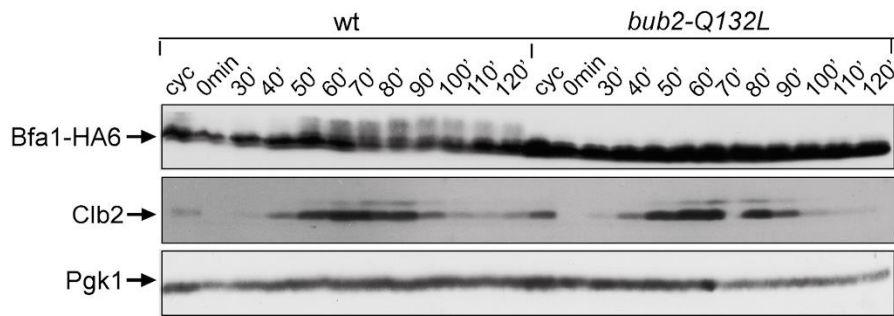
Figure 3 Cells were treated as in Fig 2A-B. TCA extracts were prepared from cell samples at the indicated time points to monitor kinetics of Bfa1-HA6 phosphorylation and Clb2 accumulation and degradation by western blot analysis. Pgk1 was used as loading control.

We then asked if Bub2-Q132L could still interact efficiently with Bfa1 and Tem1. Immunoprecipitations of Bub2 or Bub2-Q132L tagged with three HA epitopes showed that both proteins pulled down roughly the same amounts of GFP-tagged Bfa1. In contrast, Bub2-Q132L precipitated a higher amount of GFP-tagged Tem1 than wild type Bub2

(Fig. 4), suggesting that abolishing the GAP catalytic activity of the Bub2/Bfa1 complex stabilizes the interaction between Tem1 and its GAP.
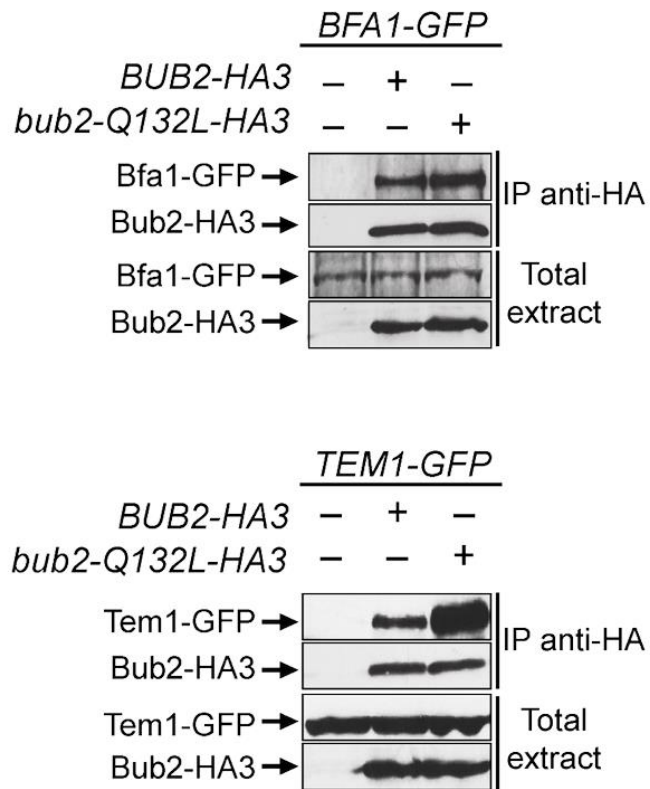
Figure 4 Protein extracts from cells expressing the indicated tagged proteins were used for immunoprecipitation with an anti-HA affinity resin. Western blot analysis was then performed with anti-GFP and anti-HA antibodies. The input represents 1/25th of the total extract used for each IP

66

Because lack of Bub2 GAP activity through the *bub2-R85A* allele leads to increased symmetric localization of Bub2 to SPBs in anaphase (Fraschini et al., 2006), we analyzed the subcellular distribution of eGFP-tagged Bub2-Q132L. In contrast to wild type Bub2, which was almost exclusively present on the bud-directed SPB in 84% of anaphase cells, Bub2-Q132L-HA3 was found on both SPBs in 97% of cells in anaphase. In addition, Bfa1 and Tem1 were also more symmetrically localized on the SPBs of *bub2-Q132L* cells than they were in wild type cells during the same cell cycle stage (Fig. 5A). We therefore conclude that, consistent with previous data, interfering with Bub2 GAP activity affects the asymmetry of the Tem1/Bub2/Bfa1 complex on anaphase spindle poles.

Finally, we analysed the localization of the Tem1 effector kinase Cdc15 in *bub2-Q132L* cells. Although previous data showed that Cdc15 is recruited to SPBs only in anaphase (Konig et al., 2010; Valerio-Santiago et al., 2011; Visintin et al., 2001), we found GFP-tagged Cdc15 on the SPBs of metaphase spindles in 55% of the cells upon fixation with formaldehyde. Deletion of *BUB2* or its replacement with the *bub2-Q132L* allele increased both the total percentage of cells with Cdc15 at SPBs (83% and 80%, respectively, Fig. 5B) and the percentage of cells with

symmetrically localized Cdc15 in metaphase (36% in *bub2Δ* and *bub2-Q132L* cells versus 11% of wild type cells). Thus, lack of Bub2 GAP activity leads to more efficient recruitment of Cdc15 at spindle poles.

A
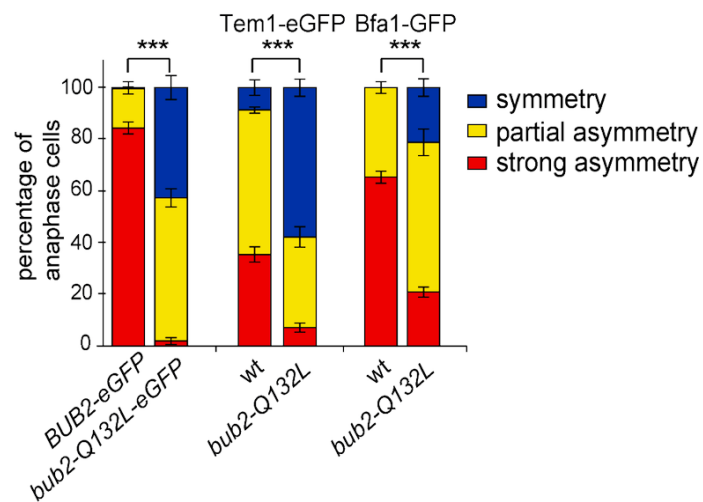
B
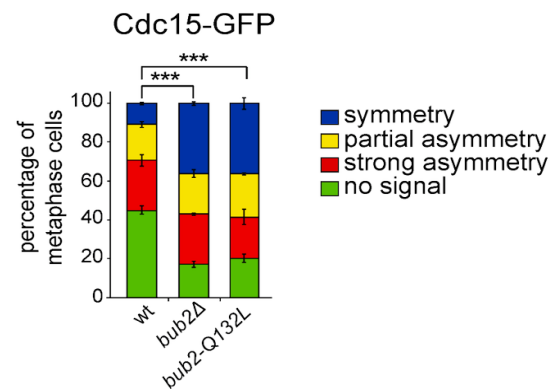
Figure 5 Localization of eGFP- tagged Bub2/Bub2-Q132L, Tem1 and Bfa1**(A)** and Cdc15 **(B)** was analysed by fluorescence microscopy after formaldehyde fixation.

Constitutive targeting of Bfa1 to SPBs facilitates mitotic exit by recruiting Tem1 to SPBs

Since spindle misalignment leads to persistent residence of Bub2/Bfa1 on both SPBs (Pereira et al., 2000), we and others proposed that symmetric distribution of the GAP complex might lead to inhibition of Tem1 (Fraschini et al., 2006; Pereira et al., 2000). This idea was further supported by our previous finding that a myc-tagged variant of Bub2 (Bub2-myc9) localizing mostly symmetrically on SPBs was lethal and prevented mitotic exit in sensitized backgrounds (Fraschini et al., 2006). On the other hand, the Bub2/Bfa1 complex is required throughout most of the cell cycle for Tem1 association with SPB, which in turn triggers its activation (Valerio-Santiago et al., 2011; Pereira et al., 2000). To assess the importance of Bub2/Bfa1 asymmetry at SPBs, we tethered Bfa1 or Bub2 to both SPBs by fusing them to the structural SPB component Spc72. We confirmed that in about 90% of the cells the Spc72-Bfa1 chimeric protein localised constitutively to the SPBs throughout the cell cycle (Fig. 6A) and was able to recruit Tem1 to both SPBs in 74% of anaphase cells, as opposed to 35% of wild type cells (Fig. 6B).

Both Spc72-Bfa1 and Spc72-Bub2 chimeric proteins were functional based on their ability to complement lack of endogenous *BFA1* or *BUB2*,

respectively, for what concerns the checkpoint response to microtubule depolymerisation. Indeed, in the presence of nocodazole, *SPC72-BFA1 and SPC72-BUB2* cells arrested in mitosis with 2C DNA contents as well as wild type cells, whereas *bub2Δ* and *bfa1Δ* cells re-replicated their genome in the same conditions (Fig. 6C-D). Thus, the Spc72-Bfa1 and -Bub2 chimera are likely functional in that they retain their inhibitory properties towards Tem1.

A

Spc72-Bfa1-eGFP
Spc42-mCherry

B

Tem1-eGFP
Tub1-mCherry
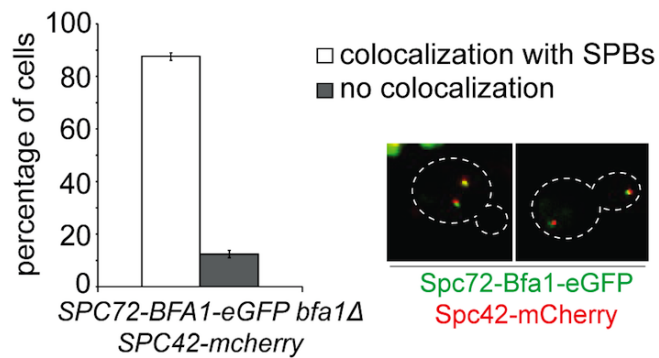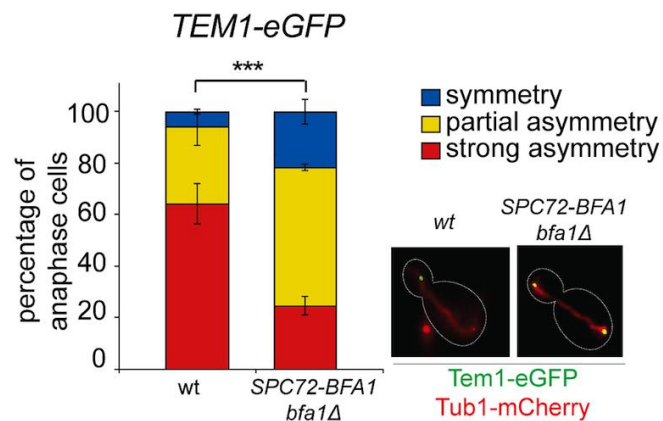
C
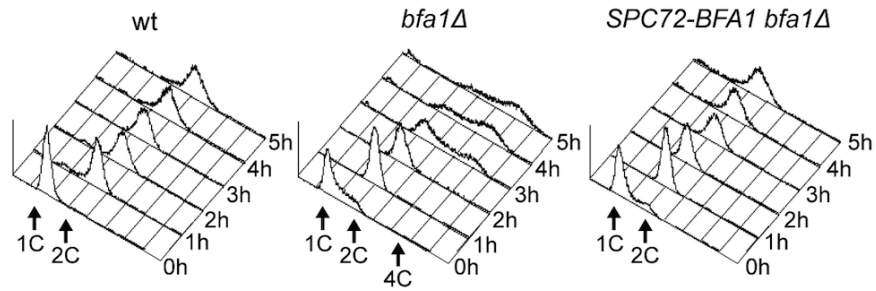
D
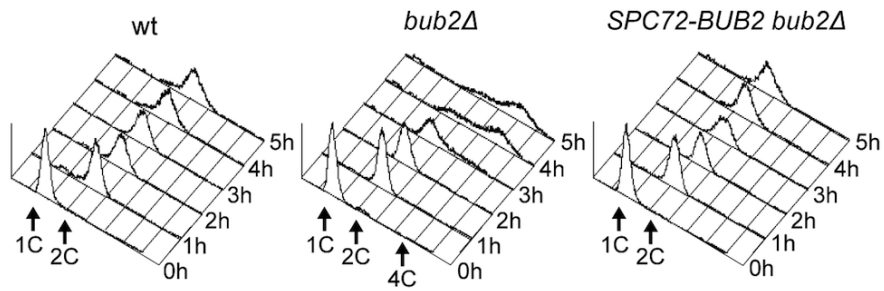
Figure 6 Cycling cells co-expressing Spc72-Bfa1-eGFP and Spc42-mCherry to mark the SPB **(A)** or co-expressing Tem1-eGFP and Tub1-GFP (to mark microtubules, (**B**)) were analysed to study the distribution of Spc72-Bfa1-eGFP and Tem1-eGFP at SPBs in *SPC72-BFA1 bfa1Δ* cells. **C-D**: Cycling cells with the indicated genotypes were shifted into nocodazole containing medium (t=0). Cell samples were withdrawn at the indicated times for FACS analysis of DNA contents.

71

Previously characterized Bub2 and Bfa1 chimeric proteins constitutively anchored to SPBs are SPOC-defective (Caydasi et al., 2006). Similarly, our Spc72-Bfa1 and Spc72-Bub2 failed to activate the SPOC upon spindle mispositioning caused by *DYN1* deletion (Fig. 7). Indeed, *dyn1Δ SPC72-BFA1 bfa1Δ* cells undergoing anaphase in the mother cell, which is symptomatic of spindle mispositioning, exited the cell cycle and re-budded, in contrast to *dyn1Δ* cells that arrested in mitosis as large budded cells (Fig. 7). The SPOC failure of *SPC72-BFA1 bfa1Δ* cells was not worsened by deletion of *BUB2* or *KIN4* or both (Fig. 7), consistent with the notion that Kin4 and Bub2/Bfa1 act in concert to inhibit Tem1. Similar results were obtained with the Spc72-Bub2 chimera. Thus, constitutive targeting to both SPBs of the GAP Bub2/Bfa1, and of Tem1 as a consequence, leads to unscheduled Tem1 activation, consistent with a previous proposal (Valerio-Santiago et al., 2011).
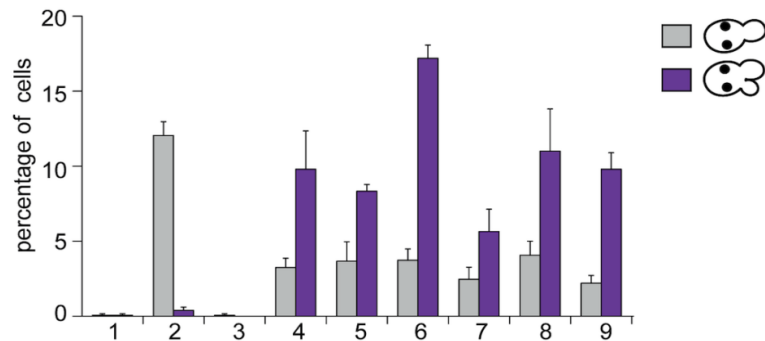
1.wt
2.*dyn1Δ*
3.*SPC72-BFA1 bfa1Δ*
4.*dyn1Δ bub2Δ*
5.*SPC72-BFA1 bfa1Δ dyn1Δ*
6.*SPC72-BFA1 bfa1Δ dyn1Δ bub2Δ*
7.*dyn1Δ kin4Δ*
8.*SPC72-BFA1 bfa1Δ dyn1Δ kin4Δ*
9.*SPC72-BFA1 bfa1Δ dyn1Δ kin4Δ bub2Δ*

Figure 7 The percentage of cells with binucleate cell bodies accompanied or not by a SPOC defect was scored after propidium iodide staining of cycling cultures of cells with the indicated genotypes after shift to 14°C for 16h

We then asked if symmetric localization of Tem1 driven by the Spc72-Bfa1 chimera leads to more efficient recruitment of Cdc15 to SPBs in metaphase. This was indeed the case. Whereas GFP-tagged Cdc15 was present at the SPBs of 55% wild type metaphase cells, 90% of metaphase cells expressing the fusion *SPC72-BFA1* displayed SPB-bound Cdc15 (Fig. 8). Furthermore, Cdc15 was significantly more symmetric in *SPC72-BFA1* than in wild type cells. Thus, stable tethering

of Tem1 to SPBs by fusion to an SPB component (Valerio-Santiago et al., 2011) or by SPB recruitment via its inhibitory GAP (Caydasi et al., 2009 and our data) leads in both cases to premature Tem1 activation.
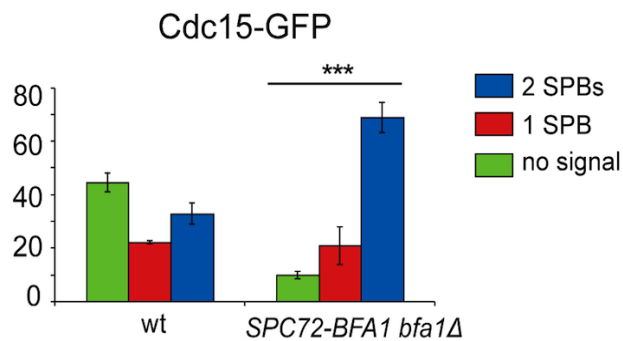
Figure 8 Percentage of metaphase cells with Cdc15-GFP at 0, 1 or 2 SPBs in the indicated strains was analysed by fluorescence microscopy after formaldehyde fixation.

We then asked if expression of the Spc72-Bfa1 chimera could have any phenotypic consequence for conditional mutants affecting the MEN. Remarkably, *SPC72-BFA1* as the only source of Bfa1 in the cells suppressed the growth defects of several MEN mutants. In particular, it could partially rescue the temperature sensitivity of *tem1-3* and *mob1-77* (Fig. 9A), as well as the cold-sensitivity of *cdc15-2* and *dbf2-2* mutant cells (Fig. 9B). A slight suppression, if any, was observed for the

temperature-sensitivity of *cdc5-2* cells, whereas the temperature-sensitivity of *cdc14-3* cells was not suppressed at all (Fig. 9C).

Suppression of *tem1-3* was recessive, as it was not observed when a wild type copy of *BFA1* was present concomitant to *SPC72-BFA1* in the cells (Fig. 9A). Importantly, suppression was not due to reduced GAP activity, as it could not be recapitulated by deletion of *BFA1* (Fig. 9A), or *BUB2* or both (Fig. 9D). Since the mitotic exit defects of *tem1-3* cells at high temperatures correlate with a loose interaction of the mutant Tem1 protein with SPBs (Asakawa et al., 2001), we conclude that Spc72-Bfa1 suppresses the temperature-sensitivity of *tem1-3* cells likely by recruiting Tem1 to the SPBs. Consistent with this notion, the Spc72-Bfa1 and Spc72-Bub2 chimera suppressed the lethality caused by overexpression of the SPOC kinase Kin4 (Fig. 9E), which increases the turnover of Bub2/Bfa1, and by consequence of Tem1, at SPBs (Caydasi et al., 2009).

Thus, these data, together with those from a previous study (Caydasi et al., 2009), indicate that symmetric persistence of Bub2/Bfa1 at SPBs does not interfere with mitotic exit. Rather, in spite of being part of an inhibitory GAP complex, Bfa1 is the receptor of Tem1 at SPBs, where Tem1 promotes MEN signaling. Stable residence of Bub2/Bfa1 at SPBs

75

causes unscheduled mitotic exit by decreasing Tem1 turnover at SPBs,

as previously suggested (Valerio-Santiago et al., 2011).

A

B

C

	25°C	30°C	35°C
wt			
wt			
SPC72-BFA1 bfa1Δ			
cdc5-2			
SPC72-BFA1 bfa1Δ cdc5-2			
SPC72-BFA1 bfa1Δ cdc5-2			

	25°C	30°C	35°C
wt			
wt			
SPC72-BFA1 bfa1Δ			
cdc14-2			
SPC72-BFA1 bfa1Δ cdc14-2			
SPC72-BFA1 bfa1Δ cdc14-2			

D

	25°C	30°C	35°C
wt			
tem1-3			
SPC72-BFA1 bfa1Δ tem1-3			
bfa1Δ tem1-3			
bfa1Δ bub2Δ tem1-3			
bfa1Δ bub2Δ tem1-3			
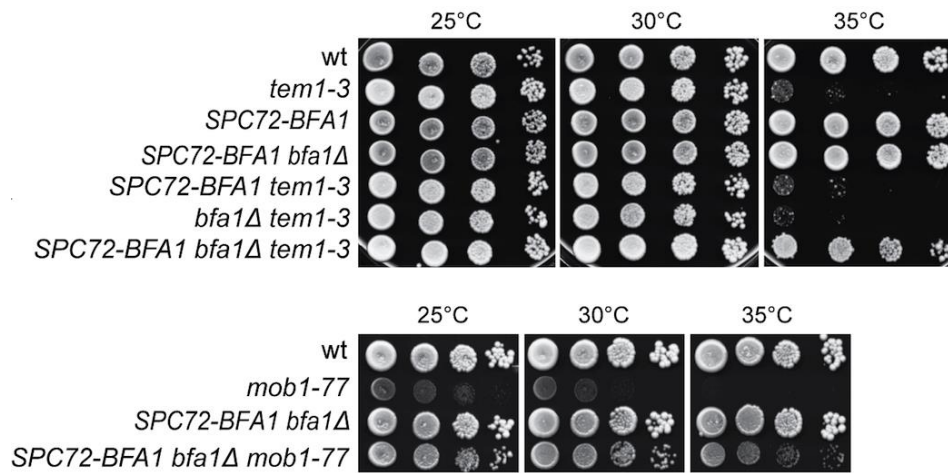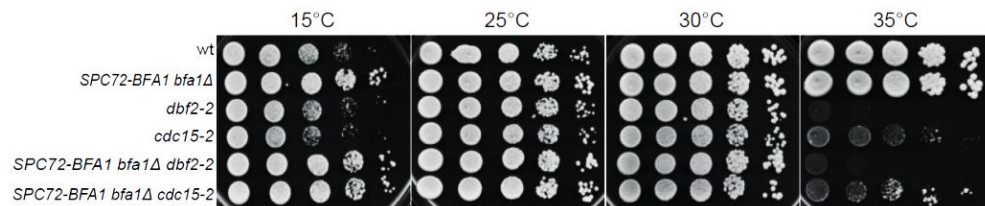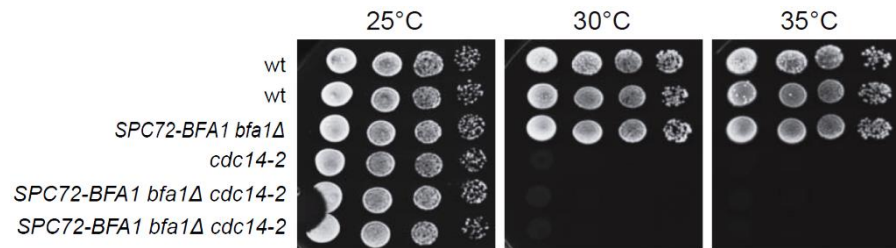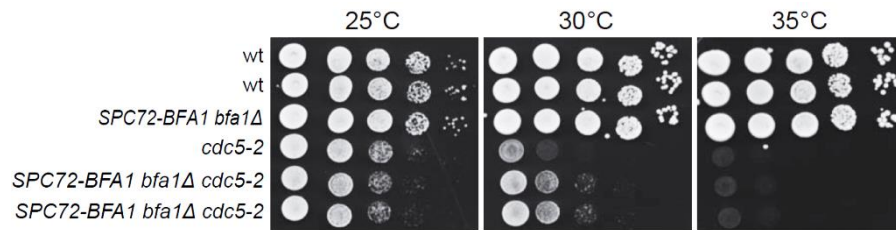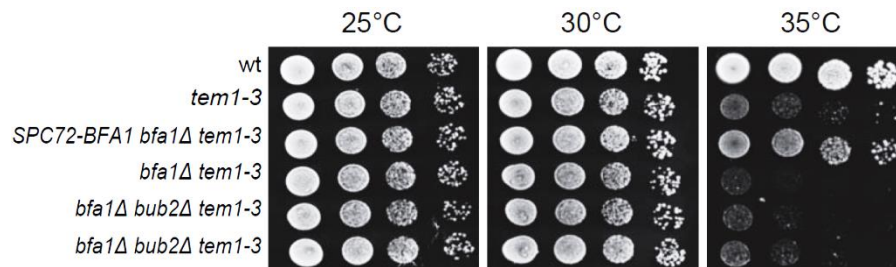
E
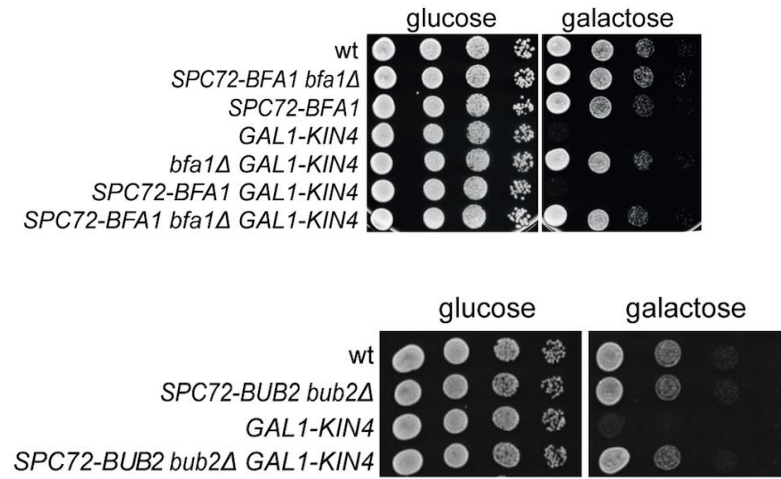
Figure 9 A-D: Serial dilutions of stationary phase cultures of the indicated strains were spotted on YPD and incubated at the indicated temperature for 48h. **E:** Serial dilutions of stationary phase cultures of the indicated strains were spotted on YP medium containing either glucose or galactose and incubated at 25°C for 48h.

Activation of the FEAR pathway in anaphase is required for the unscheduled mitotic exit triggered by Spc72-Bfa1 and -Bub2 chimeric proteins

The ability of Spc72-Bfa1 and -Bub2 tethers to efficiently prevent mitotic exit upon microtubule depolymerization, but not upon spindle mispositioning, was somewhat puzzling. A major difference between the two conditions lies in the activation of the spindle assembly checkpoint (SAC) after nocodazole treatment. Through inhibition of Cdc20/APC, SAC leads to securin stabilization, in turn preventing activation of separase and the FEAR pathway (Stegmeier et al., 2002). If inhibition of the FEAR pathway is the only reason for the failure of Spc72-Bfa1 and -Bub2 chimera to promote mitotic exit, premature FEAR activation should allow mitotic exit in cells expressing Spc72-Bfa1 and -Bub2 treated with nocodazole. Conversely, FEAR inactivation should prevent mitotic exit in the same cells undergoing spindle misalignment. To test this hypothesis, we prematurely activated the FEAR pathway and Cdc14 release from the nucleolus by either inactivation of the PP2A^{Cdc55} phosphatase through deletion of *CDC55* or *ESP1* overexpression (Queralt et al., 2006). Remarkably, PP2A^{Cdc55} inactivation had a synergistic effect with *SPC72-BFA1* and *SPC72-BUB2* on the kinetics of mitotic exit upon nocodazole

79

treatment, as judged by the ability of cells to re-replicate their DNA (Fig. 10A-B). Similar data were obtained with *ESP1* overexpression from the galactose-inducible *GAL1* promoter (Fig. 10C-D). In contrast, reducing the levels of mitotic CDKs through *CLB2* deletion did not accelerate mitotic exit in *SPC72-BFA1* cells (Fig. 10E).

A

B

C

D

E
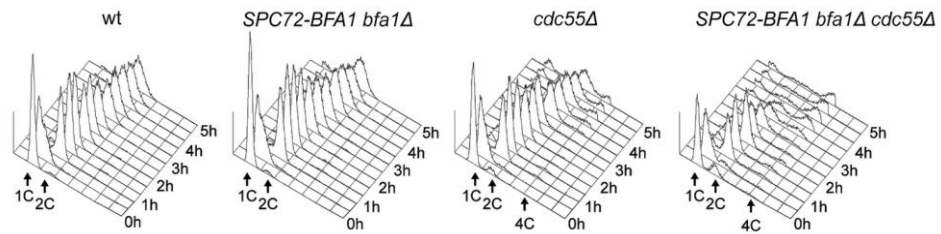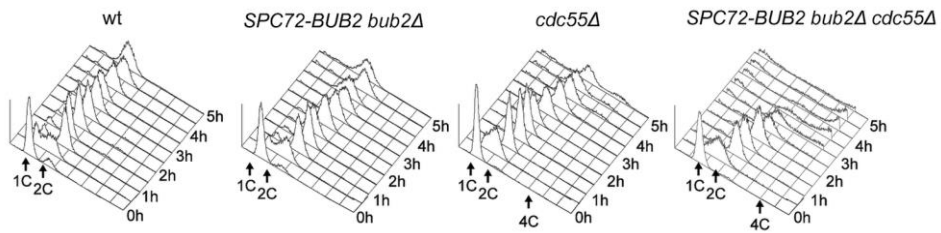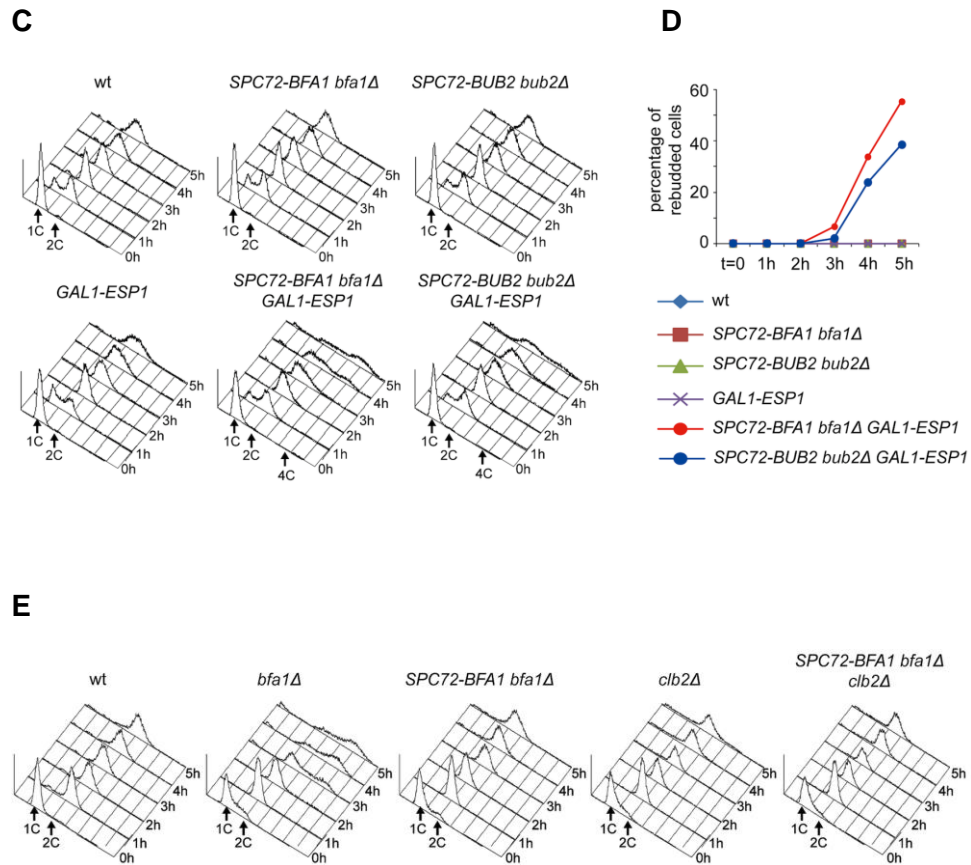
Figure 10 Logarithmically growing cultures of cells with the indicated genotypes were synchronized in G1 by α-factor and then released into nocodazole containing medium (t=0). At the indicated times cell samples were withdrawn for FACS analysis of DNA contents **(A-C** and **E)** and to score the percentage of rebudded cells **(D).**

81

Importantly, FEAR inactivation through deletion of both *SPO12* and *BNS1* reduced the unscheduled mitotic exit caused by *SPC72-BFA1* in *dyn1Δ* cells (Fig. 11).

Thus, constitutive recruitment of the Bub2/Bfa1 complex to SPBs leads to precocious Tem1 activation. Whether this translates into a premature mitotic exit depends on the activation state of the FEAR pathway.
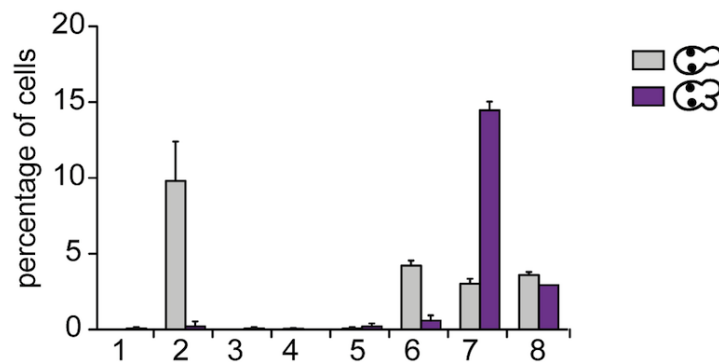
1. wt
2. *dyn1Δ*
3. *bns1Δspo12Δ*
4. *SPC72-BFA1 bfa1Δ*
5. *SPC72-BFA1 bfa1Δ bns1Δ spo12Δ*
6. *bns1Δ spo12Δ dyn1Δ*
7. *SPC72-BFA1 bfa1Δ dyn1Δ*
8. *SPC72-BFA1 bfa1Δ bns1Δ spo12Δ dyn1Δ*

Figure 11 The percentage of cells with binucleate cell bodies accompanied or not by a SPOC defect was scored after DAPI staining of cycling cells with the indicated genotypes shifted to14°C for 16h.

A constitutively active GTP-bound Tem1 variant is SPOC-deficient and is synthetically lethal for mutants affecting spindle positioning

To further investigate the links between Tem1 activity and the establishment of SPB asymmetry of the Tem1/Bub2/Bfa1 complex, we generated a *TEM1-Q79L* mutant allele, where the catalytic glutamine in the G domain (Q79, according to sequence comparison with Rab-like GTPases (Bourne et al., 1991), was replaced by leucine. We first tested the catalytic properties of Tem1-Q79L in *in vitro* GTPase assays in the presence of Bfa1 and Bub2. As previously shown (M. Venturetti, PhD thesis), Tem1-Q79L was completely refractory to stimulation of GTP hydrolysis by the GAP Bub2/Bfa1 *in vitro*, suggesting that *in vivo* it is preferentially in its active GTP-bound form. Thus, Q79 of Tem1 likely participates directly to GTP hydrolysis along with R85 and Q132 of Bub2.

When expressed in yeast cells as the sole source of Tem1, Tem1-Q79L did not cause any detectable growth defect at any temperature (data not shown). Furthermore, *TEM1-Q79L* mutant cells showed kinetics of cell cycle progression similar to those observed in wild type cells (Fig. 12).
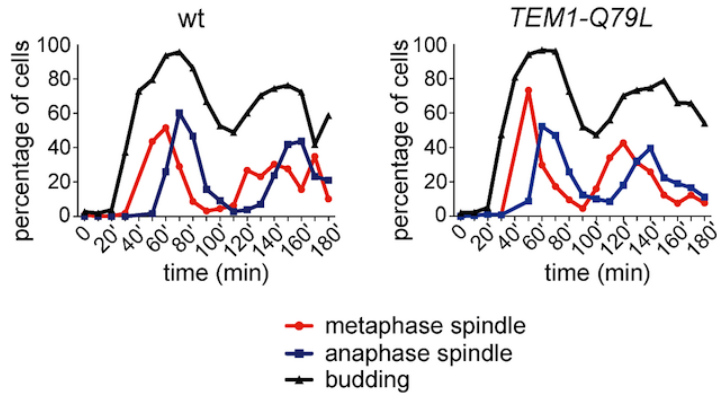
Figure 12 Wild type and *TEM1-Q79L* cells were arrested in G1 by α factor and then released into fresh medium at 25°C (t=0). Cell samples were withdrawn every 10' for FACS analysis of DNA contents (not shown) and to measure kinetics of budding and spindle formation/elongation after in situ immunostaining of tubulin

The absence of obvious cell cycle phenotypes in unperturbed conditions was somewhat surprising, as a similar mutation in fission yeast *spg1+*, encoding the SIN counterpart of the Tem1 GTPase, leads to premature cytokinesis and formation of multiple septa (Schmidt et al., 1997). We therefore analysed by time-lapse video microscopy the speed of actomyosin ring contraction, as a marker of cytokinesis (Bi et al., 1998), in wild type and *TEM1-Q79L* cells expressing GFP-tagged myosin II (Myo1). Strikingly, contraction of the actomyosin ring took place on average 2' faster in *TEM1-Q79L* relative to wild type cells (i.e. 6' and 8', respectively, Fig. 13), consistently with previous data on *bub2Δ* cells

(Park et al., 2009). Thus, the *TEM1-Q79L* allele accelerates at least some aspects of cytokinesis without affecting cell viability.
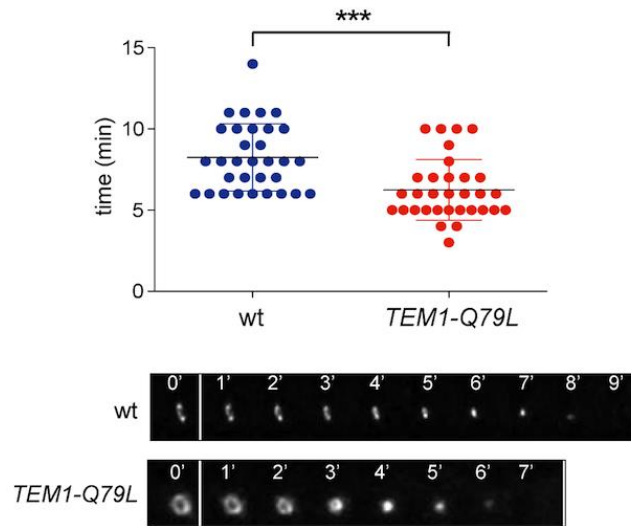
Figure 13 Actomyosin ring contraction has been visualized by live cell imaging of wild type and *TEM1-Q79L* cells expressing Myo1-GFP (n=30)

To gain further insights into the factors allowing *TEM1-Q79L* cells to grow at normal rates, we carried out a synthetic genetic arrays (SGA) screen to find deletions of non-essential genes that become synthetically lethal/sick with *TEM1-Q79L* (Table 1). This screen uncovered several genes encoding proteins involved in spindle positioning and nuclear migration, such as Kar9, the dynein light chain (*DYN2*) and components

of the dynactin complex that cooperates with dynein for spindle positioning (Kahana et al., 1998). In addition, this screen uncovered several genes implicated in microtubule biogenesis, which might indirectly influence spindle positioning. Thus, *TEM1-Q79L* aggravates the sickness of cells undergoing spindle mispositioning. A number of additional non-essential genes whose deletion displayed synthetic interactions with *TEM1-Q79L* was also uncovered with this screen and will be described elsewhere, since the significance of these genetic interactions has not been further explored in this context.

GENE	DESCRIPTION	FUNCTION
BIK1	Microtubule-associated protein	
NUM1	Nuclear migration	
BIM1	Microtubules plus end-tracking protein	
DYN2	Dynein light chain (microtubule motor protein)	Spindle positioning and nuclear migration
ARP1	Component of the dynactin complex	
LDB18	Component of the dynactin complex	
NIP100	Component of the dynactin complex	
JNM1	Component of the dynactin complex	
CIK1	Kinesin-associated protein	
KAR9	Microtubule-associated protein	
PAC10	Co-chaperone GimC/prefoldin complex	
GIM3	Co-chaperone GimC/prefoldin complex	Microtubule biogenesis
YKE2	Co-chaperone GimC/prefoldin complex	

Table1 List of non-essential genes implicated in microtubule dynamics or spindle positioning identified in the SGA screen with *TEM1-Q79L*

We then tested the ability of *TEM1-Q79L* mutant cells to respond to microtubule depolymerization and spindle mispositioning. In the presence of nocodazole, whereas wild type cells arrested in mitosis with 2C DNA contents, *TEM1-Q79L* cells re-replicated their genome similar to cells lacking Bub2 (Fig. 14A). In addition, *TEM1-Q79L dyn1∆* cells exited mitosis and re-budded in face of the spindle position defects (Fig. 14B). Thus, the *TEM1-Q79L* mutant allele affects SPOC response. As expected, the checkpoint defect was dominant, as the *TEM1-Q79L* allowed mitotic exit and re-replication in the presence of nocodazole even when expressed from an episomal plasmid in cells carrying also the endogenous *TEM1* gene (Fig. 14C). Consistent with its constitutive activation, the *TEM1-Q79L* allele was also able to suppress the lethality associated with overexpression of *KIN4* from the galactose-inducible *GAL1* promoter (Fig. 14D), which delays mitotic exit by keeping the Bub2/Bfa1 GAP active (D'Aquino et al., 2005).

A

B

C

88
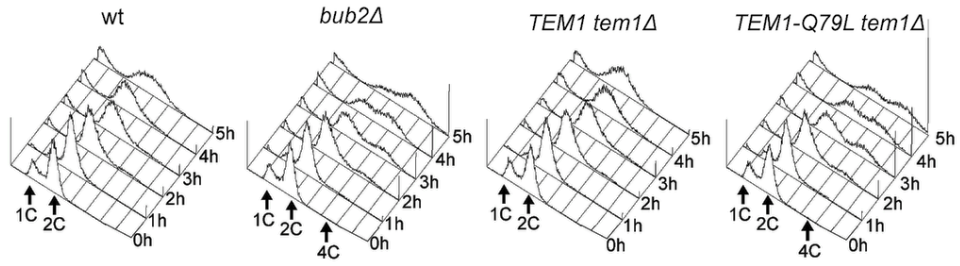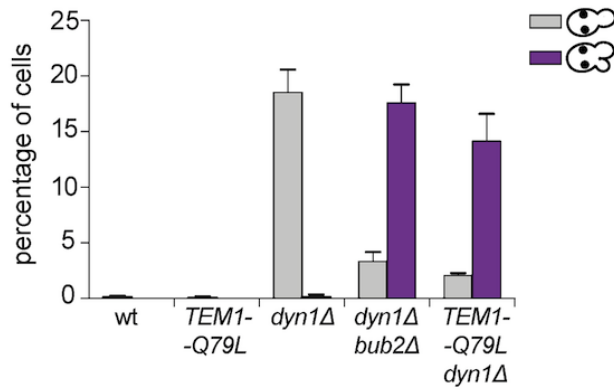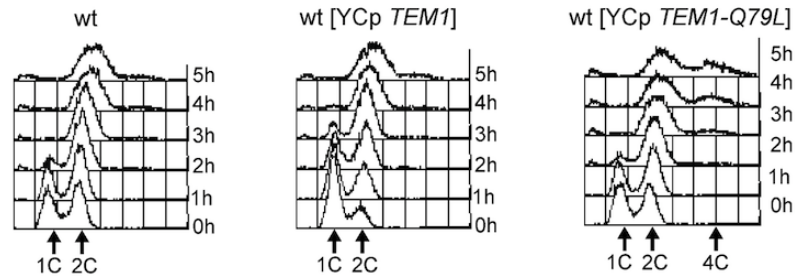
D
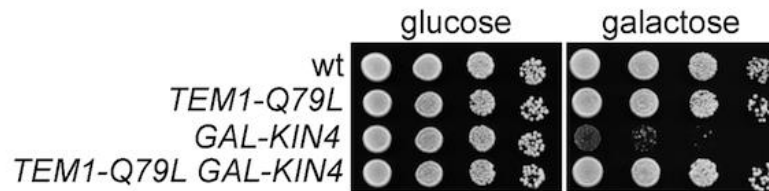
Figure 14 A: Logarithmically growing cultures of cells with the indicated genotypes were shifted into nocodazole-containing medium (t=0). DNA contents were analysed by flow cytometry at the indicated times. **B:** The percentage of cells with binucleate cell bodies accompanied or not by a SPOC defect was scored after DAPI staining of cycling cells of the indicated strains shifted to 14°C for 16h. **C:** Logarithmically growing cultures of strains with the indicated genotypes were shifted to nocodazole containing medium (t=0). DNA contents were analysed by flow cytometry at the indicated times. **D:** Serial dilutions of stationary phase cultures of the indicated strains were spotted on YPD or YP galactose plates and incubated at 30°C for 48h.

The constitutively active Tem1-Q79L variant shows reduced asymmetry at anaphase spindle poles and impairs the asymmetry of Bfa1

The "dual finger" model predicts that GTP hydrolysis is catalysed by the GAP and the so-called catalytic glutamine of the GTPase could stabilize the interaction between the GAP and the GTPase without directly contributing to the catalytic reaction (Pan et al., 2006). We formally tested this idea by analysing the interaction between Tem1 or Tem1-Q79L with Bub2 and Bfa1 in co-immunoprecipitation experiments. Remarkably, HA-tagged Tem1-Q79L pulled down a higher, rather than a lower, amount of Bub2 and Bfa1 (tagged with 3PK epitopes and GFP, respectively) (Fig. 15A). Thus, constitutive binding to GTP seems to increase the affinity of Tem1 for its GAP. To further corroborate this conclusion we co-expressed Bfa1-GFP and Bub2-GFP with HA-tagged Tem1 or Tem1-Q79L. Immunoprecipitation of Tem1-Q79L-HA3 pulled down higher amounts of both Bfa1-GFP and Bub2-GFP than Tem1-HA3 (Fig. 15B), without affecting the relative proportion of Bfa1-GFP and Bub2-GFP in the immunoprecipitates. We therefore conclude that locking Tem1 in the GTP-bound form enhances its affinity for Bub2/Bfa1 without affecting the stoichiometry of the GAP complex.

A
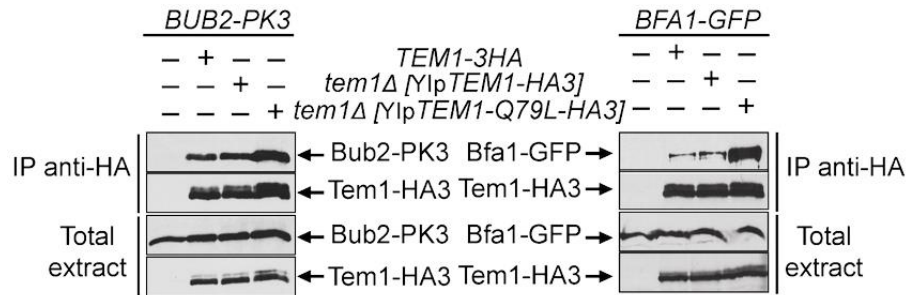
B
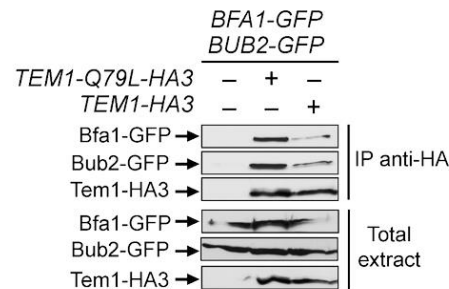
Figure 15 Protein extracts from cells expressing the indicated tagged proteins were used for immunoprecipitations with an anti-HA affinity resin. Western blot analysis was then performed with anti-PK, anti-GFP and anti-HA antibodies. The input represents 1/25th of the total extract used for each IP.

Since our data suggest that proper regulation of Tem1 GTP hydrolysis is required for asymmetry of the Tem1/Bub2/Bfa1 complex at SPBs, we analysed the subcellular distribution of Tem1-Q79L tagged with eGFP. As expected, Tem1-eGFP was already asymmetric in 53% of metaphase cells, whereas Tem1-Q79L-eGFP was asymmetric in a lower fraction of

91

cells (35%). In anaphase, whereas Tem1-eGFP localized asymmetrically to the bud-directed SPB in 90% of cells, Tem1-Q79L-eGFP was present symmetrically at SPBs in 70% of the cells (Fig. 16A). Thus, abolishing the GAP-stimulated GTPase activity of Tem1 through different kinds of mutations invariably leads to Tem1 symmetric localization at SPBs.

Interestingly, whereas *BFA1* deletion markedly affected Tem1-eGFP recruitment to SPBs as previously reported (Valerio-Santiago et al., 2011; Pereira et al., 2000; Caydasi et al., 2012), it had a less pronounced effect on Tem1-Q79L-eGFP SPB localization (Fig. 16B), suggesting that loading to SPBs of constitutively active Tem1 is partially GAP-independent.
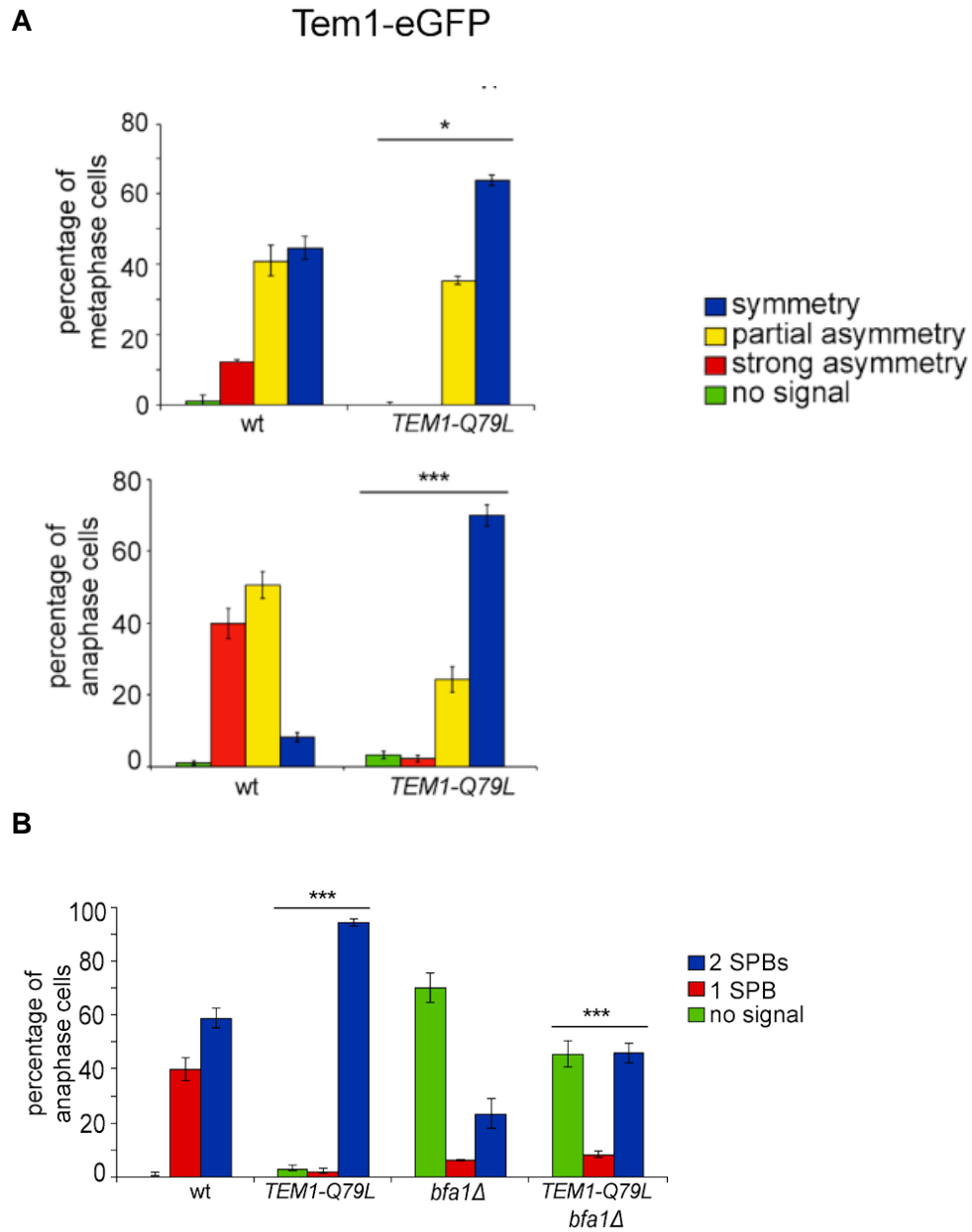
Figure 16 Localization of eGFP-tagged Tem1 and Tem1-Q79L was analysed in the indicated strains by fluorescence microscopy after formaldehyde fixation. Metaphase and anaphase cells were identified by means of the Tub1-mCherry co-expressed marker.

Previous data suggested that loading of Bfa1 and Bub2 on SPBs and their asymmetry in anaphase still occur in cells lacking Tem1 (Geymonat et al., 2009; Pereira et al., 2000). On the other hand, experimental evidence indicates that an increased residence time of Tem1 at the SPBs or its decreased GTPase activity can influence Bub2/Bfa1 localization (Valerio-Santiago et al., 2012; Fraschini et al., 2006; Kim et al.,2012). Because our results indicate that the Q79L substitution affects Tem1 activity, as well as its localization in anaphase, we asked if Tem1-Q79L had any impact on localization of Bfa1. Both wild type and *TEM1-Q79L* mutant cells showed a similar partially asymmetrical SPB localization of Bfa1-eGFP in metaphase (Fig. 17A). In contrast, at the onset of anaphase, while Bfa1 drastically dropped to hardly detectable levels on the mother-bound SPB in 95% of wild type cells, it remained completely symmetrical on SPBs in 22% of *TEM1-Q79L* cells and persisted to low but clearly detectable levels on the mother-bound SPB in 46,6% of the cells (Fig. 17A). The symmetric localization of Bfa1 in *TEM1-Q79L* cells did not depend on premature activation of downstream MEN kinases, as it was not affected by Cdc15 inactivation through the *cdc15-2* temperature-sensitive allele (Fig. 17B).

Since Kin4 promotes Bfa1 turnover at SPBs upon SPOC activation (Caydasi et al., 2009), we analysed Bfa1 localization in wild type and *TEM1-Q79L* cells lacking *KIN4* (Fig. 17A). In agreement with previous data (Caydasi et al., 2009), deletion of *KIN4* alone did not affect Bfa1 distribution on SPBs of wild type cells in unperturbed conditions. In stark contrast, it had a synergistic impact with the *TEM1-Q79L* mutant allele on Bfa1 localization at SPBs specifically in anaphase, making it completely symmetrical in 65% of the cells and only partially asymmetric in 30% of the cells (Fig. 17A). Consistently, the ratio in Bfa1-GFP fluorescence intensity at the mother- versus the bud-directed SPB was close to 0 for wild type and *kin4Δ* cells, while it significantly increased in *TEM1-Q79L* and *TEM1-Q79L kin4Δ* cells (Fig. 17C). Thus, these data reveal an unanticipated role of Kin4 in actively dislodging Bfa1 from the mother-bound SPB during anaphase of the unperturbed cell cycle. Furthermore, they indicate that Tem1 GTP hydrolysis is a primary determinant of Bfa1 asymmetry in anaphase.

A

B

Bfa1-GFP

C
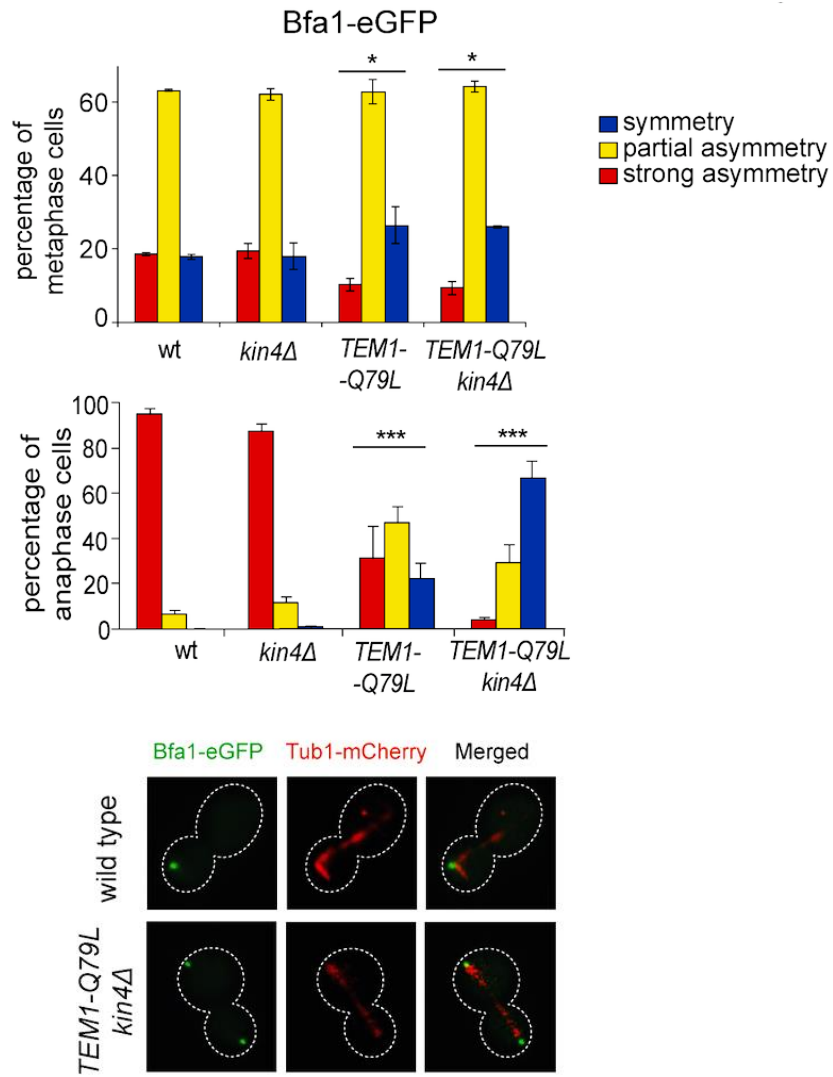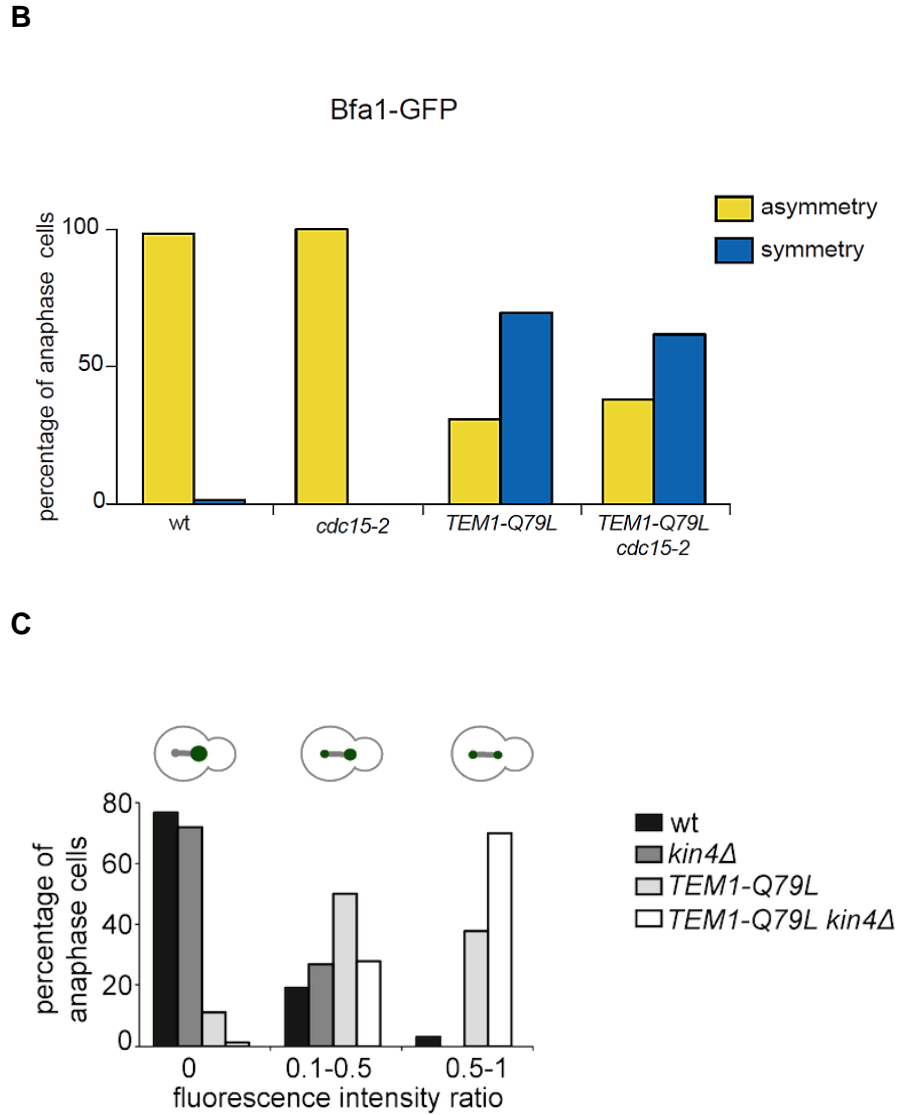
Figure 17 Localization of eGFP-tagged Bfa1 **(A-B)** was analysed in the indicated strains by fluorescence microscopy after formaldehyde fixation. Metaphase and anaphase cells were identified by means of the Tub1-mCherry co-expressed marker. Micrographs show representative cells of each strain in anaphase. **C:** Fluorescence intensity ratio were calculated between the two SPBs in anaphase cells of the indicated strains (see details in Materials and Methods)

The *TEM1-Q79L* allele enhances Cdc15 loading on SPBs, without affecting the timing of mitotic exit

To investigate further if the *TEM1-Q79L* allele leads to premature MEN activation, we analysed the subcellular localization of downstream MEN components, such as Cdc15 and Mob1. We observed that 99% of *TEM1-Q79L* mutant cells recruited Cdc15 to SPBs in metaphase, as opposed to 55% in wild type cells (Fig. 18A). Furthermore, Cdc15 was significantly more symmetric in *TEM1-Q79L* than in wild type cells. Deletion of *KIN4*, either alone or in combination with the *TEM1-Q79L* allele did not have any impact on Cdc15 distribution (Fig. 18A). In spite of Cdc15 enhanced loading on SPBs, recruitment of Mob1 to SPBs in metaphase was only slightly increased in *TEM1-Q79L* relative to wild type cells (Fig. 18B), consistent with the notion that mechanisms other than the SPOC restrain MEN activity downstream of Tem1 until late anaphase.

Phosphorylation of Cdc15 and Mob1 by cyclin B/CDKs together with Bub2/Bfa1 GAP activity provides a dual inhibition of the MEN (Konig et al., 2010). Consistently, we found that combining the *TEM1-Q79L* allele with deletion of *CLB2*, which encodes the main mitotic cyclin B, caused synthetic growth defects at 37°C (Fig. 18C). However, no synthetic

98

lethality or detrimental synthetic defects were induced by the additional deletion of *KIN4* or *BFA1*, suggesting that the components of the MEN downstream of Cdc15 are likely targets of negative regulators additional to Bub2/Bfa1 and Clb2-associated CDKs.

A
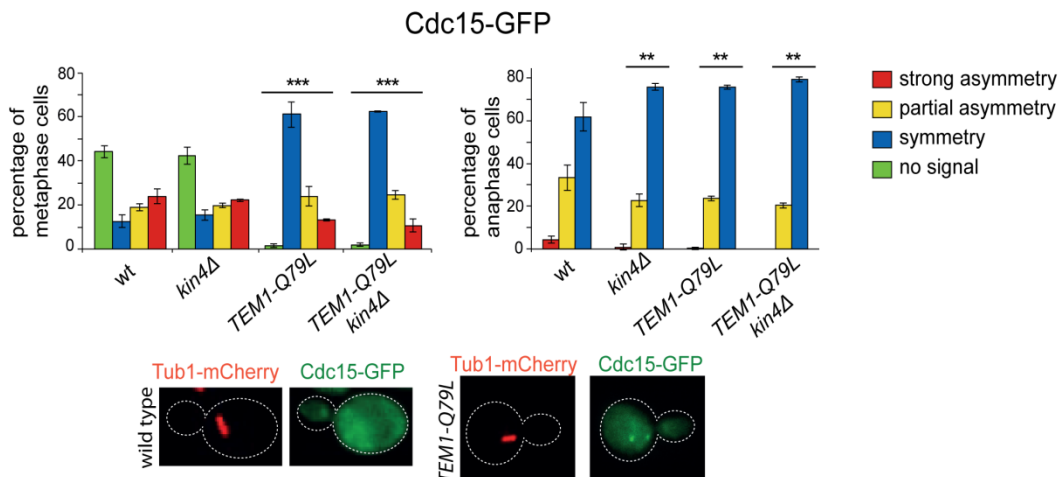
B
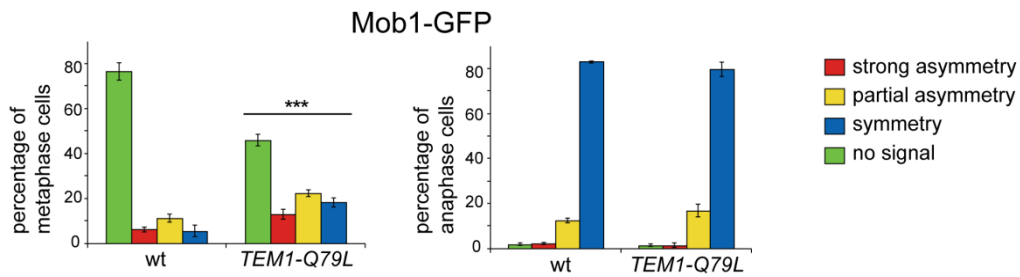
C
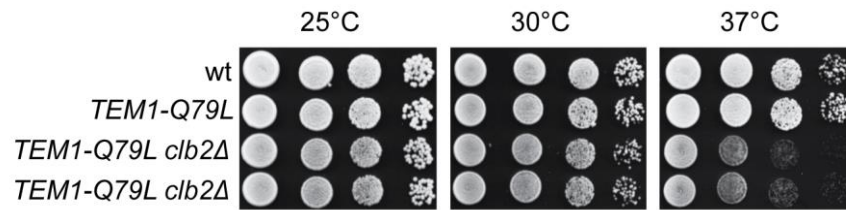
Figure 18 A: Percentage of Cdc15-GFP loading onto 1SPB, 2SPBs, or none for the indicated strains in metaphase and anaphase cells. Micrographs show representative cells of each strain in metaphase. **B:** Percentage of Mob1-GFP loading onto 1SPB, 2SPBs, or none for the indicated strains in metaphase and anaphase cells. **C:** Serial dilutions of stationary phase cells with the indicated genotypes were spotted on YPD and incubated at the indicated temperatures for 48h.

Bub2/Bfa1 and Tem1 asymmetry is important for proper Kar9 distribution and spindle positioning

Partial asymmetry of Bub2/Bfa1 at SPBs begins already in metaphase (Monje-Casas et al., 2009). Since during metaphase MEN induces asymmetric localization of Kar9 at spindle poles, which is in turn required for correct spindle positioning (Hotz et al., 2012), we checked if symmetrical Bub2/Bfa1 and Tem1 might affect Kar9 localization and spindle positioning. To this end, we analysed the distribution of Kar9 tagged with eGFP on the metaphase spindles of wild type, *SPC72-BFA1 bfa1Δ, SPC72-BUB2 bub2Δ* and *TEM1-Q79L* cells. Whereas 84.4% of wild type cells showed strongly asymmetric Kar9, this value dropped to 43.5%, 50.5% and 47.6% in *SPC72-BFA1 bfa1Δ, SPC72-BUB2 bub2Δ* and *TEM1-Q79L* cells, respectively, while the remaining fraction of cells displayed partial or complete symmetry (Fig. 19A).

Since our results indicate that the GAP activity of Bub2 and Bfa1 influences the localization of the GAP complex in the cell, we characterized Kar9 distribution in the GAP-dead Bub2 variants, *BUB2-Q132L* and *BUB2-R85A* cells, in cells expressing the symmetric GAP-inactive *BUB2-myc9* construct (Fraschini et al., 2006), as well as in *bub2Δ* and *bfa1Δ* mutant cells. All strains showed more symmetric

localization of Kar9, with 33.9% of complete asymmetry for *BUB2-Q132L*, 27.8% for *BUB2-R85A*, 53.6% for *BUB2-myc9*, 45.7% for *bub2Δ* and 41.9% for *bfa1Δ* cells, as opposed to 80.3% for wild type cells (Fig. 19B). Increased symmetry of Kar9 in the mutants (with the exception of *bub2Δ* and *bfa1Δ* that were not analysed) was accompanied by increased Bfa1 symmetry (Fig. 19B). Therefore, establishment of Bub2/Bfa1 and Tem1 asymmetry impacts on Kar9 asymmetry. However, Bub2/Bfa1 symmetric distribution at SPBs is not sufficient to drive Kar9 symmetry. Indeed, when spindles are misaligned in *dyn1Δ* mutant cells, Bub2 becomes increasingly more symmetric during the metaphase to anaphase transition, whereas Kar9 remains strongly asymmetric (Cepeda-Garcia et al., 2010; Juanes et al., 2013). Thus, once Kar9 asymmetry has been established, it cannot be reversed by spindle misalignment, in contrast to that of Bub2/Bfa1.
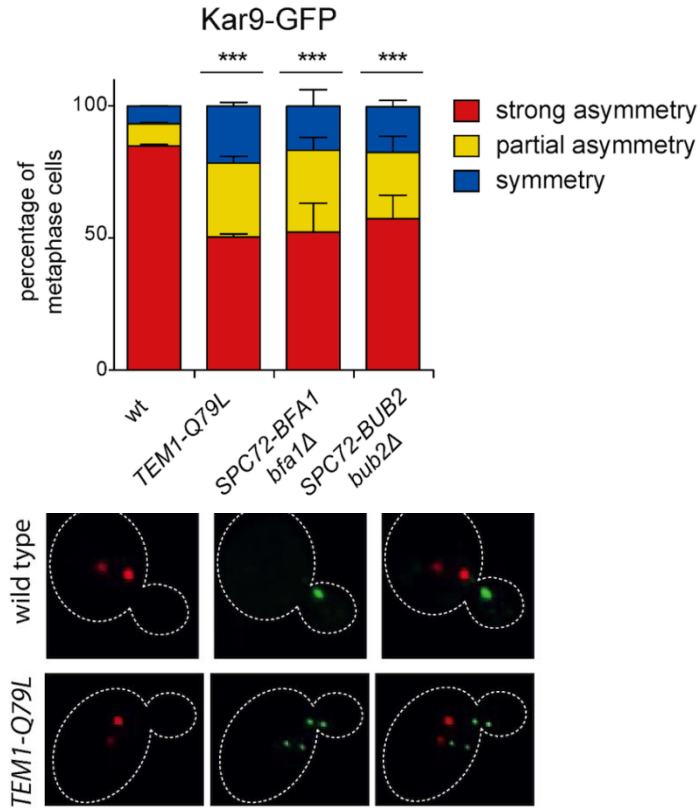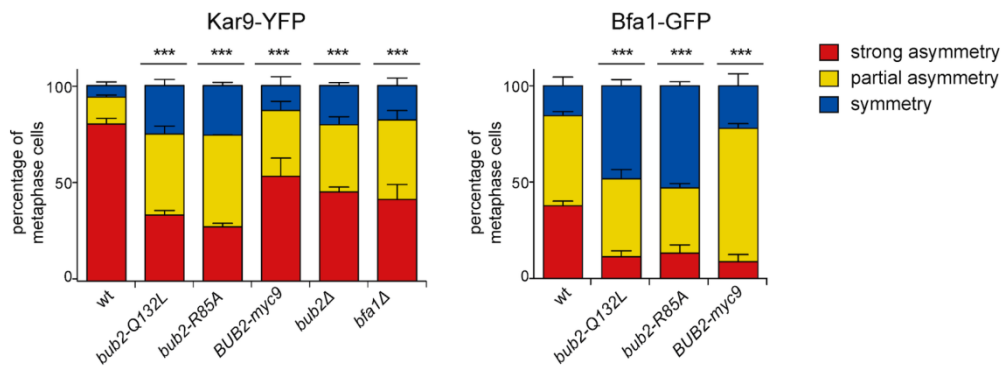
Figure 19 Percentage of metaphase cells carrying Kar9-eGFP(A) or Bfa1-eGFP on one SPB (strong asymmetry), both SPBs unequally (partial asymmetry) or both SPBs equally (symmetry) for the indicated strains after formaldehyde fixation.

We then asked if Kar9 mislocalization in our mutants affected spindle positioning. *SPC72-BFA1* and *TEM1-Q79L* cells expressing Spc42-mCherry were synchronized to collect cells in metaphase and imaged. Measurements of spindle distances from the bud neck (Fig. 20A) and spindle angles relative to the mother-bud polarity axis (Fig. 20B) indicated that both *TEM1-Q79L* and *SPC72-BFA1* cells significantly affected the position and the orientation of metaphase spindles. Thus, hyperactive Tem1 impaired Kar9-dependent spindle positioning.

In conclusion, although constitutive symmetric localization of Tem1 and its GAP Bub2/Bfa1 does not affect mitotic exit, it does compromise asymmetry of Kar9 at spindle poles, thereby causing spindle positioning and orientation defects.

A
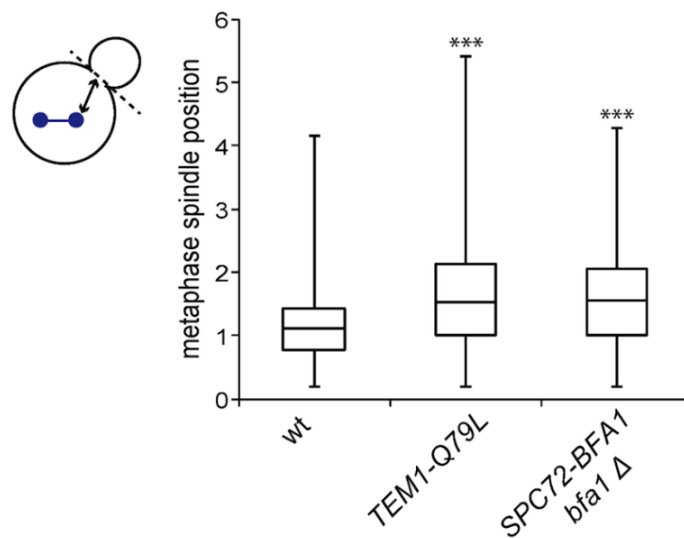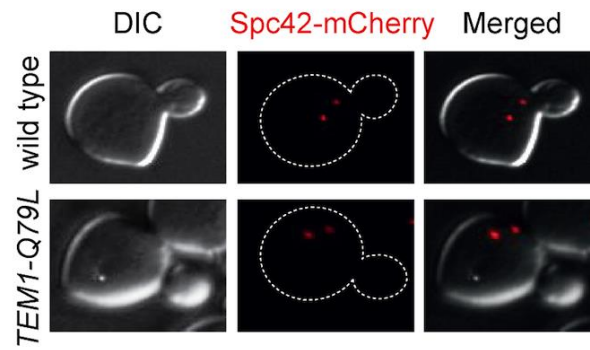
B
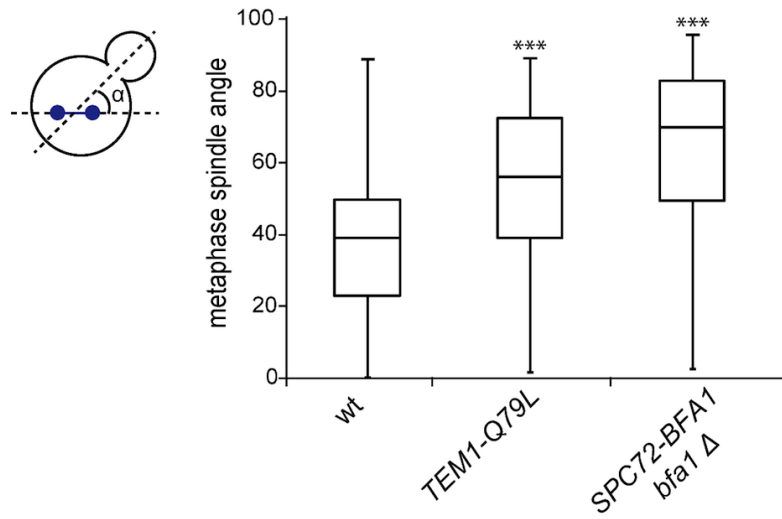
Figure 20 Spindle position (distance between the nearest SPB and the bud neck, **A**) and orientation (angle that the spindle forms with respect to the cell polarity axis, **B**) were measured in metaphase spindles of cells with the indicated genotypes after formaldehyde fixation (n≥100)

Materials and Methods

Abbreviations

BFB   Bromophenol Blue

BSA   Bovine Serum Albumine

EDTA   Ethylenediaminetetracetate

APC   Anaphase Promoting Complex

β-ME   β-MercaptoEthanol

Kb   Kilobase

kDa   Kilodalton

OD   Optical Density

PEG   Polyethylene glycol

rpm   Rounds per Minute

SDS   Sodium Dodecyl Sulphate

TCA   Trichloroacetic acid

TRIS   Tris-(hydroximethyl)-aminomethane

YNB   Yeast Nitrogen Base

NOC   Nocodazole

aa   Aminoacid

O/N   Overnight

RT   Room Temperature

SPBs   Spindle Pole Bodies

MEN	Mitotic Exit Network
FEAR	cdc Fourteen Early Anaphase Release
SAC	Spindle Assembly Checkpoint
SPOC	Spondle Position Checkpoint
GAP	GTPase Activating Protein
GEF	Guanine-nucleotide Exchanging Factor
GDI	Guanine-nucleotide Dissociation Inhibitor

Strains and plasmids

All strains, are derivatives of W303 (*ade2-1, trp1-1, leu2-3,112, his3-11,15, ura3, ssd1*).

Name	**Relevant genotype**
ySP52	*MATalpha, cdc15-2*
ySP285	*MATalpha, cdc14-3*
ySP311	*MATalpha, dbf2-2*
ySP325	*MATalpha, cdc5-2::URA3*
ySP1243	*MATa, bfa1::TRP1*
ySP1959	*MATa, BFA1-HA6::HIS3*
ySP1961	*MATa, BUB2-HA3::KlTRP1*
ySP2035	*MATalpha, BFA1-HA6::HIS3*

ySP3138	*MATa, bub2::HIS3*
ySP3197	*MATalpha, Myo1-GFP::KanMx4*
ySP3417	*MATa, tem1::URA3, [YCplac111-tem1-3]*
ySP3641	*MATalpha, TEM1-HA3::KlURA3*
ySP3673	*MATalpha, BFA1-GFP::URA3, bfa1::TRP1*
ySP3773	*MATa, BFA1-GFP::URA3, bfa1::TRP1, TEM1-HA3::KlURA3*
ySP3895	*MATa, slk19::HIS3*
ySP4091	*MATalpha, tem1::URA3, [pRS315-TEM1-GFP-KanMX4], BUB2-HA3::KlTRP1*
ySP4165	*MATalpha, tem1::URA3, [pRS315-TEM1-GFP-KanMX4]*
ySP4657	*MATa, SPC72-BUB2::BUB2::LEU2*
ySP5581	*MATalpha, SPC72::SPC72-BFA1::LEU2*
ySP5706	*MATalpha, SPC72::SPC72-BFA1::LEU2, bfa1::TRP1, tem1::URA3, [YCplac111-tem1-3]*
ySP5816	*MATa, bfa1::TRP1, tem1::URA3, [YCplac111-tem1-3]*
ySP5817	*MATalpha, bfa1::TRP1,tem1::URA3, [YCplac111-tem1-3]*
ySP5836	*MATalpha, SPC72::SPC72-BFA1::LEU2, bfa1::TRP1,*

tem1::URA3, [YCplac111-tem1-3], bub2::HIS3

ySP5837   *MATa,   SPC72::SPC72-BFA1::LEU2,   bfa1::TRP1, tem1::URA3, [YCplac111-tem1-3], bub2::HIS3*

ySP6270   *MATa, kar9::KanMX4*

ySP6292   *MATa, dyn1::KanMX4*

ySP6312   *MATa, bub2::bub2-Q132L::URA3*

ySP6432   *MATalpha, bub2::bub2-Q132L-HA3::TRP1::URA3*

ySP6435   *MATa, bub2::bub2-Q132L::URA3, BFA1-HA6::HIS3*

ySP6495   *MATa, dyn1::KanMX4, bub2::bub2-Q132L::URA3*

ySP6508   *MATalpha, kar9::KanMX4, bub2::bub2-Q132L::URA3*

ySP6552   *MATalpha, dyn1::KanMX4*

ySP6609   *MATa,   bub2:: L-HA3::TRP1::URA3,   tem1::URA3, [pRS315-TEM1-GFP-KanMX4]*

ySP6678   *MATa, bub2::HIS3, kar9::KanMX4*

ySP6680   *MATa, bub2::HIS3, dyn1::KanMX4*

ySP6744   *MATalpha,   cdc5-2::URA3,   SPC72::SPC72-BFA1::LEU2, bfa1::TRP1*

ySP6745   *MATa, cdc5-2::URA3, SPC72::SPC72-BFA1::LEU2, bfa1::TRP1*

ySP6775   *MATalpha,   bub2::bub2-Q132L-HA3::TRP1::URA3,*

BFA1-GFP::URA3, bfa1::TRP1

ySP6798 *MATa, BFA1-GFP::URA3, bfa1::TRP1, BUB2-HA3::KlTRP1*

ySP7214 *MATalpha, tem1::URA3, LEU2::TEM1*

ySP7217 *MATa, tem1::URA3, LEU2::TEM1-Q79L*

ySP7218 *MATalpha, tem1::URA3, LEU2::TEM1-HA3*

ySP7221 *MATa, tem1::URA3, LEU2::TEM1-Q79L-HA3*

ySP7270 *MATalpha, BFA1-GFP::URA3, bfa1::TRP1, tem1::URA3, LEU2::TEM1-Q79L-HA3*

ySP7277 *MATa, tem1::URA3, LEU2::TEM1-HA3, BFA1-GFP::URA3, bfa1::TRP1*

ySP7285 *MATa, BUB2-3PK::KlHIS3*

ySP7286 *MATa, TEM1-HA3::KlURA3, BUB2-3PK::KlHIS3*

ySP7287 *MATa, tem1::URA3, LEU2::TEM1-Q79L-HA3, BUB2-3PK::KlHIS3*

ySP7321 *MATa, BUB2-3PK::KlHIS3, tem1::URA3, LEU2::TEM1-HA3*

ySP7633 *MATalpha, dyn1::KanMX4, tem1::URA3, LEU2::TEM1-Q79L*

ySP7790 *MATa, GAL-ESP1::TRP1*

ySP7792 *MATa, bns1::KanMX4, spo12::HIS3*

ySP8713 *MATa,   mCherry-TUB1::URA3,   tem1::URA3, LEU2::TEM1-Q79L, BFA1::BFA1, eGFP::KanMX4*

ySP9164 *MATa, GAL-KIN4::TRP1*

ySP9448 *MATa,   BFA1::BFA1-eGFP::KanMX4,   mCherry-TUB1::URA3.*

ySP9534 *MATa,   BFA1::BFA1-eGFP::KanMX4,   mCherry-TUB1::URA3, kin4::KanMX4.*

ySP9545 *MATa, tem1::URA3, LEU2::TEM1-Q79L, BFA1::BFA1-eGFP::KanMX4, kin4::KanMX4, mCherry-TUB1::URA3*

ySP9623 *MATa,   BFA1::BFA1-eGFP::KanMX4,   mCherry-TUB1::URA3, cdc15-2*

ySP9665 *MATalpha,   tem1::URA3,   LEU2::TEM1-Q79L-HA3, CDC15-GFP::KanMX4, mCherry-TUB1::URA3*

ySP9666 *MATalpha,   CDC15-GFP::KanMX4,   tem1::URA3, LEU2::TEM1-HA3, mCherry-TUB1::URA3*

ySP9669 *MATa,   mCherry-TUB1::URA3,   tem1::URA3, LEU2::TEM1-Q79L,   BFA1::BFA1-eGFP::KanMX4, cdc15-2*

ySP9691 *MATa, SPC72::SPC72-BFA1::LEU2, bfa1::TRP1*

ySP9697   *MATa, tem1::URA3, LEU2::TEM1-Q79L-HA3, CDC15-GFP::KanMX4, kin4::KanMX4, mCherry-TUB1::URA3*

ySP9702   *MATalpha, CDC15-GFP::KanMX4, tem1::URA3, LEU2::TEM1-HA3, mCherry-TUB1::URA3, kin4::KanMX4*

ySP9736   *MATalpha, SPC72::SPC72-BFA1::LEU2, bfa1::TRP1, cdc15-2*

ySP9738   *MATalpha, SPC72::SPC72-BFA1::LEU2, bfa1::TRP1, dbf2-2*

ySP9790   *MATa, SPC72::SPC72-BFA1::LEU2, bfa1::TRP1, dyn1::KanMX4*

ySP9793   *MATa, SPC72::SPC72-BFA1::LEU2, bfa1::TRP1, clb2::LEU2*

ySP9797   *MATa, LEU2::TEM1-Q79L*

ySP9798   *MATalpha, LEU2::TEM1-Q79L*

ySP9825   *MATalpha, tem1::URA3, LEU2::tem1Q79L, Myo1-GFP::KanMx4*

ySP9829   *MATa, mCherry-TUB1::URA3, mob1::HIS3, GFP-MOB1::URA3*

ySP9830   *MATa, LEU2::TEM1-Q79L, mCherry-TUB1::URA3,*

mob1::HIS3, GFP-MOB1::URA3

ySP9831   *MATalpha, SPC72::SPC72-BFA1::LEU2, bfa1::TRP1, dyn1::KanMX4, kin4::KanMX4*

ySP9833   *MATalpha, LEU2::TEM1-Q79L, clb2::LEU2*

ySP9859   *MATalpha, SPC72::SPC72-BFA1::LEU2, bfa1::TRP1, cdc14-3*

ySP9860   *MATa, SPC72::SPC72-BFA1::LEU2, bfa1::TRP1, cdc14-3*

ySP9868   *MATa, dyn1::KanMX4, kin4::KanMX4*

ySP9870   *MATa, bns1::KanMX4, spo12::HIS3, SPC72::SPC72-BFA1::LEU2, bfa1::TRP1*

ySP9890   *MATalpha, GAL-KIN4::TRP1, SPC72::SPC72-BFA1::LEU2, bfa1::TRP1*

ySP9913   *MATa, cdc55::TRP1*

ySP9915   *MATa, bns1::KanMX4, spo12::HIS3, SPC72::SPC72-BFA1::LEU2, bfa1::TRP1, dyn1::KanMX4*

ySP9916   *MATalpha, bns1::KanMX4, spo12::HIS3, dyn1::KanMX4*

ySP9935   *MATa, LEU2::tem1-Q79L, clb2::LEU2*

ySP9938   *MATa, cdc55::TRP1, SPC72::SPC72-BFA1::LEU2,*

bfa1::TRP1

ySP9977   *MATa,   KAR9-eGFP::KanMX4,   SPC42-mCherry::NatN2*

ySP9998   *MATalpha, SPC72-BUB2::BUB2::LEU2*

ySP10042   *MATa, LEU2::TEM1-Q79L, GAL-KIN4::TRP1*

ySP10046   *MATa,   SPC72::SPC72-BFA1::LEU2,   bfa1::TRP1, TEM1-eGFP::KanMX4, mCherry-TUB1::URA3*

ySP10047   *MATalpha, CDC15-GFP::KanMX4, SPC72::SPC72-BFA1::LEU2, bfa1::TRP1, mCherry-TUB1::URA3*

ySP10064   *MATa, TEM1-eGFP::KanMX4, mCherry-TUB1::URA3*

ySP10065   *MATalpha,   TEM1-eGFP::KanMX4,   mCherry-TUB1::URA3*

ySP10066   *MATa, CDC15-GFP::KanMX4, mCherry-TUB1::URA3*

ySP10069   *MATa,   SPC72::SPC72-BFA1-eGFP::KanMX4::LEU2, bfa1::TRP, SPC42-mCherry::NatN2*

ySP10157   *MATa, clb2::LEU2*

ySP10162   *MATalpha,   SPC72-BUB2::BUB2::LEU2, dyn1::KanMX4*

ySP10268   *MATa,   KAR9-eGFP::KanMX4,   SPC42-mCherry::NatN2, tem1::URA3, LEU2::TEM1-Q79L*

ySP10289 *MATa,   SPC72-BUB2::BUB2::LEU2,   KAR9-eGFP::KanMX4, SPC42-mCherry::NatN2*

ySP10290 *MATa,   SPC72::SPC72-BFA1::LEU2,   bfa1::TRP1, KAR9-eGFP::KanMX4, SPC42-mCherry::NatN2*

ySP10392 *MATa, GAL-KIN4::TRP1, SPC72::SPC72-BFA1::LEU2*

ySP10399 *MATalpha, GAL-KIN4::TRP1, bfa1::TRP1*

ySP10447 *MATa,   SPC72::SPC72-BFA1::LEU2,   tem1::URA3, [YCplac111-tem1-3]*

ySP10472 *MATalpha, tem1-3*

ySP10560 *MATa, mob1-77::URA3*

ySP10594 *MATa, SPC72-BUB2::BUB2::LEU2, cdc55::TRP1*

ySP10622 *MATa, mob1-77::URA3, SPC72::SPC72-BFA1::LEU2, bfa1::TRP1*

ySP11224 *MATa, bfa1::TRP1, tem1::URA3, [YCplac111-tem1-3], bub2::HIS3*

ySP11225 *MATa, bfa1::TRP1, tem1::URA3, [YCplac111-tem1-3], bub2::HIS3*

ySP11453 *MATa, CDC15-GFP::KanMX4, mCherry-TUB1::URA3, bub2::bub2-Q132L::URA3*

ySP11452 *MATa, CDC15-GFP::KanMX4, mCherry-TUB1::URA3,*

bub2::HIS3

ySP11456   *MATa, SPC72-BUB2::BUB2::LEU2, GAL-ESP1::TRP1*

ySP11492   *MATa,   SPC72::SPC72-BFA1::LEU2,   bfa1::TRP1, GAL-ESP1::TRP1*

ySP11511   *MATa,   SPC72::SPC72-BFA1::LEU2,   bfa1::TRP1, slk19::HIS3*

ySP11513   *MATa,   SPC72::SPC72-BFA1::LEU2,   bfa1::TRP1, dyn1::KanMx4, slk19::HIS3*

ySP11515   *MATa, dyn1::KanMx4, slk19::HIS3*

ySP11534   *MATa, TEM1-eGFP::KanMX4, mCherry-TUB1::URA3, bub2::bub2-Q132L::URA3*

ySP11536   *MATa,   BFA1::BFA1-eGFP::KanMX4,   mCherry-TUB1::URA3, bub2::bub2Q132L::URA3*

ySP11583   *MATa, tem1::HPHMx [pRS315-TEM1-GFP-kanM46], mCherry-TUB1::URA3*

ySP11585   *MATa,   tem1::HPHMx   [pRS315-TEM1-Q79L-GFP-kanMX4], mCherry-TUB1::URA3*

ySP11619   *MATa, BUB2-eGFP::KanMx4, mCherry-TUB1::URA3*

ySP11621   *MATa,   bub2-Q132L-eGFP::KanMx4,   mCherry-TUB1::URA3*

ySP11623 *MATalpha, BFA1-GFP::URA3, bfa1::TRP1, BUB2-eGFP::KanMX4*

ySP11624 *MATalpha, BFA1-GFP::URA3, bfa1::TRP1, tem1::URA3, LEU2::tem1Q79L-HA3, BUB2-eGFP::KanMX4*

ySP11625 *MATa, tem1::URA3, LEU2::TEM1-HA3, BFA1-GFP::URA3, bfa1::TRP1, BUB2-eGFP::KanMX4*

<u>Media for *E.coli*</u>

LD	1% bactotryptone
	0,5% yeast extract
	0,5% NaCl pH7,25
LD agar	LD + 1% agar
LD ampicillin	LD + 50 μg/ml ampicillin
LD chloramphenicol	LD + 34 μg/ml chloramphenicol

Media for *S.cerevisiae*

YEP   1% yeast extract

                            2% bactopeptone

                            50mg/L adenine

YEPD   YEP + 2% glucose

YEPG   YEP + 2% galactose

YEPR   YEP + 2% raffinose

YEPRG   YEP + 2% raffinose and 1%galactose

                            1,36% $CH_3COONa_3H_2O$

Sporulation   plates   0,19% KCl

(VB)   0,0035% $MgSO_4$

                            0,12% NaCl

                            2% agar

Selection plates   0,7% Yeast nitrogen base (YNB)

                            2% glucose

                            25µg/ml aminoacids

                            2% agar

Reagents

5x SDS-PAGE running buffer	2M Glycine, 0.25M Tris, 1% SDS, pH 8.3
20x SSC	3M NaCl, 0.3M Na citrate, pH 7.5
TAE	0.04M Tris acetate, 1mM EDTA, pH 7.4
TE	10mM TRIS-HCl, 1mM EDTA, pH 7.4
10x TBS	1.5M NaCl, 0.5M TRIS-HCl, pH 8
Laemmli buffer	250 mM Tris, 1.9M Glycine, 1% SDS
Transfer buffer	250 mM Tris, 1.9M Glycine, 0.25% SDS
BLUE 6X	0.2% BFB in 50% glycerol

Strains construction

- Generation of diploid strains and sporulation

Diploid strains were generated by crossing haploid strains on the appropriate agar medium. In case of selection of diploid cells, after 24h of incubation at 25°C, crosses were transferred on selective medium and/or temperature allowing only diploid cells growth. Diploid cells were allowed to sporulate by transferring them to VB sporification medium. These plates were then incubated 3 days at 25°C. After zymolyase digestion of the cell wall, achieved by treating the cells with 0,025mg/ml

zymolyase 100T for 15 minutes at RT, tetrads were dissected with an optical micromanipulator on the appropriate agar medium. Plates were finally incubated 3 days at 25°C. Meiotic segregants were then replica plated to appropriate selective media and/or temperatures allowing analysis of their growth requirements.

- Generation of chimeric proteins

The *SPC72-BUB2* fusion was generated by triple ligation of a HindIII/XbaI PCR fragment containing the whole ORF of 340 bp of *SPC72* promoter, a XbaI/EcoRI PCR fragment containing the ORF of *BUB2* spanning codons 2-172, and the *LEU2*-based Yiplac128 vector linearized with HindIII and EcoRI. The generated plasmid (pSP275) was linearized with BamHI for integration at the *BUB2* locus, thereby generating a gene fusion under the *SPC72* promoter and containing the whole ORF of *SPC72* fused in frame to the entire ORF of *BUB2*, as well as a truncated *BUB2* gene lacking the last 134 codons. Single integration of the construct at the *BUB2* locus was checked by Southern blot.

The *SPC72-BFA1* fusion was generated by triple ligation of a HindIII/XbaI PCR fragment containing the whole ORF of 340 bp of *SPC72* promoter, a XbaI/BglII PCR fragment containing the entire ORF of *BFA1* starting from the 2nd codon and 330 bp of 3' UTR, and the

123

LEU2-based Yiplac128 vector linearized with HindIII and BamHI. The generated plasmid (pSP371) was linearized with PstI for integration at the *SPC72* locus and single integration of the construct at the *SPC72* locus was checked by Southern blot.

- Site-directed mutagenesis

The ORF of *TEM1* and about 1000 bp of promoter region was cloned in Yiplac128 (pSP596). A variant carrying the *TEM1-Q79L* mutation was generated by site-directed mutagenesis (pSP597) accordingly to the QuickChange site-directed mutagenesis kit (stratagene) instructions. The mutagenesis mix contained 2.5µl buffer, 16.7µl H2O, 0.75µl quick solution, 25ng plasmid template 125ng of each primer (SP522/523), 1µl dNTP mix, 1µl DNA polymerase. The *TEM1*-bearing plasmids have been integrated at the *LEU2* locus by BstXI digestion and single integrations have been checked by Southern blot.

- Gene deletion and tagging

Gene deletions were generated by one-step gene replacement (Wach et al.,1994). One-step tagging techniques (Janke et al.,2004; Sheff et al., 2004) were used to tag Tem1, Tem1-Q79L, Bfa1, Spc72-Bfa1 and Kar9 with 3HA or eGFP.

E.coli transformation

DH5α competent cells, kept at -80°C, were defrozen in ice. Amount of 50 – 100µl of cells was used for each reaction. After an incubation of 30 minutes in ice, 1 – 10ng of DNA was added to the cells. After an incubation of 30' in ice, cells underwent a 5' heat shock at 37°C, followed by 2' of incubation in ice. Finally, 1ml of LD medium was added to each reaction tube. Cell suspension was shaken for an hour at 37°C before being plated on selective medium and incubated at 37°C for 24 hours.

Yeast transformation

Cells were inoculated o/n at 25°C in YEP medium containing the appropriate sugar, allowing them to reach the stationary phase. Cell cultures were diluted and allowed to grow for at least 2 hours, until they reached concentration between 5×10^6 and 1×10^7 cells/ml. 10ml of culture were then centrifuged for 5' at RT. Pellet was washed with 1ml of 0.1M LiAc to completely eliminate the growth medium. The pellet was resuspended in 500µl of 0,1M LiAc. 1 – 2 µg of DNA were added to 100µl of cells suspension (sufficient for one transformation), together with 16µg of carrier DNA (salmon sperm DNA) and 45µl of 50% PEG 4000. After gently mixing, the tubes were incubated 30 – 60 minutes at RT.

Subsequently, 6µl of 50% glycerol was added to the cell suspension, followed by incubation at 30 – 60 minutes at RT. After 5 minutes of heat shock at 42°C, cells were finally plated on selective medium. In case of double crossing over at the desiderated locus, after the heat shock, cells were grown for at least 5 hours at 25°C or 30°C in non-selective conditions before plating on appropriate selective medium.

Preparation of plasmidic DNA from E. coli

Two different techniques were used, depending on the amount and the quality of DNA to be obtained.

- Mini preparations of plasmidic DNA

Plasmid-containing cells were inoculated in 2ml LD + amp and they were grown at 37°C o/n. Cells were then recovered by centrifugation in an eppendorf tube and resuspended in 0.5ml of STET. 50µl of 10mg/ml lysozyme solution was added prior to boiling the tube for 2 minutes. DNA was precipitated with isopropanol at -80°C. After centrifugation, the pellet was resuspended in 1x TE.

- Mini preparations of plasmidic DNA with E.Z.N.A plasmid Mini Kit I

Plasmid-containing cells were inoculated in 2ml LD + amp and they were grown at 37°C o/n. Cells were then recovered by centrifugation in an eppendorf tube and resuspended in 250μl of Solution I/RNase A solution. Then 250μl of Solution II was added and the suspension was incubated 2 – 3 minutes at RT, prior to adding 350μl of Solution III. Samples were spun at 13000 rpm for 10 minutes at RT. Then, the supernatant was loaded on a pre-equilibrated HiBind DNA Column and washed with 500μl of HB Buffer. Next, the column was washed twice with 700μl of DNA Wash Buffer. After drying the column, the DNA was eluted with 30 – 50μl of Elution Buffer.

Preparation of genomic DNA from yeast

Yeast cells of the desired strains were grown in 5ml YEP containing the appropriate sugar to log phase. Cells were collected by centrifuging and then washed with 1ml of a solution containing 0.9M sorbitol and 0,1M EDTA pH 7.5. Pellets were then transferred into 0.4ml of a solution containing 0,9M sorbitol, 0.1M EDTA pH 7.5 and 14mM β-ME. After mixing, 100μl of a 2μg/ml solution of Zymolyase 100T were added, and

the tubes were incubated at 37°C up to spheroplast formation (20 – 30 minutes), checked by optical microscopy. After 30 seconds of centrifugation, pellets were carefully resuspended in 0,4ml TE 1x. After addition of 90µl of a solution containing 1.5ml of EDTA pH 8.5, 600µl of Tris base and 600µl of 10% SDS, the tubes were mixed and incubated 30 minutes at 65°C. Next, 80µl of 5M potassium acetate were added and then tubes were incubated in ice for at least 1 hour. The tubes were then centrifuged for 15 minutes and the supernatant was precipitated and washed with ethanol. Dried pellets were carefully resuspended in 500µl of TE 1x. 25µl of RNase 1mg/ml were added to the tubes and the solutions were incubated 30 minutes at 37°C. DNA was precipitated by addition of 500µl of isopropanol and centrifuged. Pellets were washed with cold 70% ethanol, dried and finally resuspended in 50µl of TE 1X to obtain a final concentration of 100 µg/µl of yeast genomic DNA.

DNA digestions with restriction endonucleases and agarose gels

DNA samples were digested with the appropriate restriction enzymes, using the conditions described in Maniatis et al., 1989, or the manufacturer's instructions. 1/5 volumes of a BFB solution (6X stock solution: 0.2% BFB in 50% glycerol) were added to the digested

samples, before loading onto agarose gels at the optimal concentration (0.6% - 2%). Fragments were separated by virtue of their molecular weight, performing electrophoresis in TAE buffer. DNA was visualized by adding GelRed (diluted 1:10000) directly to the gel, and then by analysis of the gel with UV radiations of 260nm wavelength. To determine the size of the DNA fragments loaded onto the gel, a marker containing DNA fragments of known length (provided by Invitrogen) was loaded in parallel with the samples.

DNA purifications from agarose gels

DNA was purified from agarose gels according to GelExtract Mini Kit (5 PRIME).The fragment of interest was excised from the agarose gel. After weighing the gel slice, 3 volumes of buffer PS were added to 1 volume of gel and it was incubated at 50°C until it completely melted. The solution was loaded on equilibrated PCR Extract Mini Column CB2 and span shortly. Then, the column was twice with i) 700µl and ii) 500µl of Buffer PW. After being dried, the DNA was eluted with 30µl of Buffer PEB.

Ligations

Appropriate amounts of isolated fragment and of the vector, cut with restriction enzymes, were ligated in the following conditions:

10X T4 DNA Ligase Buffer   1µl

T4 DNA Ligase (Promega)   1µl

The reaction volume was corrected with water to a final volume of 10µl and the resulted mix was incubated at 16°C o/n.

Southern blot analysis

Yeast DNA was prepared according as described above and digested with the appropriate endonuclease(s). The resulting DNA fragments were separated by gel electrophoresis in 0.6% agarose gels and transferred (Maniatis et al., 1989) to Amersham HybondTM-N+ nylon membrane (GE Healthcare), followed by hybridization with an appropriate DIG-labelled probe. Standard hybridization conditions for DIG labelled probes were used. After appropriate washes, the membrane was treated with an alkaline phosphatase. The membrane was incubated with CSPD, allowing the detection of phosphatase activity by a chemiluminescence reaction, which was then revealed by exposing the blot to X-ray film.

Polymerase Chain Reaction (PCR)

PCR was performed on plasmidic DNA preparations (E.Z.N.A.) or on genomic yeast DNA. A DNA fragment amplification requires two nucleotides flanking the region of amplification, working as primers for the DNA polymerase. Different DNA

polymerases were used: Taq polymerase (GeneSpin), Vent polymerase (Biolabs), Pfu polymerase (Stratagene), depending on the kind of DNA template and fidelity of the amplified fragment. The reaction mix was:

Plasmidic DNA	10ng
10x Buffer	2.5µl
Primers	0.6µM/each
dNTPs	0.1mM/each
DNA polymerase	1-2 units
H2O	to 25µl

DNA amplification was performed with PTC-100 Peltier Thermal Cycler (MJ Research), with the following parameters:

1. denaturation step 3' at 95°C

2. denaturation step 30'' at 95°C

3. annealing step 30'' at primers Tm

4. extension step depending on DNA polymerase (1'-2' per kb)

5. repeat steps from 2 to 4 25/30 times

6. extension step 10' at 72°C

7. end

A primer's melting temperature (Tm) was calculated with the following formula:

Tm = 4(G + C) + 2(A + T) °C

Synchronization with α-factor

MATa cells were inoculated in YEP medium supplied with the appropriate sugar, allowing them to reach a concentration of 5 x 10^6 cells/ml. α-factor (provided by Genescript) was then added to a final concentration of 2μg/ml. 1 hour later α-factor was re-added to a final concentration of 2μg/ml and 1 hour later the percentage of budded cells was scored. When more than 95% of cells was unbudded (G1-arrested cells), the pheromone was removed and cells were washed once with fresh medium and then resuspended and incubated in fresh medium.

Synchronizations were performed at 25°C. If the release was into a medium at different temperature than 25°C, medium was pre-heated or pre-chilled to the appropriate temperature.

Nocodazole response

Nocodazole arrests yeast cells in metaphase, by causing microtubule depolimerization. For nocodazole arrest, cells were released from G1 arrest in the presence of 15µg/ml nocodazole (Sigma) dissolved in DMSO. The final concentration of DMSO in the cell cultures was 1%.

Protein extracts with TCA

Cells were collected by centrifugation and resuspended in 1ml of TCA20%. Cells were then transferred into eppendorf tubes and resuspended in 100µl of TCA20%. Equal amount of acid-treated glass-beads were then added to each suspension, and cells were broken by vortexing 7' at RT. Samples were then transferred into new tubes and clarified by centrifugation. Clarified extracts were resuspended in 50µl 3X Laemmli buffer (0,62M Tris, 2% SDS, 10% glycine, 0,001% BFB, 100mM DTT), boiled 3' and loaded on a polyacrylamide gel

Immunoprecipitation

50ml of 1×10^7 cells/ml concentration culture was collected, washed and resuspended in 200µl of lysis buffer (50mM Tris-HCl pH 7.5, 150mM NaCl, 1% NP-40, 10% glycerol, 1mM sodium orthovanadate, 60mM β-

glycerophosphate and a protease inhibitor cocktail provided by Boehringer Mannheim). Eppendorf tubes were always kept in ice. An equal amount of acid-treated glass beads was then added to the suspension, and cells were broken by 7 cycles of 30" of vortexing/30" ice. The samples were then transferred to new eppendorf tubes and clarified by centrifuging for 10' on 14680 rpm at 4°C. 2µl of protein extracts were taken for quantification of the amount of protein extract at spectrophotometer at UV light (280 nm wavelength). HA-tagged proteins were immunoprecipitated from 1mg of total extract by α-HA resin (provided by Roche). The samples were incubated 2 hours at 4°C. Then, the resin was washed at least three times with lysis buffer and two times with PBS 1X. Finally, 25µl of 3X Laemmli were added to samples and samples were boiled for 3 minutes in order to extract proteins bound to the resin.

Western blot analysis

Proteins were separated based on their molecular weight on 10% or 12% SDS-PAGE (denaturing polyacrylamide gel). The transfer of proteins on nitrocellulose filters was performed o/n under 200mA electric current. Filter was incubated 1 hour at RT with 5% non-fat dry milk or with 5%

Bovine Serum Albumin (BSA) prepared by dissolving in 1X TBS with 0,1%Tween-20 (TBS-T). Nitrocellulose membrane was then incubated 2 hours at RT (or o/n at 4°C) with primary antibodies directly diluted in 5% milk. To detect HA-tagged proteins we used monoclonal antibodies 12CA5 diluted 1:5000. To detect GFP-tagged proteins we used α-GFP polyclonal antibodies diluited 1:1000. The membrane was then washed three times in 1x TBS-T for 10 minutes, before incubating it for 1 hour at RT with secondary antibodies (1:10000 anti-mouse IgG, anti-rabbit IgG or anti-goat IgG). These secondary antibodies, provided by Amersham™ were conjugated to peroxidase enzyme. The membrane was finally washed three times with TBS-T for 10 minutes, dried on 3MM paper and carefully dipped in a mixcomposed of equal amounts of the two ECL solutions (ECL kit was provided by Amersham™). After drying of the filter, it was exposed for different times to a X-ray film.

FACS analysis and percentage of budded and binucleated cells

This method requires DNA staining with Propidium Iodide, and successive determination of DNA contents of the cells by Fluorescence-Activated Cell Sorter (FACS). 5×10^6-2×10^7 cells were taken at each time point, collected by centrifugation and then resuspended in 1ml of

70% ethanol, prior to 1 hour of incubation at RT. Cells were then washed once with 1ml of 50mM Tris pH 7.5 and then resuspended in 1ml of 50mM Tris pH 7.5 containing 1mg/ml RNase. After incubation o/n at 37°C, cells were collected by centrifugation, dissolved in 0.5ml of pepsin 5mg/ml, freshly dissolved, in 55mM HCl and incubated for 30 minutes at 37°C. Cells were then washed once with 1ml of FACS buffer (200mM Tris pH 7.5, 200mM NaCl, 78mM $MgCl_2$) and resuspended in the same buffer containing 50µg/ml Propidium Iodide. Samples were finally analysed with a FACSCalibur device (BD Biosciences). Percentage of budded and binucleate cells was scored microscopically on samples treated for FACS analysis.

Fluorescence microscopy

Cells were fixed in 1ml IF buffer (0.1M K^+/PO_4^{3-} buffer pH 6.4, 0.5mM MgCl2) containing 3.7% formaldehyde o/n at 4°C. Samples were washed three times with IF buffer and once with IF buffer containing 1.2M sorbitol. Cells were spheroplasted by incubating 20 - 30 minutes at RT in 200µl spheroplasting solution (250µg/ml zymolyase, 1.2M sorbitol, 0.1M K^+/PO_4^{3-} buffer pH 6.4, 0.5mM $MgCl_2$). Spheroplasting was monitored by mixing a drop of cells in spheroplasting solution with an equal amount of

10% SDS. The spheroplasts were then washed once with IF buffer containing 1.2M sorbitol and resuspended in 20 - 200µl of the same solution, depending on amount of the cells. A 30-wells slide was coated with 0.1% poly-Lysine, rinsed with H_2O and dried. A drop of cell suspension of medium density was spotted on each well and left for 5 – 10 minutes to allow the cells to attach to the slide surface. The cell suspension was then removed, the slide was placed in a methanol bath at -20°C for 6', and in acetone bath at -20°C for 30". Next, the slide was dried. Proper primary antibody was added to each well and left to incubate for two hours at RT (or o/n at 4°C) in a dark and humid chamber. Then the antibody was aspirated off and each well was washed three times with PBS/BSA solution. Then the appropriate secondary antibody was added to each well and incubated for 1 hour at RT in a dark and humid chamber. Next, the secondary antibody was aspirated off and each well was washed four times with PBS/BSA solution. For DAPI staining, a drop of pd-DAPI (0.25µg/ml DAPI – 4.6 diamino-2-Phenylindolo-, 0.1% p-phenylendiamine, and 10% PBS pH 8.0 in glycerol) was added to each well, and the coverslip was placed over and sealed using nail hardener. Slides were stored at -20°C in the dark until use. To detect spindle formation and elongation, anti-tubulin

immunostaining was performed with the YOL34 monoclonal antibody (Serotec) diluited 1:100 in BSA/PBS (1% crude BSA, 0.04M K_2HPO_4, 0.01M KH_2PO_4, 0.15M NaCl) followed by indirect immunofluorescence using Cy2-conjugated anti-rat antibody (GE Healthcare) diluited 1:100. Cells expressing GFP and mCherry-tagged proteins were grown in minimum complete medium. Digital images of live cells, cells fixed with 3.7% formaldehyde or cold EtOH were taken with an oil 63X 1.4-1.6 HCX Plan-Apochromat objective (Zeiss) with a Coolsnap HQ2-1 charge device camera (Photometrics) mounted on a ZeissAxioimager Z1/Apotome fluorescence microscope controlled by the MetaMorph imaging system software. Z-stacks of 12 planes at 0.3 µm step size were acquired.

Time Lapse analysis

For time lapse video microscopy of Myo1-GFP strain, cells were mounted in low autoflorescence selective drop-in medium shortly before viewing. Movies were recorded with a DeltaVision microscope and a 100× oil immersion objective using the Softworx software (Applied Precision). Individual Z stacks contained 10 planes with a step size of 0.6 µm. After image acquisition the movies were projected as max intensity projections.

Imaging analysis and processing

Fluorescence intensity measurements of max intensity-projected images were performed using the ImageJ software. The index of Bfa1 symmetric distribution (σ) was measured using the following equation: $\sigma_{(0<\sigma<1)} = I_1/I_2$, where I_1 is the fluorescence intensity of the brightest of the two SPBs, and I_2 is the fluorescence intensity of the dimmest. The position and the orientation of the spindle was measured on max intensity-projected images using ImageJ. The position was determined measuring the distance between the bud neck and the nearest SPB. The orientation was determined measuring the smaller of the two angles that the spindle forms intersecting the polarity axis of the cell. Adobe Photoshop and ImageJ were used to mount the images and to produce merged color images.

Drop test

For drop test analysis, cultures of cells were grown o/n at 10^8 cells/ml and then serial dilutions of the cultures were made to 1.25×10^6, 1.25×10^5, 1.25×10^4, 1.25×10^3 cells/ml. For each dilution 5µl of suspension was spotted on plate and incubated at the indicated temperature.

Discussion

Tem1 GTP hydrolysis involves a catalytic glutamine in the switch II and the GAP Bub2/Bfa1

The mechanistic details of how GTPases switch between a GTP- and a GDP-bound state build on initial structural studies on Ras. In Ras a conserved glutamine in the switch II domain of the GTPase and a conserved arginine of the GAP both contribute to GTP hydrolysis (Ahmadian et al., 1997; Scheffzek et al., 1997) and, consistently, mutations of either residue abolish GTP hydrolysis. Crystal structure of some Rab GTPases complexed with their TBC (Tre-2, Bub2 and Cdc16) GAP revealed that the conserved switch II glutamine (Q79 of Tem1) does not directly participate in GTP hydrolysis. Rather, catalysis is entirely brought about by a conserved arginine and a conserved glutamine of the TBC GAP through a mechanism referred to as "dual-finger" (Pan et al., 2006; Gavriljuk et al., 2011). Hence, the switch II glutamine of the GTPase was proposed to stabilize its interaction with the GAP (Pan et al., 2006). Recently, Rab GTPases have been shown to be more plastic than originally anticipated in their activation/hydrolysis mechanisms. In particular, the contribution of the switch II glutamine in GTP hydrolysis is variable and for some GTPases it contributes, together with a conserved lysine in the P-loop, to activation of the GTPase by

stabilizing its GEF-bound nucleotide-free form (Langemeyer et al., 2014). Therefore, the outcome of mutations of conserved catalytic residues varies depending on the GTPase, GEF and GAP, and is altogether unpredictable.

Here we have addressed the importance of Q79 in the switch II and the dual-finger mechanism in Tem1 GTP hydrolysis. First, we have established that the intrinsic rate of Tem1 GTP hydrolysis is negligible, and loss of GTP is mostly accounted for by nucleotide dissociation. In agreement with previous data (Fraschini et al 2006; Geymonat et al., 2002; Geymonat et al., 2009), Bfa1 prevents nucleotide dissociation and therefore acts as guanine-nucleotide dissociation inhibitor (GDI). Second, we show for the first time that Tem1 Q79 is directly involved in the GAP-induced GTP hydrolysis without impairing its interaction with Bub2 and Bfa1. Mutation of Q79 into leucine generates a hyperactive, dominant Tem1 that is refractory to its GAP, recruits more efficiently Cdc15 to SPBs and leads to unscheduled mitotic exit in the presence of spindle positioning defects.

Finally, we show that the dual-finger mechanism applies also to GTP hydrolysis of the Tem1-Bub2-Bfa1 complex. Indeed, glutamine 132 of Bub2 is involved in GTP hydrolysis, in addition to arginine 85 that we

144

previously showed (Fraschini et al., 2006). Consistent with an important role of Q132 in Tem1 inhibition, *bub2-Q132L* mutant cells are SPOC-defective and undergo mitotic exit upon microtubule depolymerization. Thus, we have defined Q79 of Tem1 together with R85 and Q132 of Bub2 as a catalytic triad for GAP-induced GTP hydrolysis.

Asymmetry of Bub2/Bfa1 and MEN activation

The Bub2/Bfa1 complex is required for efficient Tem1 binding to SPBs throughout most of the cell cycle, except in late mitosis (Valerio-Santiago et al., 2011; Pereira et al., 2000; Caydasi et al., 2012). In contrast, SPB recruitment of Bub2/Bfa1 does not require Tem1 (Geymonat et al., 2009; Pereira et al., 2000). The amount of Tem1 at SPBs depends on the turnover of Bub2/Bfa1 at SPBs, which in turn is accelerated by spindle mispositioning through Kin4-dependent phosphorylation of Bfa1 [35,38]. Thus, as recently proposed [50], the GAP Bub2/Bfa1 is a major Tem1 receptor at SPBs and its regulation is instrumental for establishing Tem1 asymmetry. Critical regulators of Bub2/Bfa1 asymmetry are the polo kinase Cdc5 and the phosphatase PP2A^{Cdc55}. Cdc5 phosphorylates and inactivates the Bub2/Bfa1 complex leading to Tem1 activation (Geymonat et al., 2003; Hu et al.,2001), whereas PP2A^{Cdc55} dephosphorylates Bfa1 (Baro et al., 2003). Phosphomimetic mutations in some Cdc5-dependent Bfa1 phosphorylation sites, as well as loss of PP2A^{Cdc55}, are sufficient to induce premature asymmetry of Bub2/Bfa1 at SPBs, whereas Cdc5 inactivation or phospho-ablating mutations in Bfa1 lead to its persistent symmetry (Kim et al., 2012; Baro et al., 2013). Similar mechanisms might be operational in fission yeast to establish SIN

asymmetry. Indeed, polo kinase has been proposed to phosphorylate the Bfa1 homolog Byr4 and promote its dissociation from SPBs (Johnson et al., 2011), thereby influencing the distribution of GTP-bound Spg1 and its effector kinase Cdc7. Furthermore, PP2A regulates Byr4 asymmetry through dephosphorylation of the SIN anchor at SPBs Cdc11 (Krapp et al., 2003; Singh et al., 2011). Indeed, Byr4 binds more efficiently to dephosphorylated Cdc11 (Krapp et al., 2003), wheras the Cdc15-like kinase Cdc7 binds preferentially phosphorylated Cdc11 (Feoktistova et al., 2012). Thus, common regulatory mechanisms might underlie both MEN and SIN asymmetry.

We previously proposed that Tem1 GTP hydrolysis promotes asymmetry of both Tem1 and its GAP Bub2/Bfa1 at SPBs in anaphase (Fraschini et al., 2006) and results from other studies (Valerio-Santiago et al., 2011; Kim et al., 2012) support this conclusion. Consistent with this idea, we now show that mutating the second catalytic finger of Bub2 (Q132) or mutating the catalytic Q79 of Tem1 leads in both cases to increased symmetry of Bub2/Bfa1 and Tem1 at SPBs. At a first glance these results appear at odds with the finding that in the complete absence of Tem1 Bub2/Bfa1 is not only recruited to SPBs with normal kinetics, but becomes asymmetric in anaphase exactly like in wild type cells

147

(Geymonat et al., 2009). However, we now show that when GTP hydrolysis is abolished Bub2 and Bfa1 bind more avidly to Tem1. Thus, the increased symmetry of Bub2/Bfa1 at SPBs in these conditions likely reflects its stronger affinity for GTP-bound Tem1. The different affinity of Bub2/Bfa1 for GTP- versus GDP-bound Tem1 has important implications for the SPOC, where active Tem1 needs to be quickly inactivated in the presence of a mispositioned spindle.

Based on our previous results using a version of Bub2 tagged with nine myc epitopes at the C-terminus (Bub2-myc9), we proposed that removal of Bub2/Bfa1 from the mother SPB is important for timely mitotic exit (Fraschini et al, 2006). Indeed, Bub2-myc9 is more symmetrically localized at SPBs than wild type Bub2 and is lethal for *cdc5-2* and *tem1-3* mutants because it prevents mitotic exit in these sensitized backgrounds. Now we further tested this idea by expressing chimeric proteins that constitutively recruit the GAP and Tem1 to both SPBs. Contrary to our predictions, these chimeric proteins rescued, instead of aggravating, the temperature-sensitive growth phenotype of several MEN mutants. In particular, Spc72-Bfa1 rescued the temperature-sensitivity of *tem1-3* cells likely by suppressing the SPB-binding defects of the mutant Tem1-3 protein at high temperature (Asakawa et al., 2001). Importantly,

suppression of MEN mutants by our chimeric proteins is not accounted for by their possible impaired GAP activity, because it could not be recapitulated by *BFA1* and/or *BUB2* deletion.

The chimeric proteins Spc72-Bfa1 and -Bub2 caused also unscheduled mitotic exit in the presence of mispositioned spindles, similar to Bub2- and Bfa1-Cnm67 fusion proteins previously characterized (Caydasi et al., 2009). Therefore, despite different parts of Bub2 and Bfa1 are fused to the SPB anchor (the N-terminus in our Spc72- fusions and the C-terminus in the -Cnm67 chimera), constitutive binding of the Bub2/Bfa1 complex to SPBs invariably leads to SPOC defects. Our data are totally consistent with the notion that Tem1 recruitment to SPBs is necessary for its MEN function [21]. In this scenario, SPB-locked Bub2/Bfa1 activates Tem1 by increasing its symmetry and residence time at SPBs. The molecular basis for SPB-driven Tem1 activation is not known. It is possible that the GAP Bub2/Bfa1 at SPBs is constitutively kept inactive by Cdc5-mediated phosphorylation, thereby making Tem1 at SPBs refractory to GAP-mediated inhibition. Upon spindle misalignment, Kin4-mediated dislodgement of Bub2/Bfa1 from SPBs becomes essential for Tem1 inhibition in the cytoplasm and SPOC response (Caydasi et al., 2009; Caydasi et al., 2012). An interesting non-mutually exclusive

hypothesis is that a putative GEF for Tem1 localizes at SPBs (Hotz et al., 2014). However, as mentioned above the identity of Tem1 GEF(s) remains elusive.

The finding that the chimeric proteins Spc72-Bfa1 and -Bub2, similar to Bub2- and Bfa1-Cnm67 (Caydasi et al., 2009) and Cnm67-Tem1 (Valerio-Santiago et al., 2011), support a mitotic arrest after microtubule depolymerization, but not after spindle mispositioning, was somehow puzzling. One major difference between the SAC-mediated metaphase arrest and the SPOC-mediated anaphase arrest is that in the latter, but not in the former, the PP2A^{Cdc55} phosphatase is inhibited by the FEAR pathway (Stegmeier et al., 2002; Queralt et al.,2006). We find that, indeed, *CDC55* deletion or *ESP1* overexpression in cells expressing Spc72-Bub2 or -Bfa1 drives unscheduled mitotic exit in the presence of nocodazole. In contrast, FEAR inhibition by deletion of *SPO12* and *BNS1* (Stegmeier et al., 2002) prevents mitotic exit in cells expressing the same chimeric proteins and experiencing spindle positioning defects. Thus, whether the FEAR is activated or inhibited influences the impact of the chimeric proteins on mitotic exit. PP2A^{Cdc55} has been recently shown to antagonize the Cdc5-dependent phosphorylation of Bfa1 (Baro et al., 2013, thereby providing a mechanistic explanation to our data. The

FEAR-mediated partial release of Cdc14 from the nucleolus might also contribute to MEN activation by counteracting the CDK-dependent inhibitory phosphorylation of MEN components (Konig et al., 2010).

In conclusion, persistent symmetric localization of the GAP Bub2/Bfa1 does not interfere with mitotic exit. Most likely, the Bub2-myc9 protein that we described previously prevents timely MEN activation by a different mechanism. Consistently, tagging of Spc72-Bub2 at the C-terminus with nine myc epitopes causes synthetic sickness in combination with the *cdc5-2* mutant allele affecting the polo kinase.

An unanticipated role of Bub2/Bfa1 and Tem1 asymmetry on Kar9 distribution and spindle positioning

We show that symmetric localization of the Bub2/Bfa1/Tem1 complex, independently of whether it is driven by chimeric proteins or loss of GTPase activity, interferes with Kar9 asymmetry at spindle poles in metaphase, as well as with spindle positioning and orientation relative to the cell division axis. Although Tem1 inactivation causes similar phenotypes for what concerns Kar9 localization and spindle orientation, it does not affect spindle positioning at the bud neck (Hotz et al., 2012), indicating that Tem1 hyperactivation and inactivation are not equivalent in this respect. The molecular bases of this difference remain to be established. Similarly, whether Tem1 hyperactivation primarily affects Kar9 localization and, as a consequence, spindle positioning or vice-versa remains to be investigated. Although the phenotypic analyses of our mutants did not reveal any apparent alterations of astral microtubules, at the moment we cannot exclude that subtle defects in microtubule dynamics could account for spindle mispositioning and, in turn, increased Kar9 symmetry.

Previous (Cepeda-Garcia et al., 2010) and our data indicate that not all conditions leading to symmetric distribution of the Bub2/Bfa1 complex

and Tem1 cause symmetric localization of Kar9 at spindle poles. Indeed, whereas Bub2, Bfa1, Tem1 and Kar9 are all asymmetric, to different extents, on metaphase spindles, Bub2, Bfa1 and Tem1 become increasingly more symmetric upon spindle misalignment, while Kar9 remains strongly asymmetric. These data suggest that establishment of Bub2/Bfa1/Tem1 symmetry on misaligned spindles is an active process and Kar9 asymmetry is so robust that once established it cannot be reversed by bringing the Bub2/Bfa1/Tem1 complex to both spindle poles. In contrast, in our mutants Bub2, Bfa1 and Tem1 are more symmetric already in metaphase and might therefore interfere with the establishment of Kar9 asymmetry. Furthermore, we speculate that in these mutants the residence of Tem1 and the GAP Bub2/Bfa1 at SPBs is relatively stable, while these proteins turn over very fast at the SPBs of misaligned spindles (Caydasi et al., 2009)

Factors involved in cell polarity were implicated in the asymmetry of Bub2-Bfa1 at spindle poles (Fraschini et al., 2006; Monje-Casas et al., 2009. Thus, it is tempting to speculate that in budding yeast the role of cell polarity in spindle positioning might be partly exerted through asymmetric localization of the Bub2-Bfa1-Tem1 trimeric complex at spindle poles, which in turn influences Kar9 asymmetry. Remarkably,

other eukaryotic cells (i.e. nematodes, flies and mammals) employ heterotrimeric G proteins for spindle positioning during both symmetric and asymmetric cell division (reviewed in Hampoelz et al., 2004). A striking parallel can be drawn between the asymmetric enrichment of their GDIs GPR-1/2, which is controlled by polarity factors and necessary for proper spindle alignment (reviewed in Gonczy 2008), and asymmetric localization of Bub2-Bfa1. Future work will certainly shed new light onto possible additional similarities in the mechanisms adopted by different organisms to achieve correct spindle positioning.

References

Abrieu A, Magnaghi-Jaulin L, Kahana JA, Peter M, Castro A, Vigneron S, Lorca T, Cleveland DW and Labbé JC (2001) Mps1 is a kinetochore-associated kinase essential for the vertebrate mitotic checkpoint. Cell. 106: 83-93.

Adames NR and Cooper JA (2000) Microtubule interactions with the cell cortex causing nuclear movements in Saccharomyces cerevisiae. J Cell Biol. 149: 863-74.

Ahmadian MR, Stege P, Scheffzek K, Wittinghofer A (1997) Confirmation of the arginine-finger hypothesis for the GAP-stimulated GTP-hydrolysis reaction of Ras. Nat Struct Biol 4: 686-689.

Araki Y, Lau CK, Maekawa H, Jaspersen SL, Giddings TH Jr, Schiebel E, Winey M. (2006) The Saccharomyces cerevisiae spindle pole body (SPB) component Nbp1p is required for SPB membrane insertion and interacts with the integral membrane proteins Ndc1p and Mps2p. Mol Biol Cell. 17: 1959-70.

Arquint C, Gabryjonczyk AM, Nigg EA (2014) Centrosomes as signalling centres. Philos Trans R Soc Lond B Biol Sci 369.

Asakawa K, Yoshida S, Otake F, Toh EA (2001) A Novel Functional Domain of Cdc15 Kinase Is Required for Its Interaction With Tem1 GTPase in Saccharomyces cerevisiae. Genetics 157: 1437-1450.

Azzam R, Chen SL, Shou W, Mah AS, Alexandru G, Nasmyth K, Annan RS, Carr SA and Deshaies RJ. (2004) Phosphorylation by cyclin B-Cdk underlies release of mitotic exit activator Cdc14 from the nucleolus. Science. 305: 516-9.

Bardin AJ and Amon A. (2001) Men and sin: what's the difference? Nat Rev Mol Cell Biol. 2: 815-26.

Bardin AJ, Visintin R, Amon A. (2000) A mechanism for coupling exit from mitosis to partitioning of the nucleus. Cell.102: 21-31.

Baro B, Rodriguez-Rodriguez JA, Calabria I, Hernaez ML, Gil C, et al. (2013) Dual Regulation of the mitotic exit network (MEN) by PP2A-Cdc55 phosphatase. PLoS Genet 9: e1003966.

Bedhomme M, Jouannic S, Champion A, Simanis V, Henry Y. (2008) Plants, MEN and SIN. Plant Physiol Biochem. 46: 1-10.

Bement WM, Benink HA and von Dassow G. (2005) A microtubule-dependent zone of active RhoA during cleavage plane specification. J Cell Biol.170: 91-101.

Bertazzi DT, Kurtulmus B and Pereira G (2011) The cortical protein Lte1 promotes mitotic exit by inhibiting the spindle position checkpoint kinase Kin4. J Cell Biol. 193: 1033-48.

Betschinger J, Mechtler K and Knoblich JA (2003) The Par complex directs asymmetric cell division by phosphorylating the cytoskeletal protein Lgl. Nature 422: 326-330.

Bi E, Maddox P, Lew DJ, Salmon ED, McMillan JN, Yeh E and Pringle JR (1998) Involvement of an actomyosin contractile ring in Saccharomyces cerevisiae cytokinesis. J Cell Biol. 142: 1301-12.

Bohnert KA and Gould KL. (2011) On the cutting edge: post-translational modifications in cytokinesis. Trends Cell Biol. 21: 283-92.

Bourne HR, Sanders DA, McCormick F (1990) The GTPase superfamily: a conserved switch for diverse cell functions. Nature 348: 125-132.

Bourne HR, Sanders DA, McCormick F (1991) The GTPase superfamily: conserved structure and molecular mechanism. Nature 349: 117-127.

Calabria I, Baro B, Rodriguez-Rodriguez JA, Russiñol N and Queralt E. (2012) Zds1 regulates PP2A(Cdc55) activity and Cdc14 activation during mitotic exit through its Zds_C motif. J Cell Sci. 125: 2875-84.

Carminati JL and Stearns T (1997) Microtubules orient the mitotic spindle in yeast through dynein-dependent interactions with the cell cortex. J Cell Biol. 138: 629-41.

Caydasi AK, Ibrahim B, Pereira G (2010) Monitoring spindle orientation: Spindle position checkpoint in charge. Cell Div 5: 28.

Caydasi AK, Kurtulmus B, Orrico MI, Hofmann A, Ibrahim B and Pereira G (2010) Elm1 kinase activates the spindle position checkpoint kinase Kin4. J Cell Biol. 190: 975-89.

Caydasi AK, Lohel M, Grunert G, Dittrich P, Pereira G, et al. (2012) A dynamical model of the spindle position checkpoint. Mol Syst Biol 8: 582.

Caydasi AK, Micoogullari Y, Kurtulmus B, Palani S and Pereira G. (2014) The 14-3-3 protein Bmh1 functions in the spindle position checkpoint by breaking Bfa1 asymmetry at yeast centrosomes. Mol Biol Cell. 25: 2143-51.

Caydasi AK, Pereira G (2009) Spindle alignment regulates the dynamic association of checkpoint proteins with yeast spindle pole bodies. Dev Cell 16: 146-156.

Cao LG and Wang YL (1996) Signals from the spindle midzone are required for the stimulation of cytokinesis in cultured epithelial cells. Mol Biol Cell. 7: 225-32.

Cepeda-García C, Delgehyr N, Juanes Ortiz MA, ten Hoopen R, Zhiteneva A and Segal M (2010) Actin-mediated delivery of astral microtubules instructs Kar9p asymmetric loading to the bud-ward spindle pole. Mol Biol Cell. 21: 2685-95.

Cerutti L and Simanis V.(1999) Asymmetry of the spindle pole bodies and spg1p GAP segregation during mitosis in fission yeast. J Cell Sci. 112: 2313-21.

Chan LY, Amon A (2010) Spindle position is coordinated with cell-cycle progression through establishment of mitotic exit-activating and -inhibitory zones. Mol Cell 39: 444-454.

Cheng X, Shen Z, Yang J, Lu SH and Cui Y. (2008) ECRG2 disruption leads to centrosome amplification and spindle checkpoint defects contributing chromosome instability.J Biol Chem. 283: 5888-98.

Chen RH, Waters JC, Salmon ED and Murray AW (1996) Association of spindle assembly checkpoint component XMAD2 with unattached kinetochores. Science. 274: 242-6.

Craddock C, Lavagi I, Yang Z (2012) New insights into Rho signaling from plant ROP/Rac GTPases.Trends Cell Biol. 22: 492-501.

Crosio C, Fimia GM, Loury R, Kimura M, Okano Y, Zhou H, Sen S, Allis CD and Sassone-Corsi P.(2002) Mitotic phosphorylation of histone H3: spatio-temporal regulation by mammalian Aurora kinases. Mol Cell Biol. 22: 874-85.

D'Amours D, Amon A (2004) At the interface between signaling and executing anaphase--Cdc14 and the FEAR network. Genes Dev 18: 2581-2595.

D'Aquino KE, Monje-Casas F, Paulson J, Reiser V, Charles GM, et al. (2005) The protein kinase Kin4 inhibits exit from mitosis in response to spindle position defects. Mol Cell 19: 223-234.

Dechant R and Glotzer M (2003) Centrosome separation and central spindle assembly act in redundant pathways that regulate microtubule density and trigger cleavage furrow formation. Dev. Cell. 4: 333-344.

Dobles M, Liberal V, Scott ML, Benezra R and Sorger PK (2000) Chromosome missegregation and apoptosis in mice lacking the mitotic checkpoint protein Mad2.Cell. 101(6):635-45.

Eckerdt F and Strebhardt K. Polo-like kinase 1: target and regulator of anaphase-promoting complex/cyclosome-dependent proteolysis. Cancer Res. 66: 6895-8.

Elledge SJ. (1996) Cell cycle checkpoints: preventing an identity crisis. Science. 274: 1664-72.

Falk JE, Chan LY and Amon A (2011) Lte1 promotes mitotic exit by controlling the localization of the spindle position checkpoint kinase Kin4. Proc Natl Acad Sci U S A. 108: 12584-90.

Farr KA and Hoyt MA (1998) Bub1p kinase activates the Saccharomyces cerevisiae spindle assembly checkpoint. Mol Cell Biol. 18: 2738-47.

Fankhauser C and Simanis V (1994) The cdc7 protein kinase is a dosage dependent regulator of septum formation in fission yeast. EMBO J. 13: 3011-9

Fink J, Carpi N, Betz T, Bétard A, Chebah M, Azioune A, Bornens M, Sykes C, Fetler L, Cuvelier D and Piel M.(2011) External forces control mitotic spindle positioning. Nat Cell Biol.13: 771-8.

Fraschini R, Beretta A, Sironi L, Musacchio A, Lucchini G, et al. (2001) Bub3 interaction with Mad2, Mad3 and Cdc20 is mediated by WD40 repeats and does not require intact kinetochores. Embo J 20: 6648-6659.

Fraschini R, D'Ambrosio C, Venturetti M, Lucchini G, Piatti S (2006) Disappearance of the budding yeast Bub2-Bfa1 complex from the mother-bound spindle pole contributes to mitotic exit. J Cell Biol 172: 335-346.

Fraschini R, Formenti E, Lucchini G, Piatti S (1999) Budding yeast Bub2 is localized at spindle pole bodies and activates the mitotic checkpoint via a different pathway from Mad2. J Cell Biol 145: 979-991.

Fraschini R, Venturetti M, Chiroli E, Piatti S (2008) The spindle position checkpoint: how to deal with spindle misalignment during asymmetric cell division in budding yeast. Biochem Soc Trans 36: 416-420.

Frenz LM, Lee SE, Fesquet D, Johnston LH (2000) The budding yeast Dbf2 protein kinase localises to the centrosome and moves to the bud neck in late mitosis. J Cell Sci 113 Pt 19: 3399-3408.

Furge KA, Wong K, Armstrong J, Balasubramanian M and Albright CF (1998) Byr4 and Cdc16 form a two-component GTPase-activating protein for the Spg1 GTPase that controls septation in fission yeast. Curr Biol. 8: 947-54.

Gateff E (1978) Malignant Neoplasms of Genetic Origin in Drosophila melanogaster. Science. 200:1448-59.

Gavriljuk K, Gazdag EM, Itzen A, Kotting C, Goody RS, et al. (2012) Catalytic mechanism of a mammalian Rab.RabGAP complex in atomic detail. Proc Natl Acad Sci U S A 109: 21348-21353.

Geymonat M, Spanos A, de Bettignies G, Sedgwick SG (2009) Lte1 contributes to Bfa1 localization rather than stimulating nucleotide exchange by Tem1. J Cell Biol 187: 497-511.

Geymonat M, Spanos A, Smith SJ, Wheatley E, Rittinger K, et al. (2002) Control of mitotic exit in budding yeast. In vitro regulation of Tem1 GTPase by Bub2 and Bfa1. J Biol Chem 277: 28439-28445.

Geymonat M, Spanos A, Walker PA, Johnston LH, Sedgwick SG (2003) In Vitro Regulation of Budding Yeast Bfa1/Bub2 GAP Activity by Cdc5. J Biol Chem 278: 14591-14594.

Glotzer M. (2009) The 3Ms of central spindle assembly: microtubules, motors and MAPs Nat Rev Mol Cell Bio 10: 9-20.

Gonczy P (2008) Mechanisms of asymmetric cell division: flies and worms pave the way. Nat Rev Mol Cell Biol 9: 355-366.

Gonzalez C (2007) Spindle orientation, asymmetric division and tumour suppression in Drosophila stem cells. Nat Rev Genet 8: 462-472.

Grandin N, de Almeida A and Charbonneau M (1998) The Cdc14 phosphatase is functionally associated with the Dbf2 protein kinase in Saccharomyces cerevisiae. Mol Gen Genet. 258: 104-16.

Grava S, Schaerer F, Faty M, Philippsen P and Barral Y (2006) Asymmetric recruitment of dynein to spindle poles and microtubules promotes proper spindle orientation in yeast. Dev Cell. 10: 425-39.

Gruneberg U, Campbell K, Simpson C, Grindlay J, Schiebel E (2000) Nud1p links astral microtubule organization and the control of exit from mitosis. Embo J 19: 6475-6488.

Hampoelz B, Knoblich JA (2004) Heterotrimeric G proteins: new tricks for an old dog. Cell 119: 453-456.

Hannak E, Kirkham M, Hyman AA and Oegema K. (2001) Aurora-A kinase is required for centrosome maturation in Caenorhabditis elegans. J Cell Biol.155: 1109-16

Hartwell LH and Weinert TA (1989) Checkpoints: controls that ensure the order of cell cycle events. Science. 246: 629-34.

Havens KA, Gardner MK, Kamieniecki RJ, Dresser ME and Dawson DS (2010) Slk19p of Saccharomyces cerevisiae regulates anaphase spindle

dynamics through two independent mechanisms. Genetics. 186: 1247-60.

Hawkins N. and Garriga G., (1998) Asymmetric cell division: from A to Z. Genes & Dev 12: 3625-3638.

Holubcová Z, Howard G and Schuh M. (2013) Vesicles modulate an actin network for asymmetric spindle positioning. Nat Cell Biol.15: 937-47.

Höfken T, Schiebel E (2002) A role for cell polarity proteins in mitotic exit. EMBO J.21: 4851-62.

Horvitz and Herskowitz, (1992) Mechanisms of asymmetric cell division: Two Bs or not two Bs, that is the question. Cell 68: 237–255.

Hotz M, Barral Y (2014) The Mitotic Exit Network: new turns on old pathways. Trends Cell Biol 24: 145-152.

Hotz M, Leisner C, Chen D, Manatschal C, Wegleiter T, et al. (2012) Spindle pole bodies exploit the mitotic exit network in metaphase to drive their age-dependent segregation. Cell 148: 958-972.

Hu F, Wang Y, Liu D, Li Y, Qin J, et al. (2001) Regulation of the Bub2/Bfa1 GAP complex by Cdc5 and cell cycle checkpoints. Cell 107: 655-665.

Humbert P, Russell S, Richardson H (2003) Dlg, Scribble and Lgl in cell polarity, cell proliferation and cancer. Bioessays. 25: 542-53.

Jaffe AB, Kaji N, Durgan J and Hall A (2008) Cdc42 controls spindle orientation to position the apical surface during epithelial morphogenesis. J Cell Biol. 183: 625-33.

Janke C, Magiera MM, Rathfelder N, Taxis C, Reber S, et al. (2004) A versatile toolbox for PCR-based tagging of yeast genes: new fluorescent proteins, more markers and promoter substitution cassettes. Yeast 21: 947-962.

Jaspersen SL, Charles JF, Tinker-Kulberg RL, Morgan DO, (1998) A late mitotic regulatory network controlling cyclin destruction in Saccharomyces cerevisiae Mol Biol Cell. 9: 2803-17.

Juanes MA, Twyman H, Tunnacliffe E, Guo Z, ten Hoopen R and Segal M. (2003) Spindle pole body history intrinsically links pole identity with asymmetric fate in budding yeast. Curr Biol. 23: 1310-9.

Kahana JA, Schlenstedt G, Evanchuk DM, Geiser JR, Hoyt MA, et al. (1998) The yeast dynactin complex is involved in partitioning the mitotic spindle between mother and daughter cells during anaphase B. Mol Biol Cell 9: 1741-1756.

Kammerer D, Stevermann L and Liakopoulos D (2010) Ubiquitylation regulates interactions of astral microtubules with the cleavage apparatus. Curr Biol. 20: 1233-43.

Kerr GW, Sarkar S, Tibbles KL, Petronczki M, Millar JB and Arumugam P (2011) Meiotic nuclear divisions in budding yeast require PP2A(Cdc55)-mediated antagonism of Net1 phosphorylation by Cdk. J Cell Biol. 193: 1157-66.

Kim J, Luo G, Bahk YY, Song K (2012) Cdc5-dependent asymmetric localization of Bfa1 fine-tunes timely mitotic exit. PLoS Genet 8: e1002450.

Kiyomitsu T and Cheeseman IM. (2013) Cortical dynein and asymmetric membrane elongation coordinately position the spindle in anaphase. Cell. 154: 391-402.

Knoblich JA (2010) Asymmetric cell division: recent developments and their implications for tumour biology. Nat Rev Mol Cell Biol 11: 849-860.

Konig C, Maekawa H, Schiebel E (2010) Mutual regulation of cyclin-dependent kinase and the mitotic exit network. J Cell Biol 188: 351-368.

Knop M and Schiebel E (1997) Spc98p and Spc97p of the yeast gamma-tubulin complex mediate binding to the spindle pole body via their interaction with Spc110p. EMBO J.16: 6985-95.

Lampson MA and Kapoor TM, (2005) The human mitotic checkpoint protein BubR1 regulates chromosome-spindle attachments. Nat Cell Biol. 7: 93-8.

Langemeyer L, Nunes Bastos R, Cai Y, Itzen A, Reinisch KM, et al. (2014) Diversity and plasticity in Rab GTPase nucleotide release mechanism has consequences for Rab activation and inactivation. Elife 3: e01623.

Lee L, Tirnauer JS, Li J, Schuyler SC, Liu JY and Pellman D. (2000) Positioning of the mitotic spindle by a cortical-microtubule capture mechanism. Science 287: 2260-2.

Lee PR, Song S, Ro HS, Park CJ, Lippincott J, Li R, Pringle JR, De Virgilio C, Longtine MS and Lee KS (2002) Bni5p, a septin-interacting protein, is required for normal septin function and cytokinesis in Saccharomyces cerevisiae. Mol Cell Biol. 22: 6906-20.

Leisner C, Kammerer D, Denoth A, Britschi M, Barral Y and Liakopoulos D (2008) Regulation of mitotic spindle asymmetry by SUMO and the spindle-assembly checkpoint in yeast. Curr Biol. 18: 1249-55.

Li C, Furge KA, Cheng QC and Albright CF. (2000) Byr4 localizes to spindle-pole bodies in a cell cycle-regulated manner to control Cdc7 localization and septation in fission yeast. J Biol Chem. 275: 14381-7.

Li R (2013) The art of choreographing asymmetric cell division. Dev Cell 25: 439-450.

Li R and Murray AW. (1991) Feedback control of mitosis in budding yeast. Cell. 66: 519-31.

Liakopoulos D, Kusch J, Grava S, Vogel J, Barral Y (2003) Asymmetric loading of Kar9 onto spindle poles and microtubules ensures proper spindle alignment. Cell 112: 561-574.

Lippincott J, Shannon KB, Shou W, Deshaies RJ and Li R (2001) The Tem1 small GTPase controls actomyosin and septin dynamics during cytokinesis. J Cell Sci. 114: 1379-86.

Lowe M. et al (1998). Cdc2 kinase directly phosphorylates the cis-Golgi matrix protein GM130 and is required for Golgi fragmentation in mitosis. Cell 94: 783-793.

Luca FC, Mody M, Kurischko C, Roof DM, Giddings TH and Winey M. (2001) Saccharomyces cerevisiae Mob1p is required for cytokinesis and mitotic exit. Mol Cell Biol. 21: 6972-83.

Maekawa H, Priest C, Lechner J, Pereira G, Schiebel E (2007) The yeast centrosome translates the positional information of the anaphase spindle into a cell cycle signal. J Cell Biol 179: 423-436.

Maekawa H, Usui T, Knop M, Schiebel E. (2003) Yeast Cdk1 translocates to the plus end of cytoplasmic microtubules to regulate bud cortex interactions. EMBO J. 22: 438-49.

Maupin P and Pollard TD (1986) Arrangement of actin filaments and myosin-like filaments in the contractile ring and of actin-like filaments in the mitotic spindle of dividing HeLa cells. J Ultrastruct Mol Struct Res. 94:92-103.

McNally FJ (2013) Mechanisms of spindle positioning. J Cell Biol. 200: 131-40.

Meednu N, Hoops H, D'Silva S, Pogorzala L, Wood S, Farkas D, Sorrentino M, Sia E, Meluh P and Miller RK (2008) The spindle positioning protein Kar9p interacts with the sumoylation machinery in Saccharomyces cerevisiae. Genetics. 180: 2033-55.

Menssen R, Neutzner A and Seufert W. (2001) Asymmetric spindle pole localization of yeast Cdc15 kinase links mitotic exit and cytokinesis. Curr Biol. 11: 345-50.

Mierzwa B and Gerlich DW (2014) Cytokinetic Abscission: Molecular Mechanisms and Temporal Control. Dev Cell. 31: 525-538

Miller RK, Rose MD (1998) Kar9p is a novel cortical protein required for cytoplasmic microtubule orientation in yeast. J Cell Biol 140: 377-390.

Mocciaro A and Schiebel E. (2010) Cdc14: a highly conserved family of phosphatases with non-conserved functions? J Cell Sci123: 2867-76.

Molk JN, Schuyler SC, Liu JY, Evans JG, Salmon ED, et al. (2004) The differential roles of budding yeast Tem1p, Cdc15p, and Bub2p protein dynamics in mitotic exit. Mol Biol Cell 15: 1519-1532.

Monje-Casas F, Amon A (2009) Cell polarity determinants establish asymmetry in MEN signaling. Dev Cell 16: 132-145.

Moore JK, D'Silva S, Miller RK (2006) The CLIP-170 homologue Bik1p promotes the phosphorylation and asymmetric localization of Kar9p. Mol Biol Cell. 17:178-91.

Moore JK, Cooper JA (2010) Coordinating mitosis with cell polarity: Molecular motors at the cell cortex. Semin Cell Dev Biol 21: 283-289.

Moore JK, Chudalayandi P, Heil-Chapdelaine RA and Cooper JA (2010) The spindle position checkpoint is coordinated by the Elm1 kinase. J Cell Biol. 191: 493-503.

Moore JK, Li J and Cooper JA (2008) Dynactin function in mitotic spindle positioning.Traffic. 9: 510-27.

Mukherjee S, Kong J. and Brat D.J. (2014) Cancer Stem Cell Division: When the Rules of Asymmetry Are Broken. Stem Cells Dev.

Musacchio A, Salmon ED. (2007) The spindle-assembly checkpoint in space and time. Nat Rev Mol Cell Biol. 8: 379-93.

Neuwald AF (1997) A shared domain between a spindle assembly checkpoint protein and Ypt/Rab-specific GTPase-activators. Trends Biochem Sci 22: 243-244.

Noton E and Diffley JF (2000) CDK inactivation is the only essential function of the APC/C and the mitotic exit network proteins for origin resetting during mitosis. Mol. Cell 5: 85-95.

Osmani AH, McGuire SL and Osmani SA. (1991) Parallel activation of the NIMA and p34cdc2 cell cycle-regulated protein kinases is required to initiate mitosis in A. nidulans. Cell. 67: 283-91.

Pan X, Eathiraj S, Munson M, Lambright DG (2006) TBC-domain GAPs for Rab GTPases accelerate GTP hydrolysis by a dual-finger mechanism. Nature 442: 303-306.

Pangilinan F and Spencer F (1996) Abnormal kinetochore structure activates the spindle assembly checkpoint in budding yeast. Mol Biol Cell. 7: 1195-208.

Park SY, Cable AE, Blair J, Stockstill KE and Shannnon KB. (2009) Bub2 regulation of cytokinesis and septation in budding yeast.BMC Cell Biol. 10:43.

Pereira G, Grueneberg U, Knop M and Schiebel E (1999) Interaction of the yeast gamma-tubulin complex-binding protein Spc72p with Kar1p is essential for microtubule function during karyogamy. EMBO J. 18: 4180-95.

Pereira G, Hofken T, Grindlay J, Manson C, Schiebel E (2000) The Bub2p spindle checkpoint links nuclear migration with mitotic exit. Mol Cell 6: 1-10.

Pereira G, Schiebel E (2001) The role of the yeast spindle pole body and the mammalian centrosome in regulating late mitotic events. Curr Opin Cell Biol 13: 762-769.

Pereira G, Schiebel E (2005) Kin4 kinase delays mitotic exit in response to spindle alignment defects. Mol Cell 19: 209-221.

Piatti S, Venturetti M, Chiroli E and Fraschini R. (2006) The spindle position checkpoint in budding yeast: the motherly care of MEN. Cell Div. 1:2

Piel M, Meyer P, Khodjakov A, Rieder CL and Bornens M. (2000) The respective contributions of the mother and daughter centrioles to centrosome activity and behavior in vertebrate cells. J Cell Biol. 149: 317-30.

Queralt E, Lehane C, Novak B, Uhlmann F (2006) Downregulation of PP2A(Cdc55) phosphatase by separase initiates mitotic exit in budding yeast. Cell 125: 719-732.

Queralt E and Uhlmann F (2008) Separase cooperates with Zds1 and Zds2 to activate Cdc14 phosphatase in early anaphase. J Cell Biol. 182: 873-83.

Ro HS, Song S, Lee KS (2002) Bfa1 can regulate Tem1 function independently of Bub2 in the mitotic exit network of Saccharomyces cerevisiae. Proc Natl Acad Sci U S A 99: 5436-5441.

Rock JM and Amon A (2009) The FEAR network. Curr Biol.19: R1063-8.

Rock JM, Amon A (2011) Cdc15 integrates Tem1 GTPase-mediated spatial signals with Polo kinase-mediated temporal cues to activate mitotic exit. Genes Dev 25: 1943-1954.

Rock JM, Lim D, Stach L, Ogrodowicz RW, Keck JM, Jones MH, Wong CC, Yates JR 3rd, Winey M, Smerdon SJ, Yaffe MB and Amon A. (2013) Activation of the Yeast Hippo Pathway by Phosphorylation-Dependent Assembly of Signaling Complexes. Science 340: 871-875.

Rossio V, Yoshida S. (2011) Spatial regulation of Cdc55-PP2A by Zds1/Zds2 controls mitotic entry and mitotic exit in budding yeast. J Cell Biol. 193: 445-54.

Scheffzek K, Ahmadian MR, Kabsch W, Wiesmuller L, Lautwein A, et al. (1997) The Ras-RasGAP complex: structural basis for GTPase activation and its loss in oncogenic Ras mutants. Science 277: 333-338.

Shirayama M, Matsui Y, Tanaka K and Toh-e A (1994) Isolation of a CDC25 family gene, MSI2/LTE1, as a multicopy suppressor of ira1. Yeast. 10: 451-61.

Schmidt S, Sohrmann M, Hofmann K, Woollard A, Simanis V (1997) The Spg1p GTPase is an essential, dosage-dependent inducer of septum formation in Schizosaccharomyces pombe. Genes Dev 11: 1519-1534.

Schonegg S, Constantinescu AT, Hoege C and Hyman, A (2007). A. The Rho GTPase-activating proteins RGA-3 and RGA-4 are required to set the initial size of PAR domains in Caenorhabditis elegans one-cell embryos. Proc. Natl Acad. Sci. USA 104: 14976-14981.

Schweins T and Wittinghofer A. (1994) GTP-binding proteins. Structures, interactions and relationships. Curr Biol. 4: 547-50

Sheff MA, Thorn KS (2004) Optimized cassettes for fluorescent protein tagging in Saccharomyces cerevisiae. Yeast 21: 661-670.

Shou W, Seol JH, Shevchenko A, Baskerville C, Moazed D, et al. (1999) Exit from mitosis is triggered by Tem1-dependent release of the protein phosphatase Cdc14 from nucleolar RENT complex. Cell 97: 233-244.

Siller KH, Doe CQ (2009) Spindle orientation during asymmetric cell division. Nat Cell Biol 11: 365-374.

Singh P, Ramdas Nair A and Cabernard C. (2014) The centriolar protein Bld10/Cep135 is required to establish centrosome asymmetry in Drosophila neuroblasts. Curr Biol. 24: 1548-55.

Sohrmann M, Schmidt S, Hagan I and Simanis V. (1998) Asymmetric segregation on spindle poles of the Schizosaccharomyces pombe septum-inducing protein kinase Cdc7p. Genes Dev. 12: 84-94.

Soltys BJ and Borisy GG (1985) Polymerization of tubulin in vivo: direct evidence for assembly onto microtubule ends and from centrosomes. J Cell Biol. 100: 1682-9.

Stegmeier F, Amon A (2004) Closing Mitosis: The Functions of the Cdc14 Phosphatase and Its Regulation. Annu Rev Genet 38: 203-232.

Stegmeier F, Visintin R, Amon A (2002) Separase, polo kinase, the kinetochore protein Slk19, and Spo12 function in a network that controls Cdc14 localization during early anaphase. Cell 108: 207-220.

Sullivan M and Uhlmann F. (2003) A non-proteolytic function of separase links the onset of anaphase to mitotic exit. Nat Cell Biol. 5: 249-54.

Surana U, Amon A, Dowzer C, McGrew J, Byers B, et al. (1993) Destruction of the CDC28/CLB mitotic kinase is not required for the metaphase to anaphase transition in budding yeast. Embo J 12: 1969-1978.

Tanaka TU (2010) Kinetochore-microtubule interactions: steps towards bi-orientation. EMBO J. 29: 4070-82.

Tassan JP, Schultz SJ, Bartek J and Nigg EA (1994) Cell cycle analysis of the activity, subcellular localization, and subunit composition of human CAK (CDK-activating kinase). J Cell Biol. 127: 467-78.

Trcek T, Larson DR, Moldón A, Query CC and Singer RH. (2011) Single-molecule mRNA decay measurements reveal promoter- regulated mRNA stability in yeast. Cell.147: 1484-97.

Tsou MF, Hayashi A and Rose LS (2003) LET-99 opposes Galpha/GPR signaling to generate asymmetry for spindle positioning in response to PAR and MES-1/SRC-1 signaling. Development. 130: 5717-30.

Valerio-Santiago M, Monje-Casas F (2011) Tem1 localization to the spindle pole bodies is essential for mitotic exit and impairs spindle checkpoint function. J Cell Biol 192: 599-614.

Venturetti M. (2008) Exit from mitosis in *Saccharomyces cerevisiae*: regulation of the small GTPase Tem1. PhD thesis

Vetter IR and Wittinghofer A (2001) The guanine nucleotide-binding switch in three dimensions. Science 294: 1299-1304.

Visintin R, Amon A (2001) Regulation of the mitotic exit protein kinases cdc15 and dbf2. Mol Biol Cell 12: 2961-2974.

Visintin R, Craig K, Hwang ES, Prinz S, Tyers M, et al. (1998) The phosphatase Cdc14 triggers mitotic exit by reversal of Cdk- dependent phosphorylation. Mol Cell 2: 709-718.

Visintin R, Hwang ES, Amon A (1999) Cfi1 prevents premature exit from mitosis by anchoring Cdc14 phosphatase in the nucleolus [see comments]. Nature 398: 818-823.

Visintin R, Stegmeier F and Amon A (2003) The role of the polo kinase Cdc5 in controlling Cdc14 localization. Mol Biol Cell. 14: 4486-98.

Wach A, Brachat A, Pohlmann R, Philippsen P (1994) New heterologous modules for classical or PCR-based gene disruptions in Saccharomyces cerevisiae. Yeast 10: 1793-1808.

Wang Y and Burke DJ (1995) Checkpoint genes required to delay cell division in response to nocodazole respond to impaired kinetochore function in the yeast Saccharomyces cerevisiae. Mol Cell Biol. 15: 6838-44.

Wang Y, Shirogane T, Liu D, Harper JW and Elledge SJ. (2003) Exit from exit: resetting the cell cycle through Amn1 inhibition of G protein signaling. 112: 697-709.

Wang Y and Ng TY (2006) Phosphatase 2A negatively regulates mitotic exit in Saccharomyces cerevisiae. Mol Biol Cell. 17: 80-9.

Weinert TA and Hartwell LH (1990) Characterization of RAD9 of Saccharomyces cerevisiae and evidence that its function acts posttranslationally in cell cycle arrest after DNA damage. Mol Cell Biol. 10: 6554-64.

Weiss EL. (2012) Mitotic exit and separation of mother and daughter cells. Genetics. 192: 1165-202

Wicky S, Tjandra H, Schieltz D, Yates J 3rd, Kellogg DR. (2011) The Zds proteins control entry into mitosis and target protein phosphatase 2A to the Cdc25 phosphatase. Mol Biol Cell. 22: 20-32.

Xiong Y, Dawson VL, and Dawson TM. (2012) LRRK2 GTPase Dysfunction in the Pathogenesis of Parkinson's disease. Biochem Soc Trans. 40: 1074–1079.

Xu S, Huang HK, Kaiser P, Latterich M, Hunter T (2000) Phosphorylation and spindle pole body localization of the Cdc15p mitotic regulatory protein kinase in budding yeast. Curr Biol 10: 329-332.

Yamashita YM, Mahowald AP, Perlin JR, Fuller MT (2007) Asymmetric inheritance of mother versus daughter centrosome in stem cell division. Science.315: 518-21

Yamashita YM and Fuller MA (2008) Asymmetric centrosome behavior and the mechanisms of stem cell division. J Cell Biol. 180: 261-6.

Yamashita YM, Yuan H, Cheng J, Hunt AJ (2010) Polarity in stem cell division: asymmetric stem cell division in tissue homeostasis. Cold Spring Harb Perspect Biol 2: 001313.

Yamashita YM. (2010) A new member of the spindle orientation club: mammalian intestinal stem cells. Cell Stem Cell. 6: 91-2.

Yeh E, Skibbens RV, Cheng JW, Salmon ED, Bloom K (1995) Spindle dynamics and cell cycle regulation of dynein in the budding yeast, Saccharomyces cerevisiae. J Cell Biol 130: 687-700.

Yeh YH, Huang YF, Lin TY and Shieh SY (2009) The cell cycle checkpoint kinase CHK2 mediates DNA damage-induced stabilization of TTK/hMps1. Oncogene. 28: 1366-78.

Yoshida S, Kono K, Lowery DM, Bartolini S, Yaffe MB, Ohya Y and Pellman D. (2006) Polo-like kinase Cdc5 controls the local activation of Rho1 to promote cytokinesis. Science. 313: 108-11.

Acknowledgements

This work would not be accomplished without the precious help of many persons.

First and foremost, I would like to express my sincere gratitude to my PhD supervisor, Dr. Simonetta Piatti. I am thankful to Simonetta for her invaluable guidance, constructive criticism and friendly advice. Mossi, I would like to thank you very much for your support and understanding over these past four years and for allowing me to grow as a research scientist.

I thank current and former lab mates in Piatti's Group: M. Angels, Léon, Magda, Giorgia, Laura, Thibault, Patrycja, and Rita, for the stimulating discussions, for the support and for all the nice moments we have spent together in the lab and outside.

I also thank the whole CRBM community, for creating such a great environment for working, sharing constructive discussions, encouraging and supporting.

Getting through my dissertation required more than academic support, I want to express my gratitude to many people for their friendship. Sébastien, Marion, Cao, Edwin, Daouda, Sarah, Michele, Marion and Sylvain have been unwavering in their personal and professional support during the time I spent in Montpellier. For many memorable evenings, I must thank François, Veronica and Alessandra. I would also like to thank Babeth who opened both her home and heart to me when I first arrived in the city.

Finally I thank Gianni, Valeria, Barbara, Giulia, Giovanna, Marco, Naria, Matteo, Roberta, Eleonora, Francesca and Miria, who helped me without even knowing it, as only true friends can do.

None of this could have happened without my family. Mum, Dad and Stefano, this thesis stands as a testament to your unconditional love and encouragement.